Travail d'études : Heterologous protein production in Yarrowia lipolytica: laccase as a case study.

Auteur : Keller, Constance
Promoteur(s) : Fickers, Patrick
Faculté : Gembloux Agro-Bio Tech (GxABT)
Diplôme : Master en bioingénieur : chimie et bioindustries, à finalité spécialisée
Année académique : 2024-2025
URI/URL : http://hdl.handle.net/2268.2/23978

LIÈGE université
Gembloux
Agro-Bio Tech

HETEROLOGOUS PROTEIN PRODUCTION IN *YARROWIA LIPOLYTICA*: LACCASE AS A CASE STUDY

CONSTANCE KELLER

**MASTER'S THESIS SUBMITTED IN PARTIAL FULFILLMENT
OF THE REQUIREMENTS FOR THE DEGREE OF MASTER IN BIOENGINEERING,
SPECIALIZATION IN CHEMISTRY AND BIO-INDUSTRIES**

ACADEMIC YEAR 2024-2025

SUPERVISOR: PATRICK FICKERS

LIÈGE université
Gembloux
Agro-Bio Tech

HETEROLOGOUS PROTEIN PRODUCTION IN *YARROWIA LIPOLYTICA*: LACCASE AS A CASE STUDY

CONSTANCE KELLER

**MASTER'S THESIS SUBMITTED IN PARTIAL FULFILLMENT
OF THE REQUIREMENTS FOR THE DEGREE OF MASTER IN BIOENGINEERING,
SPECIALIZATION IN CHEMISTRY AND BIO-INDUSTRIES**

ACADEMIC YEAR 2024-2025

SUPERVISOR: PATRICK FICKERS

The master's thesis presented below was carried out in the Microbial Processes and Interactions department of Gembloux Agro-Bio Tech (University of Liege, Belgium).

ACKNOWLEDGEMENTS

I would like to take this opportunity to express my gratitude to all those who supported me during the completion of this master thesis. This work represents the culmination of my studies and has been a challenging yet rewarding experience. It would not have been the same without the guidance, encouragement and support of many people.

I would like to express my gratitude to Prof. Patrick Fickers for his invaluable supervision and guidance throughout this thesis. His scientific insight and constructive feedback greatly contributed to the quality of this work and to my personal development as a researcher.

I am also deeply thankful to Cristina, Rocío and Vassia for their patience and kindness, for always taking the time to answer my numerous questions, and for generously sharing their knowledge and expertise. Their encouragement, availability and the genuinely good vibes they shared, both in the lab and beyond, helped me navigate challenges and made my experience there truly enjoyable.

I would also like to express my heartfelt thanks to my friends Alizée, Léa, Zoé and Amélie, who made my master's journey truly enjoyable. Their friendship and support brought joy to both the challenging and lighter moments of this experience. Whether through shared study sessions, laughter, or simply being there to talk and share ideas, their presence made the past years richer and more memorable. A special mention goes to Alizée, with whom I shared countless coffee breaks and conversations about challenging experiments, offering encouragement and perspective that helped me stay motivated.

I would also like to express my deepest gratitude to my mom and sister for their unwavering support throughout my studies. Their constant encouragement and belief in me provided a foundation of confidence and reassurance during challenging moments. Knowing that they were always there to listen, offer advice, and celebrate achievements made this journey much more manageable and meaningful.

ABSTRACT (EN)

Recombinant proteins (rProt) are essential in industrial, pharmaceutical and diagnostic applications. Their efficient production often requires not only high expression of their encoding gene, but also effective rProt secretion, which simplifies the downstream processing. Protein secretion relies on a so-called signal peptide (SP), located at the N-terminal sequence of the protein. It is mainly composed of a pre-leader and a pro-region that have distinctive functions in the secretion pathway.

The yeast *Yarrowia lipolytica* is commonly used for rProt production due to its ability to express genes at a high level and its effective secretion machinery. However, the secretion efficiency for a given rProt strongly depends on the specificity of the SP sequence.

This thesis explores the influence of different SPs on the extracellular production of a model protein, the Lac Vader laccase. Using the Golden Gate Assembly technology, several variants of SP that combined diverse pre- and pro-regions were constructed, including some derived from Lip2 and Xpr2 proteins, as well as synthetic parts. The efficiency of those SP on the secretion of the model protein was evaluated by monitoring the laccase activity in the culture supernatant for the different SP-rProt constructs.

The results revealed that extended pro-regions (like Lip2 pro-region) significantly enhanced secretion. However, secretion efficiency varied between the different constructs, highlighting that not all signal sequences contributed equally to secretion. The study showed that protein export in *Y. lipolytica* is highly dependent on the combination of pre- and pro-region used. Importantly, by comparing secretion performance in *Y. lipolytica* and *Pichia pastoris*, the results demonstrated that *Y. lipolytica* generally achieved higher secretion levels.

These findings confirm that secretion tags are critical for protein expression in *Y. lipolytica* and demonstrate how their choice directly influences secretion efficiency. In comparison, *P. pastoris* showed lower secretion levels, underscoring the superior performance of *Y. lipolytica*.

RÉSUMÉ (FR)

Les protéines recombinantes (rProt) sont essentielles dans les applications industrielles, pharmaceutiques et diagnostiques. Leur production efficace nécessite non seulement une forte expression du gène codant, mais également une sécrétion efficace de la rProt, ce qui simplifie les étapes de purification en aval. La sécrétion des protéines repose sur un signal peptide (SP), situé à l'extrémité N-terminale de la protéine. Celui-ci est principalement composé d'une pré-région et d'une pro-région, qui remplissent des fonctions distinctes dans la voir de sécrétion.

La levure *Yarrowia lipolytica* est couramment utilisée pour la production de rProts en raison de sa capacité à exprimer les gènes à un niveau élevé et de son appareil de sécrétion efficace. Cependant, l'efficacité de sécrétion d'une protéine donnée dépend fortement de la spécificité de la séquence du SP.

Ce travail explore l'influence de différents SP sur la production extracellulaire d'une protéine modèle, la laccase Lac Vader. En utilisant la technologie Golden Gate Assembly, plusieurs variantes de SP combinant diverses pré- et pro-régions ont été construites, incluant certaines dérivées des protéines Lip2 et Xpr2, ainsi que des parties synthétiques. L'efficacité de ces SP sur la sécrétion de la protéine modèle a été évaluée en mesurant l'activité laccase dans le surnageant de culture pour les différentes constructions SP-rProt.

Les résultats ont montré que les pro-régions complètes (comme le pro-région de Lip2) amélioraient significativement la sécrétion. Cependant, l'efficacité de sécrétion variait selon les différentes constructions, soulignant que tous les signaux de sécrétion ne contribuent pas de manière équivalente. L'étude a démontré que l'export des protéines chez *Y. lipolytica* dépend étroitement de la combinaison du peptide signal et de la pro-région utilisée. De plus, la comparaison des performances de sécrétion entre *Y. lipolytica* et *Pichia pastoris* a montré que *Y. lipolytica* atteignait généralement des niveaux de sécrétion plus élevés.

Ces résultats confirment que les signaux de sécrétion constituent un facteur critique de l'expression protéique chez *Y. lipolytica* et montrent que leur choix influence directement l'efficacité de sécrétion. En comparaison, *P. pastoris* a montré des niveaux de sécrétion plus faibles, soulignant la performance supérieure de *Y. lipolytica*.

TABLE OF CONTENTS

LIST OF FIGURES

LIST OF TABLES

LIST OF ABBREVIATIONS

Abbreviation/symbol	Signification
3’	3’ hydroxyl extremity of a nucleotide
5’	5’ phosphate extremity of a nucleotide
%	Percentage
°C	Degree Celsius
αMat	α-mating
A. nidulans	*Aspergillus nidulans*
A. niger	*Aspergillus niger*
AEP	Alkaline extracellular protease
ANOVA	Analysis of variance
AOX1	Alcohol oxidase 1
B. subtilis	*Bacillus subtilis*
CDS	Coding DNA sequence
CRISPR-Cas9	Clustered Regularly Interspaced Short Palindromic Repeats – associated protein 9
CV	Coefficient of variation
DCW	Dry cell weight
DNA	Deoxyribonucleic acid
E. coli	*Escherichia coli*
EDTA	Ethylenediaminetetraacetic acid
ER	Endoplasmic reticulum
FDA	Food and Drug Administration (U.S.)
GG	Golden Gate
GGA	Golden Gate Assembly
GOI	Gene of interest
GRAS	Generally regarded as safe
LiAc	Lithium acetate
LB	Lysogeny broth
LBA	Lysogeny broth agar
MB	Molecular biology
MeOH	Methanol
min	Minutes
mRNA	Messenger RNA
ns	Non-significant
OD	Optical density
PCR	Polymerase chain reaction
PEG	Polyethylene glycol
PO_4	Phosphate
POI	Protein of interest
p*TEF*	Promoter of the translational elongation factor 1α
qPCR	Quantitative PCR
RFP	Red fluorescent protein
RNA	Ribonucleic acid
rpm	Rotation per minute
rProt	Recombinant protein
SC	Secretion cassette
S. cerevisiae	*Saccharomyces cerevisiae*

SOC	Super optimal broth with Catabolite repression
SP	Signal peptide
SRP	Signal recognition particle
s	Seconds
SD	Standard deviation
TAE	Tris-acetate-EDTA
TE	Tris-EDTA
Tm	Melting temperature
TU	Transcription unit
U	Enzyme unit
UV	Ultraviolet
w/v	Weight-volume ratio
w/w	Weight-weight ratio
Y. lipolytica	*Yarrowia lipolytica*
YNB	Yeast nitrogen base

1. STATE OF THE ART

1.1. Recombinant proteins

1.1.1. Introduction and generalities

A recombinant protein (rProt) can be defined as « a manufactured protein that has been produced using cells programmed to express that protein of interest »[1]. The amino acid sequence may be identical to that of the "wild-type" protein. In such cases, the nucleotide sequence can be optimized to match the codon usage of the production host[2]. Different organisms prefer different codons for the same amino acid, and matching this preference can make protein production more efficient, increasing productivity without altering the protein itself[2,3]. Alternatively, the amino acid sequence can be engineered to modify or improve the catalytic properties of the enzyme[4,5].

Initially, proteins were purified from natural sources (e.g., insulin from animal pancreas, papain from papaya latex), but these sources are often limited and extraction processes are typically inefficient, which increases the production cost[6,7]. Moreover, depending on the source of the protein, there is a risk of contamination or toxicity[7].

With the advances in cell culture and molecular biology (MB) technologies, the production of rProt at large scale in naturally non-producing hosts was made possible[6–8]. Those MB technologies enable the modification of gene expression level, the rewiring of metabolic pathway and the modification of the catalytic properties of enzymes[9–11]. They made possible the transition from naturally occurring, impure and poorly characterized enzymes to tailor-made proteins and enzymes with optimized properties for their specific application[8]. Examples include high yield production of therapeutic antibodies and recombinant hormones like insulin, as well as industrial enzymes, including heat-stable amylases for starch processing or alkaline proteases used in detergents[8,12,13].

rProts can be divided into two main categories: those for pharmaceutical use and those for non-pharmaceutical purposes[12]. Non-pharmaceutical rProts include diverse enzymes (lipases, amylases, proteases, laccases …) and structural proteins (collagen, elastin, fibronectin …), with various uses in the production of food and drinks, biodiesel, clothing, cosmetics, paper pulp industry or cleaning products[8,12,13]. They are often genetically modified to improve their intrinsic characteristics, such as a better stability to pH and heat, resistance to oxidation but also to lower their aggregation or misfolding during secretion[12,14].

Pharmaceutical rProts, on the other hand, are intended for therapeutic applications such as vaccines or diagnostics. Nowadays, they can be genetically modified or even entirely engineered, with the objective of increasing their stability and therapeutic value[12].

Despite their differing applications and a significant price gap, both categories generally follow similar manufacturing processes (Figure 1)[12]. The main difference lies in the purification steps, which represents a major share of the overall production cost.

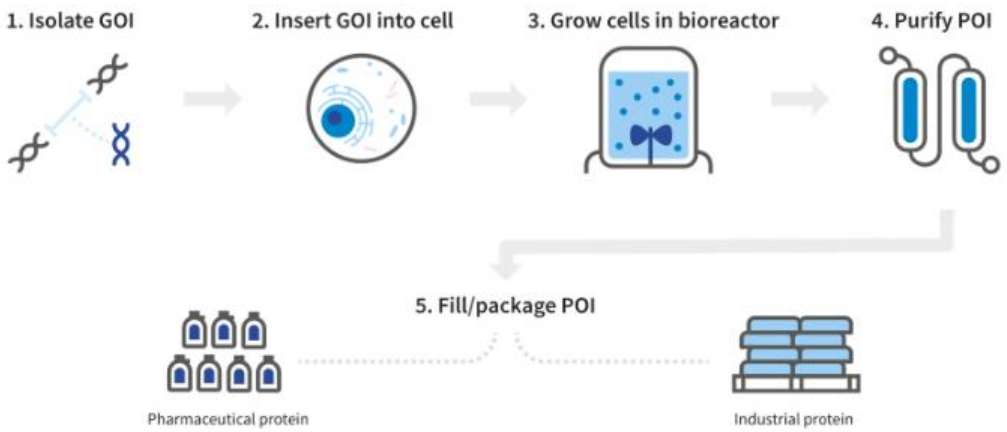

Figure 1: General workflow for recombinant protein production. *GOI = gene of interest; POI = protein of interest. From Puetz & Wurm, 2019.*

Generally, the first step in the production of a rProt is the selection of a gene of interest (GOI). This gene consists of a deoxyribonucleic acid (DNA) sequence that contains all the genomic information (nucleotide sequence) required for the synthesis of the rProt by the cellular machinery[12]. These DNA sequences can be obtained from the genomic DNA of a given organism or chemically synthesized, the latter option allowing gene sequence optimization[13]. This DNA sequence is then cloned into a specific expression vector, which is most of the time introduced at a specific locus into the genome of the producing organism[12]. This expression vector allows the expression of the GOI at high levels and on demand (regulated gene expression)[15].

The host cell is called a recombinant cell or recombinant organism. From this organism, culture is carried out to produce the protein of interest (POI)[12]. These cultures are usually performed in bioreactors in batch or fed-batch mode, allowing the production of a high quantity of rProt[7,16]. After the culture, the protein can either be in the medium (secreted) or inside the cells (non-secreted, intracellular or periplasmic). Depending on the situation, different processes are used to purify the POI, before the packaging and distribution of the final product[12,13].

However, these general steps can vary greatly depending on the protein itself and its application[12].

1.1.2. Hosts for recombinant protein production

rProts can be synthesized in many different organisms: bacteria, yeasts, filamentous fungi, mammalian cells and even in insect cells or transgenic plants and animals[6,7]. Prokaryotic or eukaryotic microorganisms, such as bacteria, yeasts and filamentous fungi, are considered beneficial hosts. This is mainly due to their high growth rates and ease of genetic manipulation, making them widely used platforms for rProt production[7].

Usually, complex proteins are expressed in eukaryotic systems, which are able to realize post-translational modifications, while less complex proteins are expressed in prokaryotic systems[6]. Therefore, the choice of organism depends on the rProt being produced. While a wide range of organisms is used to produce rProt, the present introduction will focus on bacteria, yeasts and filamentous fungi.

1.1.2.1. Bacteria

Various bacterial species have been explored as hosts for rProt production, each offering different advantages and limitations. However, this section will focus on two widely studied organisms, commonly used in biotechnology: *Escherichia coli* and *Bacillus subtilis*.

With the advent of rProt production, *E. coli* was the most widely used organism, allowing higher-yield production than other organisms at that time[12]. It allows for the most cost-efficient, rapid and simplest way to express proteins[6]. Owing to the knowledge acquired about this bacterium, including genetics, biochemistry, molecular biology, physiology and culture technologies, it has become a well-established model organism and a valuable host for various biotechnological applications[7,17]. These advantages enabled, for example, the production of high-value proteins, such as insulin or bovine growth hormone[18].

Nowadays, the expression of heterologous proteins in *E. coli* remains a common choice for many reasons. It is inexpensive, able to reach high cell densities and high protein yield, possesses a high growth rate and is easy to culture[17,19]. Moreover, its genome can be modified quickly and precisely, promoter induction can be controlled, and plasmid copy number can be efficiently regulated[6].

However, *E. coli* cultures present several drawbacks. When culture occurs at high cell density and the metabolism is overflowed, acetate produced by *E. coli* can accumulate and cause toxicity. This problem can be managed by controlling the level of oxygen[6] or by adjusting the carbon source feed rate through fed-batch mode[20]. Another important disadvantage of *E. coli* is the formation of inclusion bodies, that are protein aggregates occurring when the bacterium folding machinery is overloaded[21]. They are impacting protein production, because their quality impacts the refolding yield of the protein and the subsequent purification steps[22].

Another drawback of *E. coli* as a recombinant host is its inability to glycosylate the proteins or perform most post-translational modifications[6]. While disulfide bond formation can occur in the periplasmic space[23], *E. coli* cannot perform glycosylation or other complex post-translational modifications, such as phosphorylation, acetylation or methylation, that are often key to the proper folding, stability, and activity of many proteins[13,24]. It is therefore not the organism of choice for this type of protein production[6,17]. Moreover, *E. coli* being a Gram-negative bacterium, the proteins must cross two membranes of the cell envelope, which complicates the secretion process[25].

Another valuable bacterial species is *Bacillus subtilis*[26]. It is the Gram-positive model bacterium[27], well-characterized as a host for rProt production[28]. It possesses many advantages: strong secretion capacity; GRAS status (Generally Recognized As Safe) by the American Food and Drug Administration (FDA), due to its non-toxigenic nature; grows rapidly and easily; and the ability to be cultivated using cost-effective culture media and standard aerobic conditions[28–30].

Similarly to *E. coli*, it can be genetically engineered with ease and possess a high growth rate, which makes it a cost-effective host for large-scale protein production[26]. The main advantage of *B. subtilis* over *E. coli* is its efficient secretion machinery and the lack of the outer membrane, which allows for an extracellular production of rProts and greatly simplifies downstream processes[28,31].

In comparison with *E. coli*, *B. subtilis* offers advantages due to its Gram-positive nature, which simplifies protein secretion and purification processes[32]. Unlike *E. coli*, which mainly relies on plasmid-based expression systems, *B. subtilis* allows easier and more stable integration of recombinant genes

into its genome, improving genetic stability during protein production[33,34]. But even though *B. subtilis* can perform some post-translational modifications (phosphorylation, acetylation), it does not replicate the full complexity of mammalian modifications[26,27]. Moreover, it also possesses several disadvantages when used as a host for rProt production. Disulfide bond formation and isomerization are some of them[26].

Nevertheless, due to many advances in molecular biology, mutagenesis and genetic engineering, *B. subtilis* strains have been optimized to increase their level of rProt expression[35,36]. Besides, many other tools, such as plasmids, promoters optimization and signal peptides (SP), make it easier to genetically engineer *B. subtilis*, thus facilitating the expression and secretion of the desired proteins[37].

1.1.2.2. Yeasts

Yeasts are valuable hosts for rProt production, because they combine the advantages of microbial systems (easy genetic engineering) with eukaryotic features, such as secretory pathways and post-translational modifications[38]. Among the wide range of yeast species employed, *Saccharomyces cerevisiae*, *Pichia pastoris* and *Yarrowia lipolytica* will be addressed in this section.

S. cerevisiae is the most studied and widely used yeast host, including for heterologous protein production. This is due to the comprehensive knowledge regarding its genetics, biochemistry, metabolism, physiology and fermentation[16,39]. It can grow on inexpensive, cost-effective culture media and is easily scaled up for cultures[39]. In opposition to *E. coli*, *S. cerevisiae* can perform post-translational modifications typical of eukaryotic cells, such as glycosylation, phosphorylation and acetylation[39].

It also possesses a strong ability to both produce and metabolize ethanol and is tolerant to environmental stress, such as low oxygen levels[16]. However, ethanol production, known as the Crabtree effect (happening under aerobic conditions), can be a drawback for rProt production. Indeed, ethanol accumulation may compromise protein integrity[40]. Ethanol interacts with proteins, forming hydrogen bonds with hydrophilic residues, leading to protein denaturation and loss of function[41]. Moreover, even under high oxygen conditions, *S. cerevisiae* tends to favor ethanol production over biomass growth and rProt synthesis[40,42].

Some problems can also arise from its tendency to hyperglycosylate proteins, a process in which excessive or unusually long sugar chains are attached to proteins, which can affect secretion efficiency and alter immunogenic properties or biological functions of the target proteins[43]. It also displays mannose-rich glycosylation, that can potentially cause allergic reactions[6,16]. Another problem is the retention of expressed proteins within the periplasmic space, leading to some degradations, which complicates downstream processing and makes it difficult to purify the protein of interest[38].

P. pastoris is a methylotrophic yeast, which means it can use methanol as its carbon and energy source, when no repressing carbon source is present[16,39]. It possesses many benefits: a fast growth rate, ease of genetic engineering, and the ability to perform post-translational modifications (glycosylation, methylation, acetylation)[44]. Due to a growth based on respiration instead of fermentation, cultures are able to reach higher cell densities, as fermentation by-products like ethanol and acetic acid are not produced[44,45]. Unlike *S. cerevisiae*, which has a tendency to retain proteins in the periplasm, *P. pastoris* can secrete high molecular weight proteins, allowing for simpler purification and downstream processing[16,44]. It stands out amongst yeasts for its high efficiency in secreting rProts[6]. It also has a lower tendency for hyper-mannosylation compared to *S. cerevisiae*[16].

However, using methanol as an inducer for rProt synthesis can bring some drawbacks, like cell lysis and proteolysis, intense heat generation and risk of explosion[45]. This is a drawback of the AOX1 (alcohol oxidase 1) promoter, even though it is a strong, strictly regulated and widely used promoter from *P. pastoris* for rProt synthesis[16,45].

Similarly to *P. pastoris*, *Yarrowia lipolytica* is a non-conventional yeast, which has now become a popular organism for rProts production. This is due to several strengths it possesses, because of its unique cellular machinery and metabolic pathways. Similarly to complex eukaryotic systems, proteins secretion can take place via the co-translational translocation pathway (see below), unlike *S. cerevisiae*[16,46]. This allows proper folding and modifications of certain rProts. Sugars are also not fermented since *Y. lipolytica* growth is based on respiration[16,38]. This is beneficial because it prevents the formation of inhibitory products, such as ethanol, therefore allowing for cultures with higher cell density. Moreover, it is considered a GRAS organism for several industrial and pharmaceutical applications, it can efficiently produce large quantities of proteins with high molecular weight[16,47]. It also presents less hyperglycosylation than *S. cerevisiae*[47] and is able to grow on hydrocarbons (paraffin or different oils) as carbon sources[48,49]. These features make *Y. lipolytica* an organism of choice and an interesting alternative to more established hosts like *P. pastoris*[50,51].

Even though *Y. lipolytica* displays many advantages, it also presents hyper-mannosylation, as *S. cerevisiae*, even though the problem is to a lesser extent. Development and research have already been carried out to improve this drawback, and humanize the glycosylation pathway[16]. Another limitation is the presence of intracellular proteases, which can degrade heterologous proteins before their secretion. These proteases act internally, reducing yield and stability of the rProt[52].

Since this work specifically focuses on *Y. lipolytica* as a host for rProt production, a subsequent section will be dedicated to its expression system (see section 1.2).

1.1.2.3. Filamentous fungi

Filamentous fungi, also called molds, are well known as efficient hosts for the production and secretion of both homologous and heterologous proteins, making them useful for industrial purposes[19]. Even though their first uses concerned the production of primary metabolites[53], they are now used for heterologous protein production as well. This is due to their inherent capacities: high levels of protein secretion (as well as other molecules like metabolites, organic acids or antibiotics), high growth rate and the ability to achieve high biomass densities on cost-effective substrates[53,54]. They are also able to perform post-translational modifications, such as glycosylation[6].

These microorganisms include *Aspergillus*, *Trichoderma* and *Penicillium*. They are characterized by particular filamentous structures, also called hyphae, which are typically around 2-8 µm in diameter. Higher fungi, such as *Aspergillus*, *Penicillium* and *Trichoderma*, possess cross-walls (septa), while lower fungi (*Rhizopus* or *Mucor*) lack them[53]. Fungal cultures can have many morphologies: from mycelia suspension to packed hyphal aggregates, these different structures playing a role in growth rate and physiology of the cells[54].

Aspergillus niger is one of the most used fungal species in the context of rProt production[54]. Through genetic engineering, these fungal hosts have progressed from low production rates to impressive protein secretions. For example, in the case of glucoamylase, *A. niger* is now producing around 25 g/L[55], while initially secreting around 0.5 g/L[54]. Another example is *Trichoderma reesei*, reaching a

production of 30 g/L of cellulases[54]. Considering GRAS species, *A. niger* and *A. oryzae* are both considered GRAS by the US FDA[39].

Even though filamentous fungi are advantageous hosts, they possess some drawbacks. The production of heterologous proteins can be negatively impacted by fungal intracellular proteases, which happens to be a common problem[53]. For example, *A. nidulans* possesses around eighty protease genes[56]. Another disadvantage is that, even though they can perform glycosylation patterns on proteins, these patterns can differ significantly from those from mammals. As a result, filamentous fungi may not be the most appropriate hosts for recombinant human glycoproteins, when intended for therapeutic purposes. They could induce some immunogenicity problems[53]. However, *T. reesei* has demonstrated the ability to perform glycosylation patterns similar to mammalian ones[6].

Different strategies have been used to improve the production, both in yeasts and filamentous fungi, and with bacteria in some cases: using strong and homologous promoters, creating gene fusions with genes from well-secreted proteins, increasing the number of gene copies and using strains that lack proteases[6]. Foreign genes can be integrated into the chromosomes using plasmids, often as multiple copies integration, allowing a stable expression over time[6]. Secretion of proteins out of the cells also presents many benefits. Indeed, it minimizes the risk of degradation by intracellular proteases and simplifies downstream purification processes. It also helps to avoid potential feedback inhibition, which could happen within the production pathway, and is beneficial when the protein is toxic for the host organism[54]. Overexpression of folding enzymes and chaperones within the cell has also been explored, to improve folding and secretion efficiency[53].

1.2. *Yarrowia lipolytica* expression and secretion system

1.2.1. The secretory pathway

The secretory pathway of *Y. lipolytica* follows the eukaryotic pattern (see Figure 2), including the following steps: translational translocation into the endoplasmic reticulum (ER), folding of the proteins and quality control in the ER, trafficking through the Golgi apparatus, and final export through secretory vesicles to the extracellular environment[57–59].

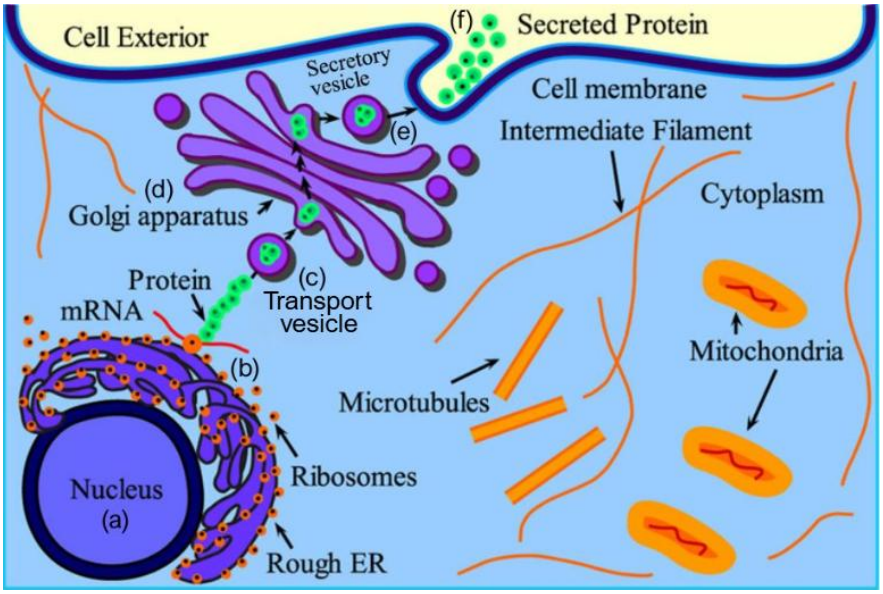

Figure 2: Schematic overview of the eukaryotic secretory pathway of proteins. *(a) Inside the nucleus, DNA is transcribed into mRNA (messenger RNA), which is itself exported to the cytoplasm via nuclear pores. (b) Ribosomes on the Rough Endoplasmic Reticulum (Rough ER) use the mRNA to synthetize proteins, which are then folded and undergo modifications in the Rough ER. (c) Proteins are packaged into transport vesicles and move to the Golgi apparatus. (d) In the Golgi apparatus, proteins are further modified, sorted and packaged into secretory vesicles. (e) Secretory vesicles carry the proteins from the Golgi apparatus to the cell membrane. (f) Vesicles fuse with the cell membrane and the proteins are released into the cell exterior. Adapted from Ehsan et al., 2018.*

At the heart of this pathway, protein targeting relies on N-terminal signal peptides (SPs), which act as molecular "addresses", guiding ribosomes to translocate nascent polypeptides into the ER and initiating entry into the secretory pathway. This early decision is crucial: without a proper SP, even abundant mRNA cannot result in high secretion levels, as the protein remains in the cytosol instead of being routed through the secretory machinery[58,60]. Their role will be discussed in more detail in section 1.2.2.

In *Y. lipolytica*, proteins are translocated into the ER more efficiently than in *S. cerevisiae*. This advantage contributes to Y. lipolytica superior protein secretion capacity, compared to conventional yeast hosts[58]. Naturally, *Y. lipolytica* is able to secrete large quantities (up to 1-2 g/L) of endogenous proteins, such as Lip2 lipase or alkaline extracellular protease (AEP)[61]. These properties can be extended to rProt via diverse engineering strategies. SPs from these two endogenous, highly secreted proteins are frequently harnessed in engineering strategies to maximize secretion of rProt[57]. These SPs have evolved for efficiency, reflecting the organism's adaptation to protein- and lipid-rich environments[61]. Its ability to secrete high quantities of enzymes has been harnessed to develop genetic and molecular tools, dedicated to the expression and secretion of heterologous proteins[57,62].

Y. lipolytica's secretory pathway also possesses features similar to those of filamentous fungi. Indeed, its dimorphic growth (yeast or filamentous form), greater adaptive membrane remodeling and vesicular transport capabilities are characteristics not found in classical yeasts[63].

However, stress conditions, such as oxygen limitation, can significantly limit secretory capacity. High oxygen uptake supports robust vesicle trafficking and higher protein secretion, highlighting the importance of bioprocess optimization as well as genetic modifications[64].

1.2.2. Mechanism and engineering of signal sequences

The efficiency of protein secretion in *Y. lipolytica* depends heavily on the architecture of these SPs, also called pre-regions. Classic eukaryotic signal peptides comprise an N-terminal, hydrophilic region (n-region), a central hydrophobic segment (h-region) and a C-terminal region (c-region), containing the cleavage site recognized by signal recognition particle (SRP) receptors on the surface of the ER[58,65,66]. SPs enable the ribosome, as soon as translation begins, to interact with the SRP. The SRP directs the ribosome-nascent chain complex to the ER membrane and mediates translocation into the ER lumen, where protein folding and quality control occur[60]. This early recognition allows the cell to distinguish secreted from cytosolic proteins immediately during translation[60]. The SP is then cleaved by signal peptidase within the ER and, in most cases, only proteins with properly cleaved SPs proceed along the secretory pathway[58,60]. The journey continues as the protein is folded and glycosylated in the ER, then packaged into vesicles for transport to and through the Golgi apparatus[58].

Beyond the SP, many secreted proteins, such as Lip2 and AEP (from the XPR2 gene), feature a pro-region, which acts as an intramolecular chaperone. This pro-region, or propeptide, can influence proper folding, maturation and secretion of the nascent protein[57]. It is then proteolytically removed by endoproteases found in the Golgi apparatus, such as XPR6 in *Y. lipolytica*[58,63]. In the case of proteases like AEP, the enzyme remains inactive while the pro-region is attached. Only after cleavage of the pro-region in the Golgi apparatus does the protease become active and able to function after secretion[67]. Similarly, in the case of LIP2, the pro-region has been shown to enhance secretion efficiency and folding of rProts, including heterologous lipases[58,63].

Empirical studies in *Y. lipolytica* have demonstrated that both the choice and engineering of signal peptides can modulate secretion rates by several-fold. For example, the widely used *LIP2* pre-pro (pre- and pro-region) signal and hybrid SP6 sequences have shown great performance compared to wild-type signal sequences, with increased secretion yields of some model proteins[65,68]. Computational analyses and screening of endogenous and synthetic signal peptides have identified features associated with efficient secretion, making it easier to design synthetic signal peptides[58]. These features include the hydrophobicity of the h-region, promoting stable insertion into the ER membrane; the presence of positively charged residues in the n-region, facilitating SRP recognition and ER targeting; and small amino acids near the cleavage site, that facilitate efficient signal peptidase recognition[58,69,70]. Empirical screening of both endogenous and novel synthetic signal peptides in *Y. lipolytica* has shown that some sequences, including SP3, SP4, SP6 and SP8 (which were selected for experimental evaluation in this work), can significantly enhance secretion yields for various heterologous proteins[58]. SP3 comes from a protease, SP4 from a glycosidase, SP6 from *Y. lipolytica* native *LIP2* lipase and SP8 from the native SoAmy amylase[58].

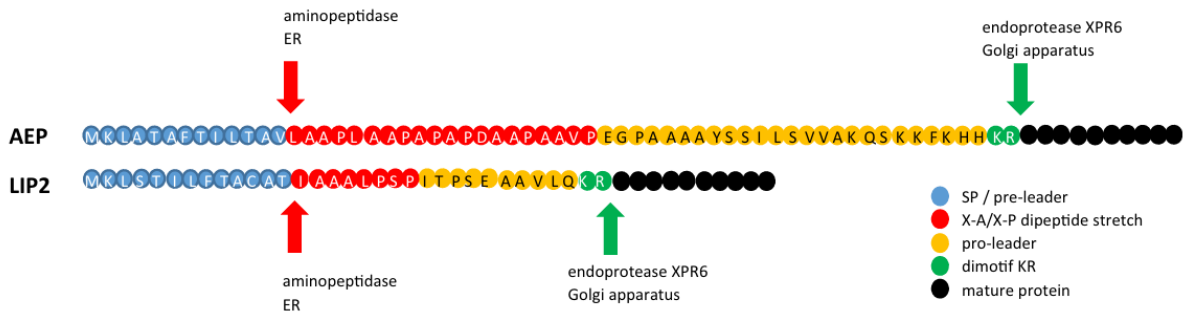

Figure 3: Map of the signal peptides of AEP and LIP2 proteins. *AEP and LIP2 are important proteins of Yarrowia lipolytica. Blue = pre-region/sequence signal, red = XA/XP dipeptide stretch, yellow = pro-region, green = dimotif*

KR, black = sequence of the mature protein. The different arrows highlight the sites recognized by specific aminopeptidase from the ER (in red) or by the endoproteases XPR6 in the Golgi apparatus (in green). From Celińska et al., 2018.

LIP-2 derived signal peptides, as well as AEP-derived signal peptides, which are commonly used as well, have displayed higher secretion levels than the native signal peptide[58]. As shown in Figure 3, the AEP and *LIP2* signal leader sequence contains a signal peptide, a stretch of XP (X-Ala or X-Pro) dipeptides susceptible to cleavage, and an extensive pro-region with glycosylation sites[58,71]. The XP dipeptide stretch (were X is any amino acid and P is proline or alanine), found just after the SP in AEP and Lip2, is specifically cleaved by ER aminopeptidases and aids efficient removal of the pro-region, ensuring proper maturation and secretion of the final protein[61,66].

By engineering this modular arrangement (e.g. optimizing XP motifs and pro-region lengths), secretion can be improved for various rProts[71,72]. While the pro-region is not necessary for heterologous protein secretion, the pre-region is a necessity for most proteins' secretion[58]. But even though it is not necessary, constructs lacking the pro-region often experience reduced stability or less efficient secretion, highlighting its role in maintaining protein integrity during transit through the whole secretory pathway[61].

It must be considered that the optimization of signal sequences is protein-specific; the optimal pre-/pro-region may differ for different heterologous proteins[58].

1.2.3. Molecular tools and engineering

With the development of many molecular tools, the engineering of *Y. lipolytica* for rProt production has improved significantly.

First of all, expression levels are highly influenced by the choice of the promoter controlling the recombinant gene. Through promoter engineering, the transcriptional output can be maximized. To do so, strong, inducible, or constitutive promoters, like p*TEF*, pPOX2 or pXPR2, can be used[61,65,68]. This allows the production of high levels of rProt, tailored to the expression conditions and the host. Among these, p*TEF* (from the gene encoding the translational elongation factor 1α) is one of the strongest and most widely used constitutive promoters in *Y. lipolytica*[73,74]. It drives continuous, high-level gene expression regardless of growth phase or nutrient availability, making it particularly suitable for consistent rProt production[73]. Its strength, robustness and reliable activity across diverse culture conditions explain its broad application in both industrial and research settings with *Y. lipolytica*[73,74].

In addition, the use of excisable selection markers (auxotrophic or antibiotic resistance markers) and precise chromosomal integration simplifies genetic engineering for stable strain construction, as it avoids plasmid loss and eliminates the need for continuous selection[75]. These strategies enable the insertion of multiple gene copies[68,76]. Multicopy integration usually correlates with high protein output, as it involves inserting several copies of the same expression cassette into the genome, therefore increasing the amount of mRNA available for translation[47]. However, this must be balanced against metabolic burden and potential impact on cell fitness, such as reduced growth[68].

Vectors for heterologous expression often carry *URA3* (uracil) or LEU2 (leucine) markers for selection and allow easy recovery of auxotrophic strains[70]. The selection of host strains with deletions of protease-encoding genes prevents degradation of secreted rProts, allowing increased accumulation in the culture medium[77].

As discussed before, another useful tool is the engineering of signal peptides. By modifying or selecting efficient pre- and pro-regions, secretion rates and protein stability can be boosted[65,69]. Expression yields also benefit from the use of hybrid secretion signals, as these often outperform native signal sequences[58].

Innovative strategies integrating these different approaches have led to significant improvements in production levels of rProt, often exceeding those achieved in other yeast systems[78,79].

1.3. Golden Gate Assembly

1.3.1. Introduction to Golden Gate cloning

The ability to assemble multiple DNA fragments in an accurate and efficient way is an important part of molecular and synthetic biology. Traditional cloning methods include, for example, restriction enzyme digestion followed by ligation, or PCR (Polymerase Chain Reaction)-based assembly. However, these methods often require multiple steps and can introduce unwanted sequences, called "scars", at the junctions between DNA fragments. These limitations have allowed for the development of improved cloning techniques, that enable rapid, precise and scarless assembly of complex DNA constructs[80].

Golden Gate Assembly (GGA) is a revolutionary advancement in molecular cloning, enabling seamless and efficient assemblies of multiple DNA fragments in a single, one-pot reaction[80]. It was originally developed in the early 2000s and now holds an important place in synthetic biology, genetic engineering and biotechnology. This is mainly due to its precision, speed and modularity[81,82].

1.3.2. Principle and mechanism

Golden Gate Assembly is based on the use of type IIS restriction endonucleases, such as *Bsa*I or BsmBI. Unlike conventional restriction enzymes, which cut within their recognition sequences, type IIS enzymes cleave DNA at a defined distance from their recognition sites[83]. This property allows the design of DNA fragments with custom overhangs (short, single-stranded DNA sequences at the end of a fragment) that will dictate the order and orientation in which the different fragments will be ligated[81,84].

In practice, as shown in Figure 4, DNA fragments flanked by type IIS recognition sites are mixed in a single tube with a destination vector, a type IIS enzyme and a DNA ligase. The reaction proceeds through alternating phases of digestion (with the type IIS enzyme) and ligation (with the DNA ligase). During the ligation phase, DNA ligase covalently joins the fragments, previously cleaved with matching overhangs by the type IIS restriction enzyme. The recognition sites of the enzyme are removed during cleavage, which results in a scarless junction between the fragments[80,82].

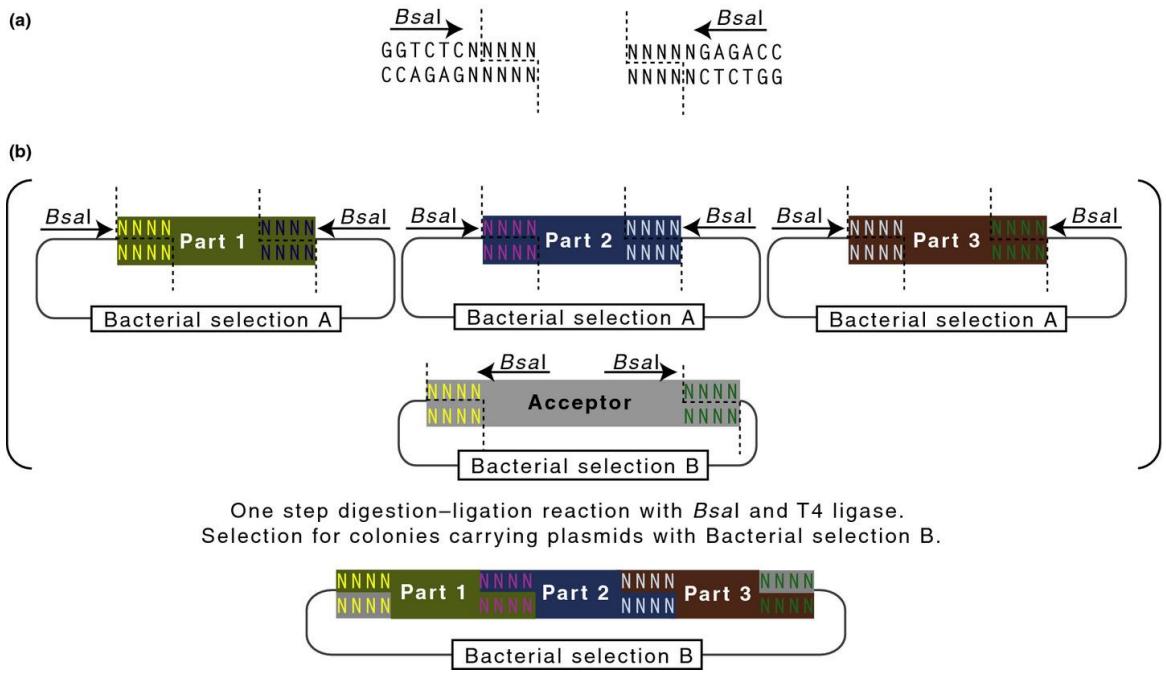

Figure 4: Schematic overview of Golden Gate Assembly using type IIS restriction enzymes. *(a) Recognition and cleavage sites of the type IIS restriction enzyme BsaI, cutting outside of its recognition sequence (GGTCTC) and generating custom overhangs. (b) Individual DNA sequences flanked by BsaI sites are left with compatible overhangs after digestion. An acceptor plasmid with marker B is used to assemble the different sequences in a single digestion-ligation reaction. The result is a final construct carrying the different sequences in a determined order, selectable via marker B. From Patron et al., 2015.*

1.3.3. Advantages over traditional cloning methods

Golden Gate Assembly offers several advantages compared to traditional cloning techniques, such as restriction enzyme cloning or Gibson Assembly.

Traditional restriction enzyme cloning uses enzymes that cut DNA at specific sequences to create compatible ends for ligation. While reliable, it requires suitable restriction sites in both vector and insert, can introduce unwanted "scar" sequences, and assembling multiple fragments is time-consuming because it involves multiple sequential cloning steps[80,85]. In contrast, GGA employs type IIS enzymes that cleave outside their recognition sites, enabling scarless and simultaneous assembly of multiple fragments in a single reaction. This allows greater fidelity and modularity, making it a more efficient and versatile alternative[82,86].

Gibson Assembly is a molecular cloning technique that enables the seamless joining of multiple DNA fragments in a single, isothermal reaction. It relies on three enzymatic activities: an exonuclease that creates complementary single-stranded overhangs at the end of DNA fragments, a DNA polymerase that fills in gaps after fragment annealing, and a DNA ligase that seals the nicks (small breaks in one strand of the DNA) to produce a double-stranded molecule[87,88]. Because the reaction does not depend on restriction enzyme recognition sites, it allows scarless assembly of fragments in any desired sequence order[88,89].

In contrast to Gibson Assembly, Golden Gate relies on type IIS restriction enzymes to create custom overhangs, enabling high fidelity and specificity by ensuring all fragments ligate in the desired order and orientation[82]. Additionally, Golden Gate's use of standardized overhangs and cloning parts makes

it a highly modular system, allowing the creation of organism-specific libraries and facilitating the reuse and combination of sequences, an important feature in synthetic biology[83].

1.3.4. Golden Gate Assembly dedicated to *Y. lipolytica*

The adaptation of Golden Gate Assembly to *Y. lipolytica* has facilitated its genetic engineering, supporting its development as a useful host in biotechnology. Several modular Golden Gate toolkits have been recently developed and optimized for *Y. lipolytica*, enabling a more efficient and adaptable construction of complex genetic pathways[90,91].

An important advance has been the creation of standardized libraries of DNA "biobricks", modular and interchangeable DNA segments flanked by standardized overhang sequences[90,92]. Each biobrick corresponds to a functional genetic element, such as a promoter, gene, terminator, or selection marker, which can all be combined in multiple configurations to create complete transcription units (TUs)[92]. As shown in Figure 5, these biobricks are stored in donor vectors, each flanked by recognition sites for the type IIS restriction enzyme *Bsa*I[81,90]. The cutting pattern of *Bsa*I generates specific 4-nucleotide overhangs (annotated A to M in panel B) that dictate the assembly order[80,90]. For example, the overhang labeled B at the end of the InsUp element is designed to perfectly match the complementary overhang B at the start of the marker M, ensuring correct and directional ligation between these two during the assembly[90]. The fixed flanking sequences enable the rapid and scarless ligation of multiple parts in a single reaction, while the variable internal regions encode the functional diversity (different promoters, genes, or terminators)[90,92].

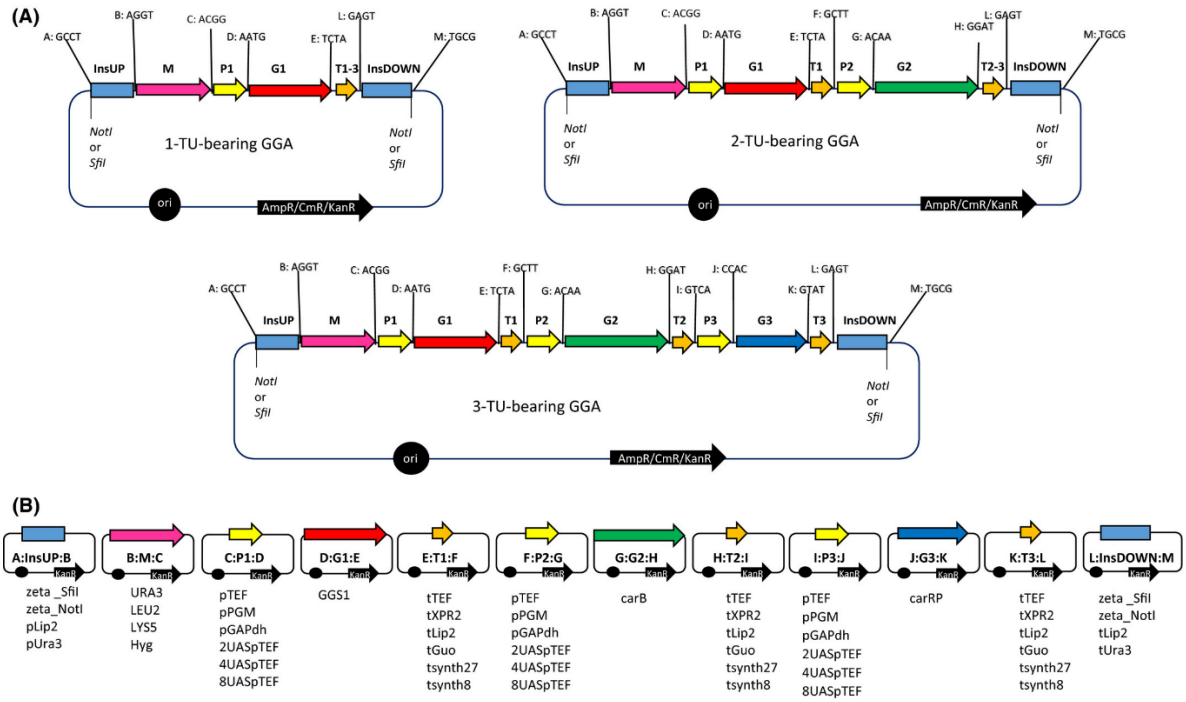

Figure 5: Modular Golden Gate Assembly (GGA) dedicated to Yarrowia lipolytica. *(A) Schematic representation of 1, 2 and 3 transcription unit (TU)-bearing plasmids assembled via Golden Gate Assembly. Each TU contains a promoter (P), a gene (G) and a terminator (T). The GGA contains the different TUs, as well as upstream and downstream insertion sites (InsUP and InsDOWN), a marker (M) and a bacterial resistance marker (ampicillin (A), chloramphenicol (C) or kanamycin (K)). (B) Library of donor vectors (with kanamycin resistance) containing Golden Gate Fragments (GGFs) used for Y. lipolytica, each fragment flanked with BsaI recognition sites. The letters flanking the different vectors (from A to M) correspond to the 4-nucleotides overhang which match those of the adjacent GGF. From Celińska et al., 2017.*

These toolkits allow for easier assembly of multiple transcription units in a single reaction, which accelerates the process of designing and testing new metabolic pathways[90,92]. These systems have been used to assemble and integrate entire biosynthetic pathways directly into *Y. lipolytica* genome, such as the one for violacein production[92]. This has allowed an easier optimization of gene expression, by combining diverse promoters, terminators and genes, which considerably accelerates the screening for optimal production assemblies[92,93]. Moreover, optimized protocols now allow for the integration of up to 13 fragments in a GGA reaction[92,94].

An important feature of these toolkits is their compatibility with different genomic integration strategies. By default, integration can be random, for example using Zeta integration sites[95]. Zeta elements are repeated DNA sequences found at many locations in the *Y. lipolytica* genome. When a construct flanked by Zeta sequences is transformed into *Y. lipolytica*, homologous recombination occurs at one of these multiple loci, leading to random insertion. While this often results in high transformation efficiency, it can also cause variability in gene expression due to differences in the transcriptional activity of the integration site, as well as the occurrence of multiple integration events[92].

In contrast, targeted integration can be achieved by flanking the GGA construct with sequences homologous to a chosen locus in *Y. lipolytica*'s genome, such as the Lip2 locus[96]. Because the genome is relatively large (20 Mb (megabases[97])), directed integration to a well-characterized locus ensures that the Golden Gate construct is inserted at a defined position, avoiding unpredictable insertions into non-coding regions[92]. In this strategy, homologous sequences corresponding to the *LIP2* gene are included in the construct, guiding recombination precisely at this locus. Furthermore, if the targeted gene is normally expressed at high levels, its genomic region is often associated with a more open chromatin conformation, improving accessibility for transcription factors[98].

In this work, the GG reaction was performed with the following standardized parts: the strong constitutive promoter *TEF*, the tLIP2 terminator, a *URA3* selection marker, and *LIP2* homology arms (flanking sequences) for targeted genomic integration at the *LIP2* locus. All these parts were inserted into vector GGE029 (see Figure 6), containing an ampicillin resistance gene and the gene coding for the red fluorescent protein (RFP). The RFP gene is flanked by *Bsa*I recognition sites and is excised during assembly[91]. This allows checking for correct integration of the Golden Gate constructs: colored colonies indicate that the mRFP1 gene remains intact, whereas successful GGA excises the mRFP1 coding sequence and replaces it with the insert, resulting in white colonies[91].

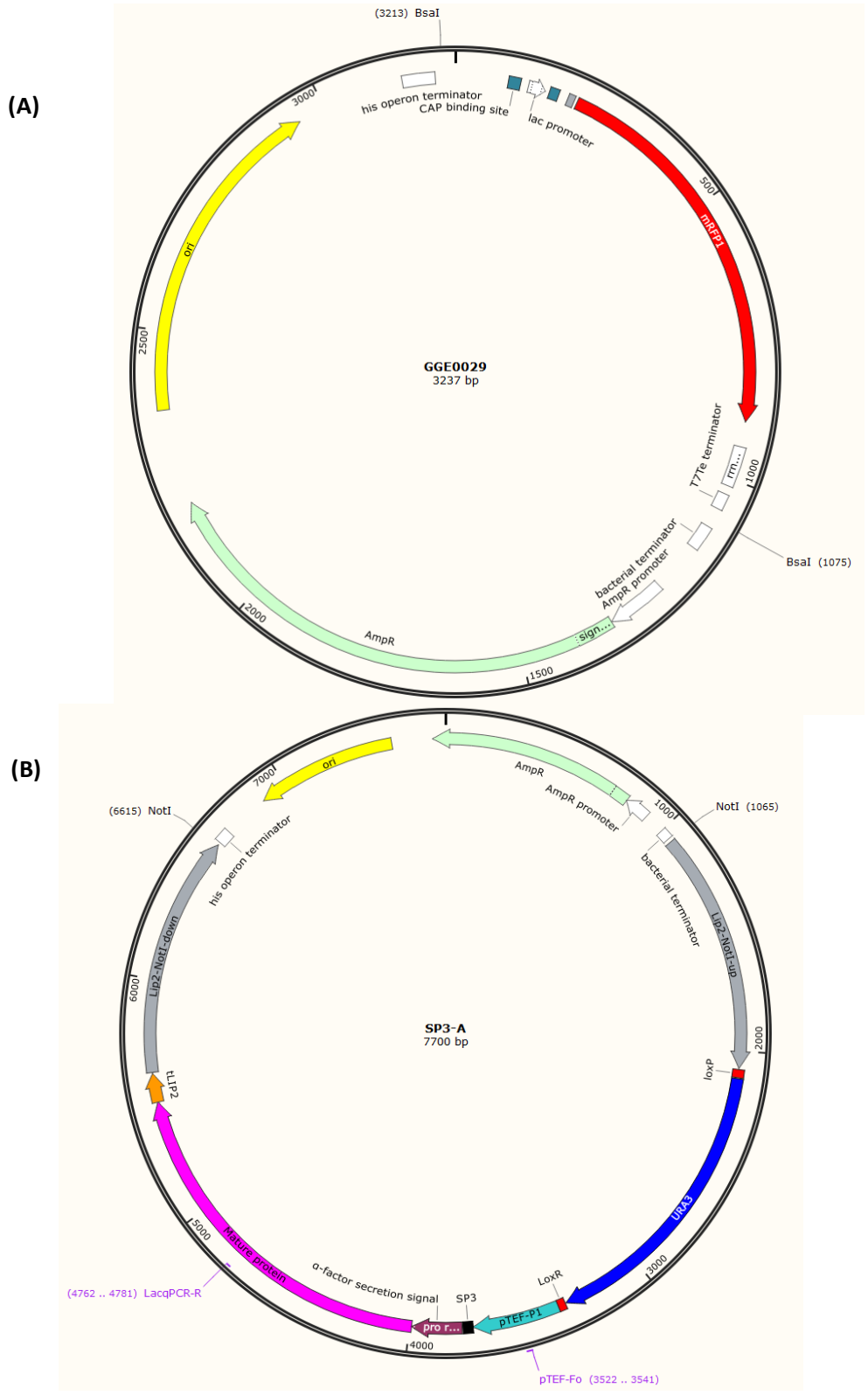

Figure 6: Golden Gate modular assembly strategy in Y. lipolytica. *(A) GGE029 vector, containing an ampicillin resistance gene. The BsaI recognition sites are visible. The mRFP1 gene codes for a colored protein, which results in the colonies growing red/pink. In contrast, the successful Golden Gate Assembly leads to the excision of the mRFP1 coding sequence and its replacement by the insert, resulting in white colonies. (B) SP3-A Golden Gate vector assembled from standardized biobricks including pTEF promoter, SP3, α-factor pro-region, the protein coding sequence (CDS), terminator tLIP2, URA3 selection marker and flanking integration sequences for LIP2 locus integration (Lip2-NotI-up/down). Maps constructed using SnapGene (v8.1).*

1.4. Laccase as a recombinant protein

1.4.1. Introduction to laccases

Laccases are multicopper oxidases widely distributed across bacteria, fungi, plants and even some insects. They are able to catalyze the oxidation of a broad range of compounds, both aromatic and non-aromatic. During the enzymatic reaction, molecular oxygen is used as an electron acceptor, and water is produced as a byproduct[99,100]. Structurally, a laccase monomer possesses four copper atoms, divided into three key sites: Type-1, Type-2 and Type-3 (see Figure 7)[100–102].

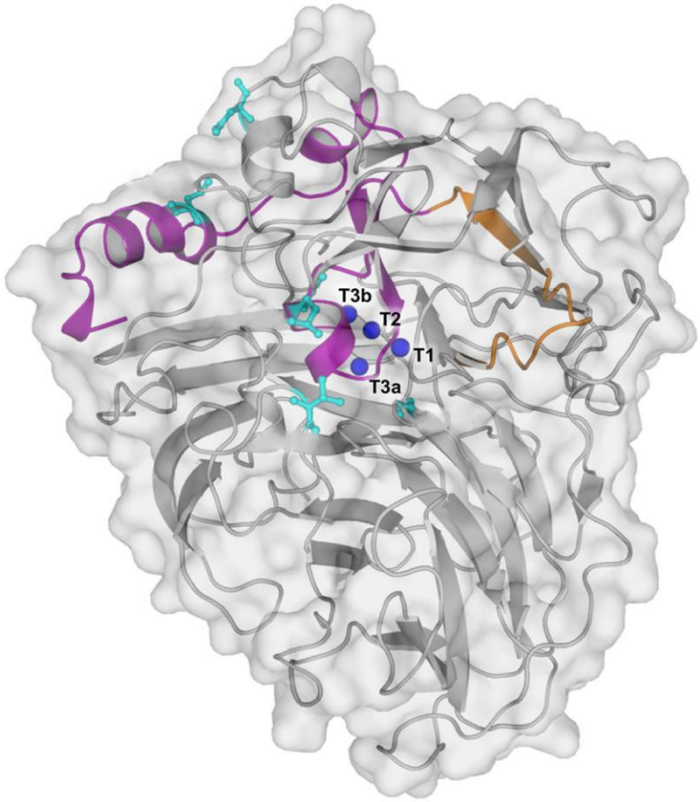

Figure 7: Map of the catalytic site of the Lac-Vader laccase. *The Lac Vader enzyme is the laccase that was produced and quantified during the experimentations. Copper atoms are visible as dark blue spheres. T1 = Type-1 copper site, which is primarily responsible for electron transfer. T2 = Type-2 copper site, T3a and T3b = Type-3 copper site, which contains two copper atoms. The Type-2 and Type-3 sites, which comprise a total of three copper atoms, constitute the trinuclear cluster. It enables the reduction of dioxygen to water. Adapted from Mateljak & Alcalde, 2021.*

The catalytic mechanism involves three steps: the oxidation of substrates at the Type-1 site, followed by an internal electron transfer to the trinuclear copper cluster, leading to the reduction of oxygen[100,101]. Due to this mechanism, laccases are versatile biocatalysts, able to oxidize a broad range of substrates. Their substrates of choice are phenolic compounds, but they are also able to oxidize other compounds[99].

Biologically, laccases play diverse roles. They participate in processes such as lignin degradation (for example in white-rot fungi), cuticle sclerotization in insects (contributing to exoskeleton formation), pigment formation or detoxification of phenolic compounds in plants[100,101]. They are frequently referenced as “green catalysts”, due to their use of oxygen and the eco-friendly nature of their byproducts[103].

1.4.2. Applications

Due to their broad substrate range and their mild reaction conditions, laccases are widely used for several industrial and environmental applications[99,104]. In the textile industry, they are used for the decolorization of dyes and the treatment of effluents[105]. They are also useful in the pulp and paper sector, including environmentally friendly bleaching and delignification processes. Indeed, they help to reduce the use of chlorine-based chemicals[106]. In the food and beverage industry, laccases are utilized to stabilize fruit juices and beers by removing phenolic compounds that could alter the color and taste of the products[105].

Laccases also present many applications in different environmental contexts, underscoring their importance as sustainable tools in green chemistry. They are valuable in environmental remediation, such as in the treatment of wastewater containing recalcitrant organic pollutants. These pollutants include compounds such as phenolic substances and synthetic dyes[103,107]. They are used as well in the context of bioremediation, to get rid of pesticides, herbicides, or certain explosive residues present in the soil[105]. Moreover, laccases' affinity for various phenolic compounds has been exploited to design biosensors, to monitor these molecules, notably in food[105]. They have also been used as sustainable catalysts in organic syntheses and in the design of biofuel cells[108].

1.4.3. Heterologous production

Despite their potential, the natural production of laccases is often limited by low yields and challenges in purification. To address these limitations, heterologous expression systems have been developed. They enable high-level production, easier downstream processing and tailored engineering of the produced enzymes[109,110]. Different hosts have been explored: bacteria (e.g., *E. coli*), yeasts (e.g., *S. cerevisiae*, *P. pastoris* or *Y. lipolytica*) and fungi (*Aspergillus, Trichoderma*). As discussed in section 1.1.2, each organism presents different advantages and drawbacks regarding post-translational modifications, protein folding and secretion capacity[109,111].

Concerning *Y. lipolytica* in particular, even though yields can be lower than in some filamentous fungi, it offers high transformation efficiencies and robust protein secretion mechanisms. It also allows for detailed genetic modifications, which are useful for industrial production and engineering of laccases[112]. Optimization strategies, including the choice of secretion signals, culture media, or the regulation of the host physiology, have contributed to increase laccase yields[112].

2. OBJECTIVES

The main objective of this master thesis is to maximize the production of a recombinant laccase enzyme, used as a model protein, by evaluating different secretion signal sequences and pro-regions in the yeast *Y. lipolytica*. For that purpose, a set of constructs was designed and subsequently assembled using the Golden Gate Assembly method. These constructs differ in their pre- and/or pro-sequences, while the coding sequence of the mature laccase remains identical across all assemblies. This design enables a direct comparison of the influence of secretion signals and pro-regions on extracellular laccase activity.

The choice of secretion signals is based on previously characterized elements from *Y. lipolytica*, synthetic or hybrid sequences, combined with or without pro-regions such as α-pro or XP-LIP2 pro. The objective was then to cultivate the transformed *Y. lipolytica* strains under controlled conditions and quantify their extracellular laccase activity. The reference strain was *P. pastoris*, containing the Lac Vader laccase construct. This construct combined the protein coding sequence with the α-factor secretion signal and pro-region from *S. cerevisiae*.

This project therefore aims to identify the most effective signal peptides and/or pro-regions combinations for secretion in *Y. lipolytica*, and to assess the potential of this host as an alternative expression platform.

3. MATERIAL AND METHODS

3.1. Media preparation

Several culture media were prepared and used throughout this work for bacterial and yeast growth, transformation, and protein production. The compositions of the different media are detailed below.

SOC (Super Optimal broth with Catabolite repression) medium was composed as follows: tryptone 20 g/L, yeast extract 5 g/L, glucose 3.6 g/L, $MgSO_4$ 1.2 g/L, $MgCl_2$ 0.97 g/L, NaCl 0.58 g/L, KCl 0.2 g/L, pH = 7.0.

LB(A) medium (Lysogeny Broth (Agar)) was used for selection plates, supplemented with either ampicillin (100 µg/mL) or kanamycin (50 µg/mL), depending on the plasmid. The LB base medium contained: casein tryptone 10g/L, yeast extract 5 g/L, and NaCl 10g/L.

YNB (Yeast Nitrogen Base) minimal medium with casamino acids was composed of: YNB (without NH_4 sulfate and amino acids) 1.7 g/L, glucose 20 g/L, NH_4Cl 5 g/L, $Na_3(PO_4)_2$ buffer (pH 6.8) 50 mM and casamino acids 2 g/L. YNB-C medium was prepared by adding 0.1 mM $CuSO_4$.

YPD (Yeast Peptone Dextrose) contained glucose 20 g/L, casein peptone 20 g/L and yeast extract 10 g/L.

BM-X medium was composed of 175 mL of water, 50 mL of 1 M PO_4 (pH 6.8) buffer, and 25 mL of YNB (17 g/L). BMM2 medium was obtained by mixing 9.9 mL of BM-X with 100 µL of methanol (MeOH), while BMM10 consisted of 9.5 mL of BM-X and 500 µL of MeOH.

For solid medium, 15 g/L of agar was added. All mediums were sterilized by autoclaving, except antibiotic solutions, casamino acids and YNB, that were filtrated.

3.2. Construction of expression vectors

Plasmid Lac Vader containing the pre-region and the pro-region from the α-factor secretion signal, followed by the protein coding sequence (see Appendix 1

) was used as template for PCR. This plasmid, as well as the *P. pastoris* strain, were provided through a collaboration with Dr. Miguel Alcalde from the Consejo Superior de Investigaciones Científicas (CSIC), in Madrid.

To explore different combinations of pre- and/or pro-region with the protein sequence, several PCRs were performed using specific primers, designed to amplify the desired constructs.

The primer sequences are listed in Table 1. These primers were designed using SnapGene (v8.1), based on the Lac Vader sequence, and ordered from Eurogentec.

Table 1: Primers used in the design of the different constructs, from the Lac Vader complete original sequence. *Fw = forward primer, Rv = reverse primer.*

Primer's name	Sequence (5' – 3')	Characteristic
Lac01B (Fw)	GGGGGTCTCTAATGAGATTTCCTTCAATTTTTACTGATGTTTTATTCGC	Complete sequence (α pre-sequence, α pro-region + protein)
Lac02 (Rv)	CCCGGTCTCTTAGATCAGAGGTCGCTGGGGT	Reverse primer (annealing at the end of the protein's sequence)

Lac03 (Fw)	CTGTGACGGACTCAGGGGTCCG	Forward primer, used to remove the *Bsa*I site initially present in the middle of the protein sequence
Lac04 (Rv)	CGGACCCCTGAGTCCGTCACAG	Reverse primer, used to remove the *Bsa*I site initially present in the middle of the protein sequence
Lac05 (Fw)	GGGGGTCTCTTGCCGAATTCAGCATTGGGCCAGTCG	Mature protein (Contains only the protein's sequence)
Lac06 (Fw)	GGGGGTCTCTTGCCGCTCCAGTCAACACTACAACAGAAG	α pro-region + protein
Lac07 (Fw)	GGTCTCTTGCCCTCCCTTCCCCCATCACTCCTTCTGAGGCCGCAGTTCTCCAGAAGCGAGAATTCAGCATTGGGCCAGTCG	Addition of the XP-Pro LIP2 sequence + α pro-region + protein
p*TEF*-Fo (Fw)	GCGTAGGGTACTGCAGTCTG	Annealing on the p*TEF* promoter, used to check the Golden Gate Assembly constructs
LacqPCR-R (Rv)	GAAGGGCACGGATCCAGTAG	Annealing in the middle of the protein sequence, used to check the Golden Gate Assembly constructs

3.2.1. PCR amplification - Q5 High-Fidelity DNA polymerase

The Q5 High-Fidelity DNA polymerase (2000 U/mL, New England BioLabs) was used according to the manufacturer's protocol. The reaction components can be found in Table 2. The PCR conditions were as follows: initial denaturation at 98°C for 30s; 30 cycles of 98°C for 10s (denaturation), 65°C for 30s, and 72°C for 1 min (extension); followed by a final extension at 72°C for 2 min, and a final hold at 4°C. Reactions were performed using a Biometra T3000 Thermocycler.

After testing the conditions in 10 µL reactions, 50 µL PCRs were performed to obtain sufficient product for DNA extractions.

Table 2: Reaction components for Q5 High-Fidelity DNA polymerase. *dNTPs = deoxyribonucleoside triphosphates.*

	Volume of reagents (µL)	**Volume of reagents (µL)**
Q5 High-Fidelity DNA polymerase	0.1	0.5
dNTPs 10mM	0.25	1.25
Forward primer (10 mM)	0.6	3
Reverse primer (10 mM)	0.6	3
5x Q5 reaction buffer	2	10
Template DNA	1	5
Water (nuclease-free)	5.45	27.25
Total volume	**10 µL**	**50 µL**

3.2.2. PCR amplification - Phusion High-Fidelity DNA polymerase

Phusion High-Fidelity DNA polymerase (2 U/mL, Thermo Scientific) was carried out using the protocol provided by Thermo Scientific. Reactions were conducted using the same thermocycling conditions as those used with Q5 DNA polymerase, along with the determined annealing temperatures (Tm). The reaction components are listed in Table 3.

Table 3: Reaction components for Phusion High-Fidelity DNA polymerase. *dNTPs = deoxyribonucleoside triphosphates.*

	Volume of reagents (µL)	Volume of reagents (µL)
Phusion High-Fidelity DNA polymerase	0.1	0.5
dNTPs 10mM	0.2	1
Forward primer (10 mM)	0.6	3
Reverse primer (10 mM)	0.6	3
5x Phusion HF buffer	2	10
Template DNA	1	5
Water (nuclease-free)	5.5	27.5
Total volume	**10 µL**	**50 µL**

3.2.3. DreamTaq Green PCR

This PCR was performed using the DreamTaq Green PCR Master Mix (2X) (Thermo Scientific), following the manufacturer's instructions. To realize PCRs on colonies, a dot of cells was collected and added directly to the PCR mix.

The same PCR method was also applied to extracted plasmid DNA, in addition to colony screening, to further confirm correct fragment integration. Table 4 shows the reagent volumes used depending on the type of PCR.

Table 4: Reaction components for DreamTaq Green PCR on colonies and on extracted plasmids.

	PCR on colonies volumes of reagents (µL)	PCR on extracted plasmids volumes of reagents (µL)
DreamTaq Green PCR Master Mix (2X)	5	7.5
Forward primer (10 mM)	0.7	1
Reverse primer (10 mM)	0.7	1
Template DNA	-	1
Water (nuclease-free)	3.6	4.5
Total volume	**10 µL**	**15 µL**

The thermocycling conditions for this PCR were as follows: initial denaturation at 95°C for 3 min; followed by 30 cycles of 95°C for 30s (denaturation), 58°C for 30s (annealing) and 72°C for 1 min (extension); with a final extension at 72°C for 5 min, and final hold at 4°C. PCRs were performed on a Biometra T3000 Thermocycler.

3.2.4. Agarose gel electrophoresis

To visualize PCR amplification, agarose gel electrophoresis was performed using Tris-acetate-EDTA (TAE) Electrophoresis Buffer (Thermo Scientific; 20 mM Tris, 10 mM acetic acid, 0.5 mM EDTA). Gels were prepared with 0.8% (w/v) of agarose (Nippon Genetics) in TAE buffer and microwaving until the agarose was completely melted. After cooling slightly, 5 µL of Midori Green Advance DNA Stain (Nippon Genetics) was added to the solution before it was poured into a gel mold. Once solidified, the gel was placed in an electrophoresis tank filled with TAE buffer.

PCR samples were mixed with Gel Loading Dye Purple (New England BioLabs): 3 µL of dye for 10 µL of reaction volume or 10 µL of dye for 50 µL of reaction volume. The mixtures were then loaded into the wells of the gel, with the well size adapted to the sample volume. For PCRs performed using DreamTaq Green PCR Master Mix (see section 3.2.3.), no loading dye was added, as it is already included in the master mix.

To estimate DNA fragment size, 5 µL of FastGene 1 kb DNA ladder (Nippon Genetics) was loaded into the first well. Electrophoresis was carried out using the Bio-Rad PowerPac Basic system, applying a voltage of 120 Volts. DNA migration proceeded for 20 to 30 min, depending on the dye front progression. After migration, the gel was visualized under UV (ultraviolet) light (320nm) using a Pullnix system (VWR GenoView & GenoSmart).

3.2.5. DNA purification from gels

The NucleoSpin Gel and PCR Clean-up kit (Macherey-Nagel) was used for DNA extraction from agarose gel following electrophoresis. After visualization under UV light, the desired DNA band was excised from the gel using a scalpel on a UV transilluminator table (New Brunswick Scientific). The manufacturer's protocol for "DNA extraction from agarose gel" was followed to perform the extraction. Elution was performed using 15 µL of elution buffer.

DNA concentrations were measured using a Nanodrop 2000 spectrophotometer (Thermo Scientific).

3.2.6. TOPO cloning of DNA fragments

For all DNA fragments obtained by gel extraction, cloning into a TOPO vector was performed. The Zero Blunt TOPO PCR Cloning Kit (Invitrogen, Thermo Fisher Scientific) was used for this purpose. The cloning reaction was carried out following the manufacturer's instructions. As visible in Figure 8, the vector possesses a kanamycin resistance marker; therefore, kanamycin was used for selection of all sequences cloned into TOPO cloning vectors.

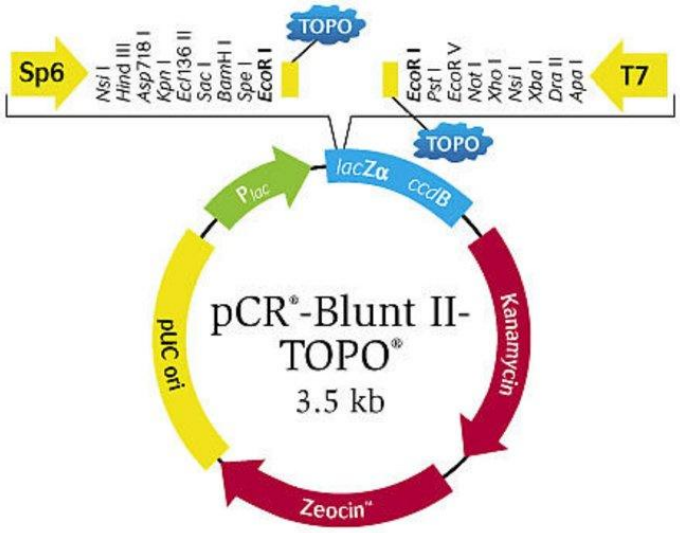

Figure 8: Map of the pCR-Blunt II-TOPO vector. *From Thermo Fisher Scientific (Zero Blunt™ TOPO™ PCR Cloning Kit, without competent cells).*

For the incubation step, after mixing the reagents, the solution was left at room temperature overnight, prior to transformation into *E. coli* the following day (see section 3.2.7.).

3.2.7. Transformation into *E. coli*

To perform the transformation, DH10B chemically competent *E. coli* cells were used. The cells were thawed on ice and gently mixed. Then, 1-5 µL of plasmid DNA (containing between 1 pg and 100 ng) was added to the cells. The tubes were gently flicked to mix the DNA and cells, then placed on ice for 30 min. A heat shock at 42°C for 1 min was applied, followed by an additional 5-min incubation on ice.

Afterward, 950 µL of room-temperature SOC medium was added, and the mixture was incubated at 37°C for one hour with shaking. LBA plates with adequate antibiotic (depending on the plasmid integrated) were used for plating.

For each transformation, cell suspension was spread on petri dishes: two plates with 200 µL, two with 100 µL and two with 50 µL of the cell suspension. The plates were incubated overnight at 37°C. After incubation, approximately 20 transformant colonies per transformation were selected and streaked onto fresh selection plates, then incubated again overnight at 37°C.

Finally, colony PCR was performed on 5 colonies to confirm the presence of the plasmid insert (see section 3.2.3.).

3.2.8. Plasmid purification

To perform the extractions, the NucleoSpin Plasmid EasyPure kit (Macherey-Nagel) was used, following the manufacturer's instructions. The day prior to extraction, liquid cultures were realized in LB medium supplemented with the appropriate antibiotic.

The cultures were incubated overnight at 37°C with shaking. After incubation, plasmid extraction was performed. Cells were pelleted by centrifugation for 2 min at 10 000 rpm using an Eppendorf MiniSpin Plus centrifuge, and the supernatant was discarded. The remaining steps followed the standard protocol provided with the kit, except for the elution, which was carried out using 30 µL of elution volume instead of 50 µL.

DNA concentrations after extraction were measured using the Nanodrop 2000 spectrophotometer (Thermo Scientific).

3.3. Assembly and transformation in *Yarrowia lipolytica*

3.3.1. Golden Gate Assembly reactions

To perform the different Golden Gate Assemblies, it was necessary to obtain the various parts (promoter, terminator, upstream and downstream inserts, etc.) that have been cloned in TOPO cloning vectors (of the Golden Gate toolkits). These vectors are maintained in *E. coli* strains at -80°C. A loop of cells was taken from cryovials and introduced into a flask containing LB liquid medium supplemented with the appropriate antibiotic (kanamycin 50 µg/mL for all "parts" vectors; ampicillin 100 µg/mL for the backbone vector). After overnight incubation at 37°C with shaking, plasmids were extracted (see section 3.2.8.).

Based on plasmid concentrations and insert sizes, the volumes of each plasmid for the Golden Gate reactions were calculated to obtain equimolar amounts of each DNA fragment (2 nM). The size of the backbone vector was also considered in the calculations.

Except for the protein sequence and the signal peptide that varied between constructs, all other components were identical across assemblies. The shared components included: the upstream and downstream integration sequences (Lip2-NotI-Up and Lip2-NotI-Down) targeting the *LIP2* locus; the

URA3 selection marker, allowing yeast growth without uracil; the p*TEF*-P1 promoter; the tLIP2 terminator; and the backbone vector GGE029, which contains an ampicillin resistance gene.

To carry out the Golden Gate reactions, these DNA parts were combined. To this mixture, 3 µL of T4 DNA Ligase Reaction Buffer (New England BioLabs), 1 µL of T4 DNA Ligase (400,000 cohesive end units/mL, New England BioLabs), and 1 µL of *Bsa*I-HF v2 (20,000 units/mL, New England BioLabs) were added, and the reaction was brought to a final volume of 30 µL with water.

The thermocycling reaction was performed using a Biometra T3000 Thermocycler. It consisted of 50 cycles of 5 min at 37°C and 5 min at 16°C, followed by 10 min at 55°C (restriction enzyme inactivation), 10 min at 80°C (complete enzymes denaturation), and hold at 4°C.

3.3.2. Transformation into *Yarrowia lipolytica* via lithium acetate method

The Golden Gate plasmids extracted previously had to be linearized. For this purpose, the plasmid DNA was mixed with 1 µL of NotI-HF (20,000 U/mL), 2 µL of rCutSmart buffer (both from New England BioLabs), and nuclease-free water to reach a final volume of 20 µL. The amount of plasmid added was calculated to obtain a concentration of approximately 175 ng/µL. These reactions were incubated overnight at room temperature.

For the transformation procedure, TE buffer (Tris-EDTA) was prepared with 50 mM Tris-HCl and 5 mM EDTA (Ethylenediaminetetraacetic acid), adjusted to pH 8.0. Lithium acetate (LiAc) solution (0.1 M, pH 6.0) was prepared, and the pH was adjusted with acetic acid. PEG 4000 (polyethylene glycol, 40% w/w) was prepared in 0.1 M LiAc solution. All these solutions were sterilized by autoclaving or filtration. For the carrier DNA, it was prepared by dissolving 5 mg/mL of Sonicated Salmon Sperm DNA (Stratagene) in TE buffer.

The day before transformation, the *Y. lipolytica* strain RIY146 (Po1d, eyk1::LEU2ex, Ura-) was streaked on a YPD plate and incubated overnight at 30°C. This strain was used as it cannot grow on YNB minimal medium lacking uracil, whereas the GG assemblies contain a *URA3* marker, allowing transformants to grow under such conditions.

After 16h of incubation, one loopful of cells was scraped from the plate and washed in 1 mL of TE buffer, then centrifuged at 13 000 rpm for 1 min, using the Eppendorf Centrifuge 5424. The supernatant was discarded, and the cell pellet was resuspended in 600 µL of 0.1 M LiAc solution, followed by 1h incubation at 28°C without shaking in an Eppendorf Thermomixer Compact, to generate competent cells.

Cells were then centrifuged at 2000 rpm for 2 min, and resuspended in 60 µL of 0.1 M LiAc solution. 40 µL of this cell suspension were transferred to a new tube, then mixed with: 4 µL of linearized plasmid DNA (≈700 ng) and 3 µL of carrier DNA (5 mg/mL). The mixture was incubated for 15 min at 28°C, followed by addition of 350 µL of PEG 4000 solution, which was mixed gently. After a further 1h incubation at 28°C, a 10 min heat shock at 39°C was performed. Following the heat shock, 600 µL of 0.1 M LiAc were added and mixed gently. Cells were plated on YNB casamino acid plates, with volumes of 200 µL, 100 µL and 50 µL, using two plates per volume. Plates were incubated at 28°C for up to two days until transformant colonies appeared.

Transformants were subcloned on fresh selective YNB casamino acid plates and incubated at 28°C for one day.

3.3.3. Yeast colony screening with Phire Plant PCR

The Phire Plant Direct PCR Master Mix (Thermo Scientific) was used to perform colony PCR on yeast. The protocol provided by the manufacturer was followed, and the reagents used are listed in Table 5.

A dot of cells was picked from a yeast colony and resuspended in 10 µL of dilution buffer. Four colonies were checked per transformation. From these solutions, 0.5 µL was added as the template for the PCR reaction, which was prepared according to the manufacturer's instructions.

The thermocycling program was carried out on a Biometra T3000 Thermocycler and consisted of the following steps: initial denaturation, 98°C for 5 min; followed by 35 cycles of 5s at 98°C (denaturation), 5s at 58°C (annealing), 40s at 72°C (extension); final extension, 1 min at 72°C and hold at 4°C.

Table 5: Reaction components for Phire Plant PCR on yeast colonies.

	Volume of reagents (µL)
Master Mix	5
Forward primer (10 mM) - p*TEF*-Fo	1
Reverse primer (10 mM) - LacqPCR-R	1
DNA (cells in dilution buffer)	0.5
Water (nuclease-free)	2.5
Total volume	**10 µL**

3.4. Cultivation and laccase activity analysis

3.4.1. Deep-well cultures

The first step of the process consisted of a 24-hour preculture. The night before starting the preculture, selected colonies were streaked on YPD plates and incubated at 30°C.

For the preculture, 1.5 mL of YNB-C medium was dispensed into 24-deep-well plates and inoculated with the corresponding strains. After 24 hours, the optical density (OD) was measured at 600 nm with a Genesys 10S UV-Vis spectrophotometer (Thermo Scientific). The main cultures were inoculated from the preculture and realized with the same medium, adjusted to an initial OD of 0.5, with a total volume of 1.5 mL per well.

For experiments, two clones per transformation were selected, and cultures were performed in triplicate. A blank control consisting of culture medium only was included. Samples were collected at 48, 60 and 72h.

In the case of *P. pastoris* cultures, the strain was used as a reference for comparison with the various *Yarrowia* strains. Two precultures were started, and six biological replicates were prepared for each. Cultures were initiated with 550 µL of YNB casamino acid $CuSO_4$ medium and subjected to successive induction steps. For this purpose, BMM2 and BMM10 induction media were used. After 36h of growth, the first induction was carried out with 700 µL of BMM2. Second and third inductions were performed at 48 and 60h, following sample collection, by adding 215 µL of BMM10. Inductions were realized since the promoter *AOX1* is inducible by methanol.

For sampling, 150 µL (for kinetic experiments) or 200 µL (for standard cultures) were withdrawn. OD was measured by diluting 50 µL of culture in 950 µL of distilled water, reaching a total volume of 1 mL.

The remaining sample was centrifuged for 5 min at 10 000 rpm using an Eppendorf Centrifuge 5424. The supernatant was stored at -20°C until laccase activity was measured.

3.4.2. Laccase activity assay

Sodium acetate buffer (0.1 M, pH 4.5) was used for this assay. On the day of the assay, a fresh working solution was prepared by mixing this buffer with ABTS (2,2'-Azino-bis (3-ethylbenzthiazoline-6-sulfonic acid)) to reach a final ABTS concentration of 0.5 mM. Since this solution is unstable, it was freshly prepared and kept on ice until use to prevent degradation or spontaneous reaction.

This assay was performed using previously collected culture supernatants, which were kept on ice until use to preserve enzyme activity. To measure laccase activity, a TC 96-well standard flat-bottom plate (Sarstedt) was used, and absorbance was monitored using a Tecan Spark plate reader.

Each sample was tested in triplicate. 10 µL of sample was pipetted into each well, followed by 280 µL of the ABTS-buffer solution, rapidly dispensed using a Thermo Scientific multichannel Finnpipette.

Absorbance at 420 nm was recorded every 30s for 5 min, with orbital shaking between readings, while the temperature was maintained at 25°C. If the absorbance exceeded 1.0, the sample were diluted 1:10 in sodium acetate buffer (without ABTS), and the assay was repeated.

The calculation of enzyme activity was based on the change of absorbance over time, using the following formula:

$$Laccase\ activity\ (U/mL) = \left(\frac{\Delta Abs_{420}}{\Delta time}\right) * V_{tot} * (\varepsilon * L * V_{enz})^{-1} * DF$$

Where:

- ΔAbs_{420} = change in absorbance at 420 nm
- $\Delta time$ = time of the reaction (5 minutes)
- V_{tot} = total reaction volume (290 µL)
- ε = molar extinction coefficient of ABTS at 420 nm (36 000 $M^{-1}.cm^{-1}$)
- L = path length (0.75cm for the 96-well plates used)
- $Venz$ = Volume of sample (10 µL)
- DF = dilution factor

To calculate specific activity, OD measurements were converted into DCW using the two following equations:

For *Pichia pastoris*, the following formula was used to calculate the DCW:

$$OD_{600} = 1.5025 * DCW + 0.0256$$

Where:

- OD_{600} = optical density at 600 nm
- DCW = dry cell weight (g/L)

This formula was experimentally determined in the laboratory by colleagues, based on a calibration curve relating optical density at 600 nm (OD_{600}) to measured dry cell weight (DCW).

In the case of *Y. lipolytica*, the following formula was applied (using the same variables as previously defined)[113]:

$$OD_{600} = 0.35\ g/L$$

3.5. Statistical analyses

All statistical analyses were conducted using RStudio software (version 4.2.2). Due to the limited number of replicates (fewer than 10), normality was assumed rather than formally tested. Homogeneity of variances was tested using Levene test. When the egality of variances was not verified, Welch ANOVA was used instead of the standard one-way ANOVA. Post-hoc pairwise comparisons were performed using Games-Howell test, which does not assume equal variances. Significance levels for Welch test were indicated as *, **, *** and **** for p-values less than 0.05, 0.01, 0.001 and 0.0001, respectively.

4. RESULTS AND DISCUSSION

4.1. Construction of Golden Gate Assemblies

Golden Gate assembly technique was used to construct integration cassettes for expressing a heterologous laccase gene in *Y. lipolytica*. This method enables the rapid and reliable assembly of DNA parts in a defined order, including a promoter for gene expression, a pre-(pro) region for protein secretion, the protein coding sequence (CDS), and a transcription terminator.

As depicted in Figure 9, several constructs were generated to test different combinations of the laccase CDS with signal peptides composed of various pre- and pro-regions. In all constructs, the constitutive p*TEF* promoter and *LIP2* transcriptional terminator were used. The expression cassettes were cloned into vector GGE029. The *URA3* marker and *LIP2* flanking regions were incorporated as well, the latter designed for targeted genomic integration at the *LIP2* locus in *Y. lipolytica*.

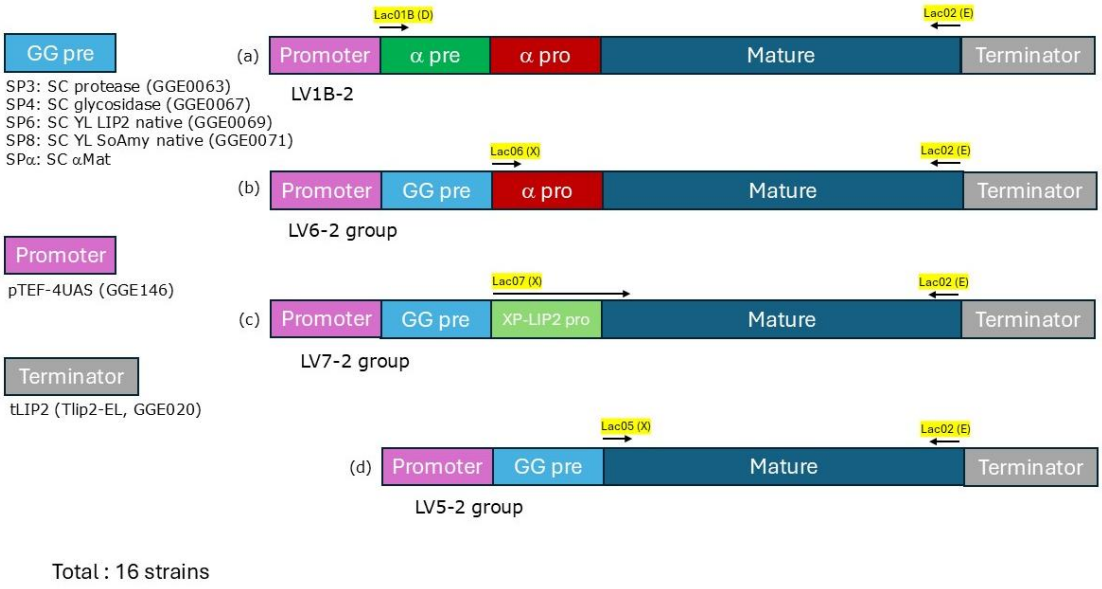

Figure 9: Map of the different DNA constructs. *SC = Secretion Cassette, αMat = α-mating factor pre-signal sequence, derived from Saccharomyces cerevisiae. In yellow, the different primers are displayed. (a) The fragment LV1B-2 (α pre-region, α pro-region and mature protein) corresponds to the original sequence expressed in Pichia pastoris. (b) The fragment LV6-2 contains the α pro-region and the mature protein. (c) The fragment LV7-2 contains the XP-LIP2 pro-region and the mature protein. (d) The fragment LV5-2 only contains the mature protein.*

The first steps consisted of generating the different biobricks and cloning them into a TOPO cloning vector. Each biobrick was designed to start and end with a specific *Bsa*I recognition sequence (GGTCTC). Upon digestion with *Bsa*I, specific cohesive ends were generated, allowing the ordered assembly of the different biobricks during the ligation steps of the GG assembly (Table 6).

Table 6: BsaI recognition sites and overhang sequences for Golden Gate Assemblies. *This table lists the biobricks employed in the assembly, along with their respective 5' and 3' overhang sequences and associated codes. The overhangs correspond to the 4-base pair sequences generated upon BsaI digestion, which allow directional assembly of adjacent fragments. Each overhang is assigned a unique code for reference, and the overhang sequences are designed to be complementary between fragments that are intended to ligate*[58,90].

Biobrick	Code	5' overhang	Code	3' overhang
Insert up	A	GCCT	B	AGGT
Marker *URA3*	B	AGGT	C	ACGG
Promoter *TEF*	C	ACGG	D	AATG
LV1B-2 (α-pre and pro)	D	AATG	E	TCTA
SPs	D	AATG	X	TGCC
LV5-2 (mature protein)	X	TGCC	E	TCTA
LV6-2 (α-pro)	X	TGCC	E	TCTA
LV7-2 (XP-Lip2 pro)	X	TGCC	E	TCTA
Terminator tLIP2	E	TCTA	L	GAGT
Insert down	L	GAGT	M	TGCG
Vector GGE029	M	TGCG	A	GCCT

In order to remove the internal *Bsa*I site of the Lac Vader CDS (see Appendix 1

), which would otherwise have interfered with subsequent GG assembly reactions, the Lac Vader CDS was obtained by overlap PCR. For that purpose, DNA fragments LV1-4 and LV3-2 were amplified using a high-fidelity DNA polymerase and using the Lac Vader plasmid as a template. Primers Lac01B/Lac04 and Lac03/Lac02 were used for the amplification. The primers Lac03 and Lac04 were designed to remove the internal *Bsa*I site, by introducing a single-nucleotide change. Although these primers exhibited a melting temperature (Tm) of 68°C and 70°C respectively, gradient PCRs were performed, and the optimal annealing temperature was found to be 65°C for both reactions.

The resulting PCR fragments were purified from agarose electrophoresis gel, and a second PCR was performed using these two fragments as a template and the primers Lac01B and Lac02, to generate the full-length α-pre-pro Lac Vader fragment lacking the internal *Bsa*I recognition site. These primers were designed to introduce *Bsa*I restriction sites with type D and E overhangs. The final PCR product was purified from gel and cloned into a TOPO cloning vector. The correctness of the resulting biobricks was confirmed by DNA sequencing. The *E. coli* strain carrying the obtained vector was stored at -80°C for further use.

To obtain the laccase CDS with or without pro-region (LV5-2, LV6-2 and LV7-2 groups (see Figure 9)), PCR amplifications with high-fidelity DNA polymerase were performed. These fragments were amplified using forward primers Lac05, Lac06 and Lac07, respectively, with Lac02 as the common reverse primer. For these fragments, the primers were designed to introduce *Bsa*I restriction sites with type X and E overhangs, to be able to link the SPs at the 5' end of the final construct.

All four PCR fragments (LV1B-2, LV5-2, LV6-2 and LV7-2) were cloned into a TOPO cloning vector, transformed into *E. coli* and the sequence checked by DNA sequencing.

Additional parts used for the assemblies (promoter, signal peptide, terminator, inserts up and down, selection marker, and backbone vector) were also obtained from plasmid DNA extracted from *E. coli*

cells grown in liquid culture. For ease of understanding, constructs were named based on their pre- and pro-regions (Table 7).

Table 7: Golden Gate Assemblies. *Variable parts (pre- and pro- regions) are displayed for each assembly. SC = Secretion Cassette, αMat = α-mating factor pre-signal sequence, derived from S. cerevisiae. For the constructs name, A = α pro-region, 0 = no pro-region, L = XP-LIP2 pro-region.*

Name	Protein sequence	Pre-sequence
YL-C	LV1B-2 (complete original Lac Vader)	/
SP3-A	LV6-2 (α pro-region + mature protein)	SP3 (SC protease)
SP4-A	LV6-2	SP4 (SC glycosidase)
SP6-A	LV6-2	SP6 (SC Lip2 native)
SP8-A	LV6-2	SP8 (SC SoAmy native)
SPα-A	LV6-2	SPα (SC αMat)
SP3-0	LV5-2 (mature protein)	SP3
SP4-0	LV5-2	SP4
SP6-0	LV5-2	SP6
SP8-0	LV5-2	SP8
SPα-0	LV5-2	SPα
SP3-L	LV7-2 (XP-LIP2 pro-region + mature protein)	SP3
SP4-L	LV7-2	SP4
SP6-L	LV7-2	SP6
SP8-L	LV7-2	SP8
SPα-L	LV7-2	SPα

Golden Gate assembly reactions were initially performed using a one-step protocol. Successful assembly was achieved for constructs YL-C, SP3-A, SP8-A and SPα-A. However, other combinations failed to yield correct assemblies.

As we expected that the number of DNA parts was too high to allow correct assembly in a single step under our experimental conditions, the assembly for the remaining constructs was performed in two sequential steps. In the first step, the signal peptide and the laccase CDS were assembled, while the remaining parts (promoter, terminator, selection marker, inserts up and down, and the plasmid backbone) were assembled in parallel. In the second step, the products from both assemblies were combined in a new GG reaction. Additionally, the ligation temperature was reduced by 1°C to enhance ligation efficiency[114].

The resulting assemblies were transformed into *E. coli*, and colonies were screened by PCR using primers p*TEF*-Fo and LacqPCR-R. Plasmid DNA from positive colonies was then extracted and underwent a second PCR for confirmation, before being sent to sequencing as a final verification step. Maps of all the assemblies can be found in Appendix 2

Out of the 16 intended construct combinations, 14 were successfully assembled. The two failed constructs were SP4-A and SP4-0.

The 14 obtained constructs were then transformed into *Y. lipolytica*. Transformants were verified via colony PCR using Phire Plant Direct PCR, with primers p*TEF*-Fo and LacqPCR-R as well.

4.2. Determination of optimal sampling time points for laccase production

To compare laccase production across the constructed strains, it was first necessary to determine the optimal sampling time. For this purpose, a time-course analysis of the laccase activity was first performed for three different clones (F11.7, F11.10 and F11.18) of strain SP8-A. This strain was selected because, at that time of the experiment, it showed the highest laccase activity among the four strains that had already been constructed. Samples were collected every 12 hours from 24h to 84h.

For each clone, 2-3 colonies (biological replicates) were used to initiate precultures. The cultures that reached sufficient optical density after 24h were subsequently used to inoculate the main cultures for the time-course analysis.

As shown in Figure 10, laccase activity increases over time, with a marked increase in activity between 48 and 72h for the three clones, suggesting this period as the most active phase of enzyme production. Before 48h and after 72h, laccase activity remained relatively constant for most cultures, indicating a plateau phase. Since expression was driven by the constitutive p*TEF* promoter, the observed activity profile likely reflects changes in biomass growth and resource availability. During the mid- to late-exponential phase, rapid cell division and abundant carbon and nitrogen sources support higher enzyme synthesis rates, whereas activity reaches saturation as nutrient depletion and stationary phase set in[115,116].

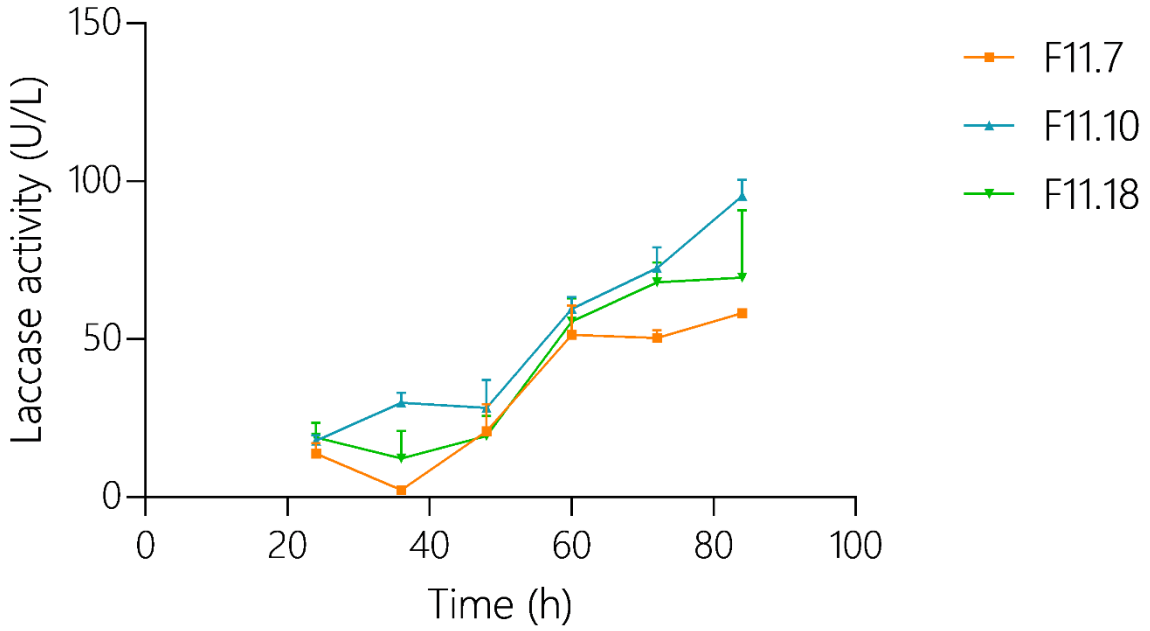

Figure 10: Kinetics of laccase activity in three selected clones of strain SP8-A. *Laccase activity (U/L) was measured every 12 hours from 24 to 84 hours post inoculation for clones F11.7, F11.10 and F11.18.*

Based on these findings, time points 48, 60 and 72 hours were identified as the most relevant for further characterization. Consequently, samples for subsequent experiments were collected at these three time points.

4.3. Assessment of gene integration consistency

Upon yeast transformation, multiple copies of the expression cassette might integrate into the genome, thus affecting the final laccase activity. To evaluate whether all constructed strains carried the same copy number, the enzymatic activity of two clones from each laccase-producing strain was measured. The underlying assumption was that if both clones displayed similar activity levels, they likely contained the same number of integrated cassettes, most probably a single copy. Indeed, the probability of randomly selecting two independent clones that both possess multiple-copy integration is considered very low. Since the Golden Gate constructs were integrated at the *LIP2* locus rather than randomly, similar laccase activity levels between two clones were interpreted as indicative of single-copy integration. Given the targeted nature of the integration, the probability of obtaining two independent clones with multiple-copy integration and similar expression levels is extremely low[92,117]; therefore, the clones were considered to carry a single-copy insertion.

Cultures were performed in triplicate for two clones of each strain generated via Golden Gate assembly, and the laccase activity was determined in triplicate after 48h of culture for each clone.

Table 8: Average laccase activity (X in U/L), standard deviation (SD) and coefficient of variation (CV) at 48h of culture for each selected clone (a and b) for all strains.

	YL-C a	YL-C b	SP3-A a	SP3-A b	SP6-A a	SP6-A b	SP8-A a	SP8-A b
X (U/L)	6.1	5.7	14.5	18.5	40.6	48.0	23.2	25.9
SD	1.6	0.9	5.0	4.8	7.1	12.8	4.2	8.2
CV	26.2	16.4	34.3	26.1	17.5	26.6	18.3	31.4

	SPα-A a	SPα-A b	SP3-0 a	SP3-0 b	SP6-0 a	SP6-0 b	SP8-0 a	SP8-0 b
X (U/L)	5.7	5.8	47.9	37.7	72.9	19.1	28.1	31.0
SD	2.2	0.6	0.5	2.0	18.2	10.4	7.4	6.9
CV	39.1	11.1	1.0	5.4	24.9	54.6	26.3	22.2

	SPα-0 a	SPα-0 b	SP3-L a	SP3-L b	SP4-L a	SP4-L b	SP6-L a	SP6-L b
X (U/L)	0.3	0.57	78.5	103.8	87.8	78.9	117.4	114.7
SD	0.2	0.1	14.0	14.3	9.3	7.91	19.8	42.7
CV	58.4	16.2	17.9	13.8	10.5	10.0	16.9	37.2

	SP8-L a	SP8-L b	SPα-L a	SPα-L b
X (U/L)	95.8	87.8	65.5	61.3
SD	7.0	12.1	19.5	22.1
CV	7.3	13.8	29.8	36.1

Among the evaluated clone pairs, all except one showed comparable laccase activity levels, as shown in Table 8. Some strains like SP3-0, SP3-L or SP8-L exhibited higher variability between both clones, with 47.9 U/L and 37.7 U/L for SP3-0, 78.5 U/L and 103.8 U/L for SP3-L, and 95.8 U/L and 87.8 U/L for SP8-L. In the case of SP3-L, the standard deviations of both clones were relatively high as well (17.9 and 13.8 U/L). However, these differences were not indicative of multiple-copy integration. In theory,

if one clone carried twice as many copies of the expression cassette as the other, its laccase activity would be expected to be roughly doubled compared with the single-copy clone. Since the measured activities remained within a similar range and no clone exhibited an activity level approximately twice of its counterpart, the differences were attributed to natural biological or cultures variability, rather than differences in copy number. The observed variability was therefore considered acceptable, and both clones were assumed to carry a single-copy integration.

These results highlight the natural biological variability that can occur even in genetically identical clones. Clones with the same genetic background can exhibit differences in gene expression and metabolic activity under identical conditions[118,119]. Some of these differences may also arise from subtle variations in culture conditions, such as nutrient availability or oxygen levels, which can occur in deep-well plate cultures[120]. Nonetheless, this variability was not sufficient to undermine the interpretation of the results, assuming that these clones carried single-copy genomic integrations.

For most strains, although the average laccase activities of both clones were similar, the standard deviations were relatively high, reflecting variability within the replicate cultures. However, this intra-culture variability doesn't affect the overall interpretation, as the average activities of the two clones were similar, supporting the idea that a single-copy integration likely occurred.

However, the SP6-0 strain exhibited a significative difference in laccase activity between its two clones, with values of 72.9 U/L and 19.1 U/L for clones *a* and *b*, respectively. This clear difference suggests that clone *a* may have undergone multiple-copy integration. Therefore, clone *b*, which showed a more moderate activity level indicative of single-copy expression, was selected for further experiments.

This highlights the importance of assessing multiple clones when evaluating integration strategies, as outliers such as clone SP6-0 *a* could potentially bias downstream data if not identified. It also confirms that a targeted integration approach, in this case at the *LIP2* locus, generally leads to reproducible secretion levels across clones.

For subsequent measurements and comparisons, laccase activity was assessed and compared at the three time points using only one of the two clones, specifically clone *b* in the case of SP6-0 strain.

4.4. Comparative analysis of laccase activity

4.4.1. Volumetric and specific laccase activity

To characterize the production and secretion efficiency of selected constructs, laccase activity was assessed at the time points previously selected: 48, 60 and 72 hours. Results are presented both as volumetric activity in U/L (see Figure 11) and as specific activity, normalized to biomass, in U/g (see Figure 12). *P. pastoris* strain RIY667 was used as a control, alongside *Y. lipolytica* strain YL-C, which carries the same pre-region, pro-region and protein sequence as in strain RIY667.

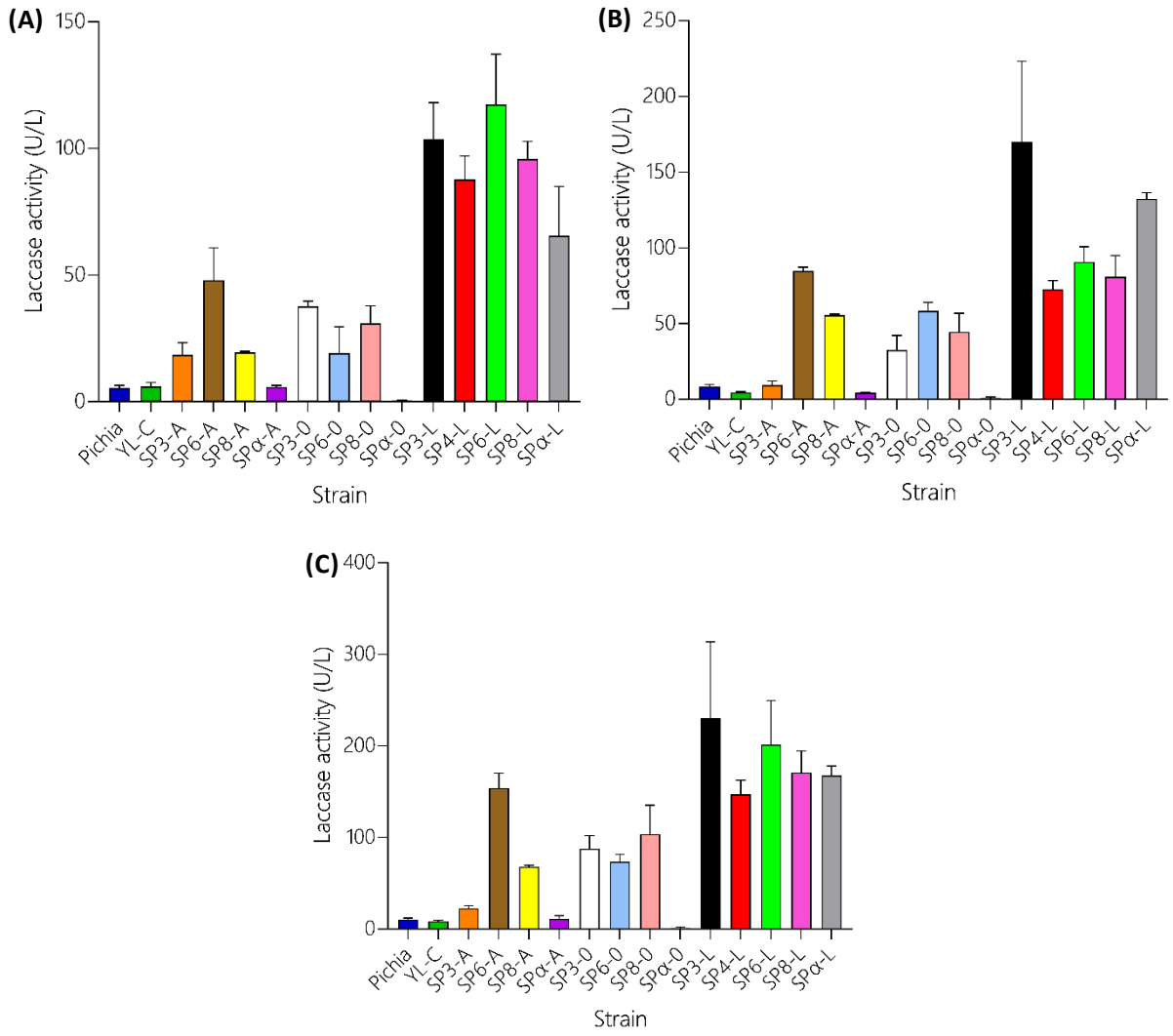

Figure 11: Histograms of the volumetric laccase activity (U/L) at 48, 60 and 72h. *(A) 48h, (B) 60h, (C) 72h. Average laccase activity values (U/L) ± standard deviations (SD) are presented for each strain. Control strains (P. pastoris and Y. lipolytica YL-C) are visible on the left of the graphs for comparison.*

The control strain *P. pastoris* showed low activity, increasing over time (from 5.5 ± 1.1 at 48 h to 10.5 ± 1.7 at 72 h). The YL-C strain, however, produced slightly lower levels of laccase, with activity peaking at only 8.6 ± 1.0 U/L at 72 h.

Laccase activity generally increased over time for most constructs, even though some exhibited a decrease in activity at 60h. Strains carrying the LV7-2 construct (XP-Lip2 pro-region) all showed the highest levels of laccase activity, reaching peak values after 72 h. The strains SP3-L and SP6-L, with final activities of respectively 230.2 ± 83.4 U/L and 201.4 ± 48.2 U/L at 72 h, are amongst the most efficient strains in terms of laccase production. All other constructs (SP8-L and SPα-L) displayed levels of activities over 150 U/L, except for SP4-L which was slightly below 150 U/L (with 147.0 ± 15.5).

In contrast to these high-performing constructs, several strains did not display considerable higher laccase production compared to the control strains. Specifically, strains expressing the LV6-2 construct showed low volumetric activity across all time points. For example, SPα-A reached only 11.2 ± 3.3 U/L at 72 h, a level comparable to *P. pastoris* strain (10.5 ± 1.7 U/L) and not significantly higher than the YL-C strain (8.6 ± 1.0 U/L). Similarly, SP3-A exhibited low activity levels compared to the two control

strains, remaining below 25 U/L even at the final time point. SP8-A showed moderate levels of activity, reaching 68.1 ± 1.7 U/L at 72 h. An exception withing the LV6-2 group was SP6-A, which reached 154.3 ± 15.9 U/L at 72h, significantly outperforming the other strains within the group.

The construct without pro-sequence (LV5-2) displayed intermediate activity levels, with increase in activity from 48 to 72 h. Although their performances did not match those of the LV7-2 group, several strains within this group achieved high levels of enzyme production. For instance, SP8-0 reached 103.9 ± 31.4 U/L at 72 h, while SP3-0 and SP6-0 reached 87.7 ± 14.3 U/L and 73.7 ± 8.0 U/L, respectively. However, not all strains in this group performed equally well. SPα-0 showed low activity levels, reaching only 1.2 ± 0.1 U/L at 72 h, which was lower than both control strains.

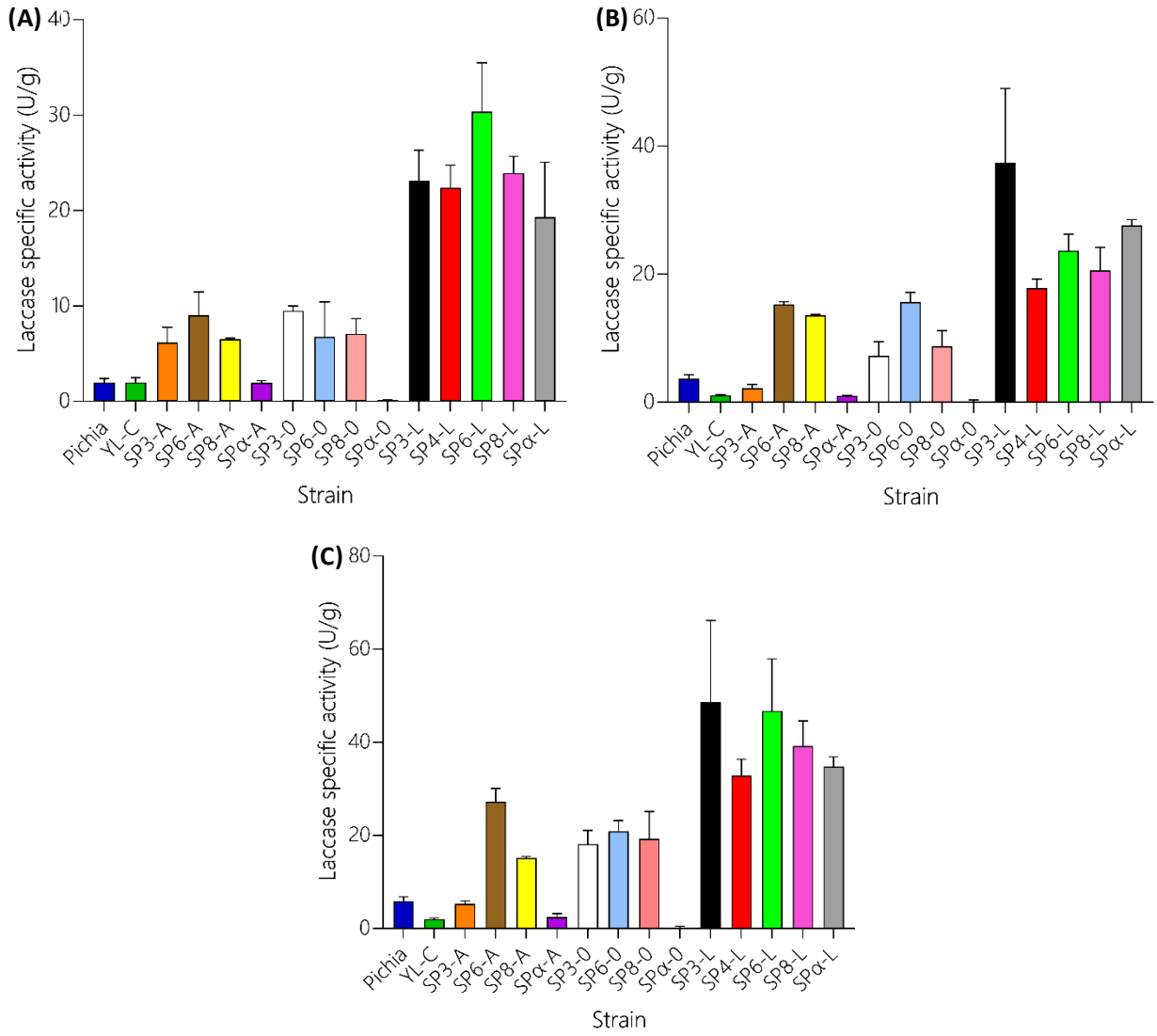

Figure 12: Histograms of the laccase specific activity (U/g) at 48, 60 and 72h. *(A) 48h, (B) 60h, (C) 72h. Average laccase activity values (U/g) ± standard deviations (SD) are presented for each strain. Control strains (P. pastoris and Y. lipolytica YL-C) are visible on the left of the graphs for comparison.*

Because the enzymatic titer is influenced by the biomass present at the sampling time, specific enzyme activity, defined as the enzymatic titer normalized to biomass, was also considered (Figure 12). In general, the same tendencies as volumetric activity can be observed. Enzyme activity increases over time for most constructs, with 72h showing the highest values. Strains from the LV7-2 group exhibited

the highest specific laccase activities, with values exceeding 30 U/g at 72 h. As for volumetric activity measurements, SP3-L and SP6-L demonstrated the highest normalized activity within this group, with respectively 48.6 ± 17.6 U/g and 46.8 ± 11.2 U/g at 72h.

In contrast, LV6-2 group showed consistently low specific activity at all time points, except SP6-A which showed higher specific activity (27.2 ± 2.8 U/g) than the others in this group. SP8-A exhibited specific activity of 15.1 ± 0.4 U/g, while the two remaining strains displayed specific activity levels below 10 U/g. For LV5-2, moderate levels of specific activity have been observed. SPα-0 was still exhibiting low levels of activity, with a specific activity of 0.3 ± 0.2 U/g, similarly to the volumetric measurements.

However, differences between individual signal peptides within each LV construct group appeared less pronounced when specific activity was considered, rather than the volumetric activities. This pattern suggests that the observed differences in volumetric activity are likely influenced by factors such as variations in growth rather than fundamental differences in secretion efficiency. This trend was observed across most strains, although some, such as SP6-A, SP3-L and SP6-L, still stood out within their respective groups due to notable higher activity levels. But for example, strains like SP3-0, SP6-0 and SP8-0 (all within the LV5-2 group), which exhibited volumetric activities of 87.7 ± 14.3 U/L, 73.7 ± 8.0 U/L and 103.9 ± 31.4 U/L respectively, showed specific activities of 18.1 ± 3.0 U/g, 20.9 ± 2.3 U/g and 19.3 ± 5.8 U/g. These three strains, which showed significantly different volumetric activities, displayed similar levels of specific activities.

When comparing specific activities, most engineered strains, except SPα-0, still outperformed the *Pichia* control (5.9 ± 0.9 U/g at 72 h) and the YL-C strain (2.0 ± 0.2 U/g), which both displayed low laccase production efficiency. But in comparison with volumetric activity, YL-C and SPα-A exhibited lower specific activity than *Pichia* strain.

Overall, specific activity values tended to be much closer across strains than volumetric activity, especially when comparing strains within the same LV construct group. Differences between signal peptides tended to be less marked when enzyme activity was normalized to biomass, though certain constructs still exhibited clear advantages.

While volumetric activity reflects the overall amount of enzyme present in the culture broth, it can be affected by differences in cell density[121]. Specific activity, on the other hand, helps distinguish between high biomass producers and truly high-yield enzyme producers[121,122]. Interestingly, despite its lower biomass in comparison to the other strains, *P. pastoris* control strain exhibited a specific activity that was comparable, or even superior, to several poorly performing *Yarrowia* strains.

In this context, specific activity offers a more balanced and realistic view of secretion performance, as it reflects how efficiently a strain produces enzyme, regardless of its growth[122]. It also helps minimize the impact of variability in culture conditions or growth rates, allowing for a more reliable comparison across the different *Y. lipolytica* strains. Specific activity values were therefore used for subsequent statistical analyses to verify if the observed trends held statistical significance.

4.4.2. Statistical comparison of specific laccase activity

To determine whether the observed differences in laccase specific activity (U/g) among the engineered strains were statistically significant, a statistical analysis was conducted for samples taken at 48h, 60h and 72h. As mentioned in section 3.5., significance levels were interpreted as follows: $p < 0.05$ (*), $p < 0.01$ (**), $p < 0.001$ (***) and $p < 0.0001$ (****); while ns indicates non-significant differences.

Statistical comparisons were performed using data from three biological replicates (independent cultures for each construct), each measured in triplicate for laccase activity (9 values in total).

Across all strains, a general increase in specific laccase activity was observed over time, confirming 72h as the optimal sampling point for comparative analysis. At 48h, most strains displayed relatively low specific values, with a few exceptions. By 60h, these differences became more noticeable, and at 72h, they reached maximum divergence, allowing statistically significant differentiation between constructs.

The following sections explore these differences in more detail with a specific focus on the 72-hour time point, which corresponded to the peak of specific activity and revealed the clearest distinctions between constructs. The results at 48h and 60h are presented in Appendix 18

and 19, for information.

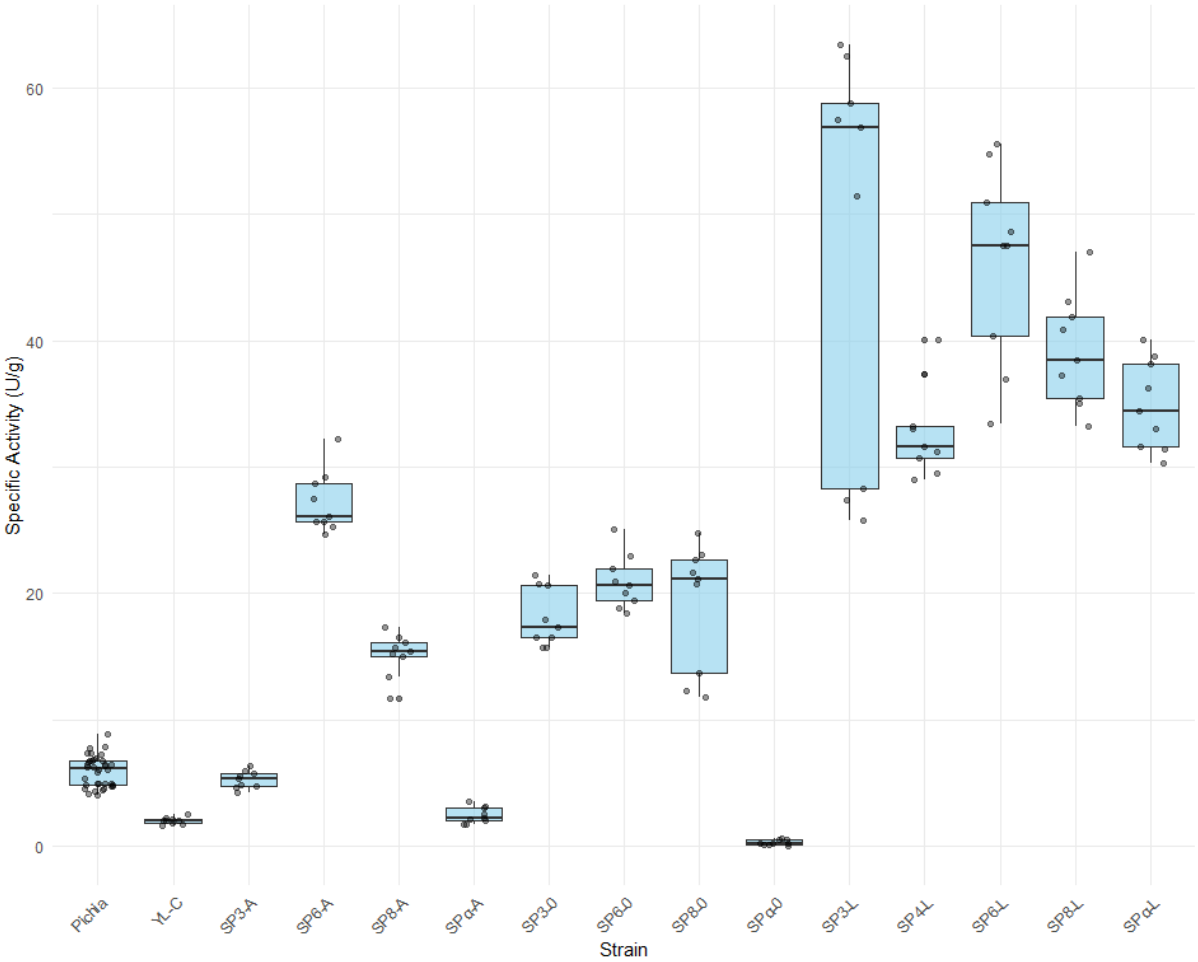

Figure 13: Box plot of the specific laccase activity (U/g) of the different Y. lipolytica strains and P. pastoris control after 72 hours of culture.

As visible in Figure 13, the LV7-2 group, encoding the XP-Lip2 pro-region and counting strains SP3-L to SPα-L, clearly outperformed all other constructs. Within this group, all five strains exhibited statistically significant differences over both control strains. SP3-L showed an increase of 46.0 U/g compared to YL-C (***), while SP6-L and SP8-L followed closely with respective increases of 44.2 U/g (****) and 37.1 U/g (****). SPα-L and SP4-L also showed strong increases with differences of 32.9 U/g (****) and 30.9 U/g (****) compared to YL-C.

These five strains also significantly outperformed *P. pastoris*, which showed low specific activity at 72h (5.9 U/g). For instance, SP6-L compared to *P. pastoris* showed a difference of 40.3 U/g (****), SP8-L 33.2 U/g (****) and SP3-L 42.1 U/g (**). The significance level of *P. pastoris* and SP3-L was lower, even though this pair displayed one of the largest differences in mean specific activity. This is due to the high variability observed in SP3-L (SD = 17.6 U/g), which contrasts with the much lower variability in *P. pastoris* (SD = 0.9 U/g). Moreover, Games-Howell post-hoc test, which accounts for unequal variances between groups, is particularly conservative in such cases, leading to a less significant p-value despite the large difference in means.

Importantly, no statistically significant differences were found among the top four LV7-2 strains (SP3-L, SP6-L, SP8-L, SPα-L) in pairwise comparisons (ns). This confirmed the robustness and reproducibility of the XP-Lip2 pro-region design, regardless of the signal peptide used. These constructs formed a clearly distinct top-performing cluster, with activities between 33 and 46 U/g, well above all other groups.

In contrast, the LV5-2 (mature protein only) group showed intermediate performance, with some variability depending on the signal peptide. SP6-0 reached 18.9 U/g higher than YL-C (****), while SP8-0 and SP3-0 followed closely with 17.1 U/g (***) and 16.1 U/g (****) increases, respectively. However, these strains were still significantly outperformed by LV7-2 constructs when comparing strains possessing the same SP. For instance, SP6-L was significantly better than SP6-0 with a difference of 25.3 U/g (***), SP8-L outperformed SP8-0 by 20.1 U/g (****), and SP3-L outperformed SP3-0 by 29.9 U/g (*). This confirms that the LV5-2 construct, while moderately effective, does not reach the secretion efficiency of constructs carrying the XP-Lip2 pro-region. Notably, SPα-0 displayed the lowest activity of all strains, with specific activity even lower than YL-C (-1.74 U/g, ****) and *P. pastoris* (-5.67 U/g, ****). It was significantly outperformed by every other engineered strain. This result highlights the detrimental effect of the SPα alone when paired with the LV5-2 construct, containing only the coding sequence of the protein.

The LV6-2 group, which includes the α-pro region, showed more heterogeneous results. SP6-A emerged as the strongest strain in this group, with a specific activity 25.2 U/g higher than YL-C (****), and also significantly better than SP3-A, SP8-A and SPα-A, with respective difference of 21.9 U/g (****), 12.1 U/g (****) and 24.8 U/g (****). SP8-A also showed a significant improvement over YL-C, with an increase of 13.1 U/g (****). In contrast, SPα-A was significantly indistinguishable from YL-C (ns). This was expected, since both constructs are constituted of the same elements: YL-C contains the complete Lac Vader sequence, including the α pre- and pro-regions, while SPα-A was reconstructed using the SPα signal peptide fused to the same α-pro region and coding sequence. Compared to *P. pastoris* strain, only SP6-A and SP8-A showed significantly higher specific activity values, with SP6-A outperforming by 21.3 U/g (****) and SP8-A by 9.2 U/g (****). SP3-A showed no significant differences with *P. pastoris*, while SPα-A exhibited a specific activity 3.49 U/g lower (****).

4.5. Biological interpretation and comparative trends

This work evaluated laccase secretion efficiency across a series of *Y. lipolytica* strains engineered with different combinations of expression cassettes, varying in construct architecture (LV5-2, LV6-2 and LV7-2) and signal peptides (SP3, SP4, SP6, SP8, SPα).

4.5.1. Comparison with reference strains

P. pastoris control showed low but consistent activity, while the YL-C strain (*Y. lipolytica* construct identical to *P. pastoris*) had even lower activity. Most engineered strains significantly outperformed these controls. When considering both biomass and volumetric activity, *Y. lipolytica* reached higher biomass levels, and most strains secreted more laccase than *P. pastoris* over the same cultivation period. Previous studies have shown a similar trend, even though they used different promoters (like p*EYK1*), with *Y. lipolytica* producing over five times more heterologous protein, in this case a lipase, and reaching maximal production faster than *P. pastoris* under comparable conditions[50,123]. Similarly, in this work, the best engineered signal peptide and construct combinations led to 15 to 20-fold increase in volumetric activity and nearly 10-fold increase in specific activity, compared to *P. pastoris*.

4.5.2. Construct architecture trends

The LV7-2 construct, incorporating the XP-Lip2 pro-region, yielded the highest laccase activity both in absolute terms and per biomass. Strains SP3-L, SP6-L, SP8-L and SPα-L all reached specific activity values between 33 and 49 U/g, and volumetric activities over 200 U/L for the two top strains. Statistical analysis confirmed these improvements as significant compared to the two controls (*P. pastoris* and YL-C), and importantly, no significant differences were found among the top LV7-2 strains. This demonstrated that the XP-Lip2 pro-region consistently enhances secretion regardless of SP. Recent studies highlight that the Lip2 pro-region improves heterologous protein secretion in *Y. lipolytica* by promoting efficient ER targeting, folding, and trafficking, with modifications leading to substantial secretion increases[57,58]. It was further confirmed that native pro-regions, including Lip2-derived ones, play critical roles in secretion and processing efficiency[71,72]. Moreover, it was demonstrated that the use of X-Pro (XP) motif yielded strong level of heterogenous protein, underscoring its secretion-boosting potential[71].

The LV5-2 construct, which encodes the mature protein without a pro-region, showed moderate performance, with SP3-0, SP6-0 and SP8-0 displaying intermediate activity. However, these strains were all significantly outperformed by their LV7-2 counterparts carrying the same SP, confirming that the absence of a pro-region can limit secretion efficiency, even with favorable SPs. Similar reductions in secretion efficiency in the absence of pro-regions have been described in heterologous laccase expression in yeasts, consistent with the enhanced folding and transport roles suggested for pro-regions[123].

The LV6-2 group, which includes the α-pro region, was more heterogeneous. Most strains had low to moderate activity, but SP6-A stood out with a performance close to some LV7-2 strains (27.2 U/g at 72h), while SP8-A also performed moderately well. In contrast, SP3-A and SPα-A showed poor secretion levels, with no significant improvements over the controls. Interestingly, aside from SP6-A, most LV6-2 strains performed worse than their LV5-2 counterparts, which only contain the mature protein without any pro-region. This observation suggests that in several cases, the presence of the α-pro region may impair secretion. While certain SPs (like SP6) may partly enhance secretion, others (like SP3 or SPα) are not effective in this context. This observation aligns with literature indicating that pro-region efficiency can vary depending on the strain and construct context[69], implying that the α-pro

region's performance is strongly influenced by the protein and the compatibility of the signal peptide used for optimal secretion. Studies demonstrated that removal of the pro sequence can increase secretion of certain heterologous proteins[57,58]. The pro-region, while generally thought to aid folding and secretion, can sometimes be detrimental, potentially by interfering with mRNA export or causing inefficient processing, thus impairing efficiency in specific contexts[57,58]. The impact of pro-regions on secretion can be protein- and context-dependent, with removal of the pro-region enhancing secretion of some proteins but not others[57].

4.5.3. Signal peptide performance

Across constructs, several trends regarding signal peptide efficiency emerged. Although the overall performance of a strain depended on both the construct architecture and the SP used, certain signal peptides consistently outperformed others across multiple construct types.

SP6, derived from the native Lip2 signal peptide of *Y. lipolytica*, was used in SP6-A, SP6-0 and SP6-L, and contributed to high secretion levels in all construct types. In particular, SP6-L was among the top-performing strains overall, while SP6-A showed the highest activity within the LV6-2 group. SP6-0 was also in the high-performing strains of the LV5-2 group. The consistent efficiency of SP6 across all construct types suggests it has broad compatibility with both mature and pro-region-containing designs, making it one of the most reliable SPs in this work. These results agree with reports that certain native signal peptides derived from highly secreted native proteins in *Y. lipolytica*, in this case Lip2, enhance heterologous protein secretion, due to their effective targeting of nascent peptides to the ER and efficient co-translational translocation[67,69].

SP3 (corresponding to the SP of a secreted protease) also supported high laccase production, particularly in SP3-L, which was the highest-performing strain overall in terms of specific activity. However, its performance was more variable than SP6. While SP3-0 exhibited moderate secretion efficiency, as the other strains in the LV5-2 group, SP3-A showed poor activity, similar to control levels. This contrast suggests that SP3 is more effective when paired with a pro-region that demonstrated high secretion efficiency, such as the XP-Lip2 sequence present in LV7-2. This is consistent with observations that the signal peptide efficacy can be highly dependent on the presence of compatible pro-regions to enhance folding and secretion yields[123].

SP8, the pre-sequence of the signal peptide SoAmy (from the rice α-amylase) of *Y. lipolytica*, emerged as a consistently good performer, though with some variation depending on the construct. SP8-L ranked among the best strains, with secretion levels close to those of SP6-L and SP3-L. SP8-0 showed moderate activity, while SP8-A also reached intermediate levels. This pattern indicates that SP8 can support efficient secretion across constructs, though its impact is amplified when combined with an efficient pro-region. Once again, these observations align with observations in engineered yeast systems, where the effectiveness of a signal peptide in facilitating secretion can be influenced by its interaction with elements such as pro-regions[123]. This emphasizes the need to combine compatible secretion signals to optimize heterologous protein production[124]. Moreover, like discussed before with SP6, heterologous protein secretion can be enhanced using native signal peptides[67,69].

Due to technical issues encountered during the construction of the Golden Gate assemblies, SP4 (corresponding to the SP of a secreted glycosidase) was only tested with LV7-2. Despite this limitation, SP4-L exhibited good performance, though slightly lower than other strains in the same group. This

suggests that SP4 may be less optimal, even when used within a favorable construct framework like XP-Lip2 pro-region.

In contrast, SPα showed a strongly context-dependent performance. SPα-L performed well, consistent with the general trend for LV7-2 strains. However, SPα-A and especially SPα-0 showed very low activity, with SPα-0 being the worst-performing strain overall. This pattern suggests that SPα is only effective when used with efficient pro-region like the XP-Lip2, and that its use alone is insufficient or even detrimental to secretion in *Y. lipolytica*. Such context dependence of signal peptides has been previously documented in *Y. lipolytica*, where α-factor based signal peptides sometimes underperform without correct pro-region synergy[123].

Together, these results indicate that, while construct architecture has a dominant impact on secretion performance, the choice of signal peptide still plays a critical role, particularly in enhancing or limiting the effect of a given pro-region. SP6, SP3 and SP8 emerged as the most promising SPs, with SP6 being the most broadly compatible, while SPα appeared to be less suited for efficient secretion in *Y. lipolytica*. This overall conclusion is supported by broader literature in yeast heterologous expression, which underscores the importance of optimizing both signal peptides and pro-regions for maximal secretion efficiency[67,69].

5. CONCLUSION AND PERSPECTIVES

This master thesis investigated the production of a recombinant laccase enzyme in *Y. lipolytica*, using a modular cloning approach to compare different secretion signals and construct designs. While all tested constructs enabled enzyme production and secretion to some extent, the results highlighted significant variability in secretion efficiency and activity levels.

The results showed that both the signal peptide and the presence or absence of a pro-region significantly influenced activity levels. While some constructs led to low or inconsistent activity, others, particularly those combining the XP-Lip2 pro-region with certain pre-sequence, notably SP3 and SP6, showed improved performances.

Looking ahead, several directions could be pursued to further confirm in more controlled culture conditions. Firstly, scaling up the most promising strains to bioreactor conditions would allow assessment of performance under industrially relevant environments. This would enable the evaluation of oxygen transfer rates and carbon sources, which might be suboptimal in deep-well plates and could limit enzyme production.

Additionally, quantitative PCR (qPCR) on genomic DNA could be performed to rigorously confirm that the selected clones carry single-copy integrations, providing direct evidence beyond the assumption based on enzymatic activity levels.

Efforts should also be made to construct the two missing Golden Gate assemblies, which would complete the panel of tested constructs and provide a more comprehensive comparison of signal peptides and pro-region combinations.

6. PERSONAL CONTRIBUTION

The practical part of this master thesis was entirely carried out by myself. I was responsible for the experimental work in the laboratory, while benefiting from the scientific advice and regular feedback of my supervisor, Prof. Patrick Fickers. His guidance helped me plan the experiments, but all manipulations and experimental procedures were performed by myself.

For the data treatment, I organized and processed the results using Excel and performed the statistical analyses with RStudio. This allowed me to evaluate the experimental outcomes and present them in a clean and structured way.

The complete manuscript was written by me. Prof. Fickers provided corrections and suggestions that improved the clarity and accuracy of the text. Since English is not my first language, I additionally relied on AI-based tools to reformulate certain sentences, to make the English more fluent while preserving the scientific meaning.

The figures included in this work were taken or adapted from published papers when appropriate, while some were designed directly by me to illustrate specific results. The vector maps of the constructs were created with SnapGene.

7. REFERENCES

(1) *Recombinant Protein Information - BE*. https://www.thermofisher.com/uk/en/home/life-science/cell-culture/cell-culture-learning-center/recombinant-protein-information.html (accessed 2025-04-17).

(2) Demissie, E. A.; Park, S.-Y.; Moon, J. H.; Lee, D.-Y. Comparative Analysis of Codon Optimization Tools: Advancing toward a Multi-Criteria Framework for Synthetic Gene Design. *J. Microbiol. Biotechnol.* **2025**, *35*, e2411066. https://doi.org/10.4014/jmb.2411.11066.

(3) Paremskaia, A. I.; Kogan, A. A.; Murashkina, A.; Naumova, D. A.; Satish, A.; Abramov, I. S.; Feoktistova, S. G.; Mityaeva, O. N.; Deviatkin, A. A.; Volchkov, P. Y. Codon-Optimization in Gene Therapy: Promises, Prospects and Challenges. *Front. Bioeng. Biotechnol.* **2024**, *12*. https://doi.org/10.3389/fbioe.2024.1371596.

(4) Ndochinwa, G. O.; Wang, Q.-Y.; Okoro, N. O.; Amadi, O. C.; Nwagu, T. N.; Nnamchi, C. I.; Moneke, A. N.; Odiba, A. S. New Advances in Protein Engineering for Industrial Applications: Key Takeaways. *Open Life Sci.* **2024**, *19* (1), 20220856. https://doi.org/10.1515/biol-2022-0856.

(5) Li, C.; Zhang, R.; Wang, J.; Wilson, L. M.; Yan, Y. Protein Engineering for Improving and Diversifying Natural Products Biosynthesis. *Trends Biotechnol.* **2020**, *38* (7), 729–744. https://doi.org/10.1016/j.tibtech.2019.12.008.

(6) Demain, A. L.; Vaishnav, P. Production of Recombinant Proteins by Microbes and Higher Organisms. *Biotechnol. Adv.* **2009**, *27* (3), 297–306. https://doi.org/10.1016/j.biotechadv.2009.01.008.

(7) Porro, D.; Sauer, M.; Branduardi, P.; Mattanovich, D. Recombinant Protein Production in Yeasts. *Mol. Biotechnol.* **2005**, *31* (3), 245–259. https://doi.org/10.1385/MB:31:3:245.

(8) Kirk, O.; Borchert, T. V.; Fuglsang, C. C. Industrial Enzyme Applications. *Curr. Opin. Biotechnol.* **2002**, *13* (4), 345–351. https://doi.org/10.1016/S0958-1669(02)00328-2.

(9) Lee, S. Y.; Kim, H. U. Systems Strategies for Developing Industrial Microbial Strains. *Nat. Biotechnol.* **2015**, *33* (10), 1061–1072. https://doi.org/10.1038/nbt.3365.

(10) Kries, H.; Trottmann, F.; Hertweck, C. Novel Biocatalysts from Specialized Metabolism. *Angew. Chem. Int. Ed.* **2024**, *63* (4), e202309284. https://doi.org/10.1002/anie.202309284.

(11) Zhou, Y.; Liu, Y.; Sun, H.; Lu, Y. Creating Novel Metabolic Pathways by Protein Engineering for Bioproduction. *Trends Biotechnol.* **2025**, *43* (5), 1094–1103. https://doi.org/10.1016/j.tibtech.2024.10.017.

(12) Puetz, J.; Wurm, F. M. Recombinant Proteins for Industrial versus Pharmaceutical Purposes: A Review of Process and Pricing. *Processes* **2019**, *7* (8), 476. https://doi.org/10.3390/pr7080476.

(13) Singh, R.; Kumar, M.; Mittal, A.; Mehta, P. K. Microbial Enzymes: Industrial Progress in 21st Century. *3 Biotech* **2016**, *6* (2), 174. https://doi.org/10.1007/s13205-016-0485-8.

(14) Vojcic, L.; Pitzler, C.; Körfer, G.; Jakob, F.; Ronny Martinez; Maurer, K.-H.; Schwaneberg, U. Advances in Protease Engineering for Laundry Detergents. *New Biotechnol.* **2015**, *32* (6), 629–634. https://doi.org/10.1016/j.nbt.2014.12.010.

(15) Liu, L.; Yang, H.; Shin, H.; Chen, R. R.; Li, J.; Du, G.; Chen, J. How to Achieve High-Level Expression of Microbial Enzymes. *Bioengineered* **2013**, *4* (4), 212–223. https://doi.org/10.4161/bioe.24761.

(16) Çelik, E.; Çalık, P. Production of Recombinant Proteins by Yeast Cells. *Biotechnol. Adv.* **2012**, *30* (5), 1108–1118. https://doi.org/10.1016/j.biotechadv.2011.09.011.

(17) Assenberg, R.; Wan, P. T.; Geisse, S.; Mayr, L. M. Advances in Recombinant Protein Expression for Use in Pharmaceutical Research. *Curr. Opin. Struct. Biol.* **2013**, *23* (3), 393–402. https://doi.org/10.1016/j.sbi.2013.03.008.

(18) Swartz, J. R. Advances in Escherichia Coli Production of Therapeutic Proteins. *Curr. Opin. Biotechnol.* **2001**, *12* (2), 195–201. https://doi.org/10.1016/S0958-1669(00)00199-3.

(19) Rosano, G. L.; Ceccarelli, E. A. Recombinant Protein Expression in Escherichia Coli: Advances and Challenges. *Front. Microbiol.* **2014**, *5*. https://doi.org/10.3389/fmicb.2014.00172.

(20) Gecse, G.; Labunskaite, R.; Pedersen, M.; Kilstrup, M.; Johanson, T. Minimizing Acetate Formation from Overflow Metabolism in Escherichia Coli: Comparison of Genetic Engineering Strategies to Improve Robustness toward Sugar Gradients in Large-Scale Fermentation Processes. *Front. Bioeng. Biotechnol.* **2024**, *12*, 1339054. https://doi.org/10.3389/fbioe.2024.1339054.

(21) Burgess, R. R. Chapter 17 Refolding Solubilized Inclusion Body Proteins. In *Methods in Enzymology*; Burgess, R. R., Deutscher, M. P., Eds.; Guide to Protein Purification, 2nd Edition; Academic Press, 2009; Vol. 463, pp 259–282. https://doi.org/10.1016/S0076-6879(09)63017-2.

(22) Jürgen, B.; Breitenstein, A.; Urlacher, V.; Büttner, K.; Lin, H.; Hecker, M.; Schweder, T.; Neubauer, P. Quality Control of Inclusion Bodies in Escherichia Coli. *Microb. Cell Factories* **2010**, *9* (1), 41. https://doi.org/10.1186/1475-2859-9-41.

(23) Manta, B.; Boyd, D.; Berkmen, M. Disulfide Bond Formation in the Periplasm of Escherichia Coli. *EcoSal Plus* **2019**, *8* (2), 10.1128/ecosalplus.ESP-0012–2018. https://doi.org/10.1128/ecosalplus.esp-0012-2018.

(24) Walsh, G. Post-Translational Modifications of Protein Biopharmaceuticals. *Drug Discov. Today* **2010**, *15* (17–18), 773–780. https://doi.org/10.1016/j.drudis.2010.06.009.

(25) Mergulhão, F. J. M.; Summers, D. K.; Monteiro, G. A. Recombinant Protein Secretion in *Escherichia Coli*. *Biotechnol. Adv.* **2005**, *23* (3), 177–202. https://doi.org/10.1016/j.biotechadv.2004.11.003.

(26) Yang, H.; Qu, J.; Zou, W.; Shen, W.; Chen, X. An Overview and Future Prospects of Recombinant Protein Production in Bacillus Subtilis. *Appl. Microbiol. Biotechnol.* **2021**, *105* (18), 6607–6626. https://doi.org/10.1007/s00253-021-11533-2.

(27) Macek, B.; Forchhammer, K.; Hardouin, J.; Weber-Ban, E.; Grangeasse, C.; Mijakovic, I. Protein Post-Translational Modifications in Bacteria. *Nat. Rev. Microbiol.* **2019**, *17* (11), 651–664. https://doi.org/10.1038/s41579-019-0243-0.

(28) Errington, J.; Aart, L. T. van der. Microbe Profile: Bacillus Subtilis: Model Organism for Cellular Development, and Industrial Workhorse. *Microbiology* **2020**, *166* (5), 425–427. https://doi.org/10.1099/mic.0.000922.

(29) Yang, H.; Ma, Y.; Zhao, Y.; Shen, W.; Chen, X. Systematic Engineering of Transport and Transcription to Boost Alkaline α-Amylase Production in Bacillus Subtilis. *Appl. Microbiol. Biotechnol.* **2020**, *104* (7), 2973–2985. https://doi.org/10.1007/s00253-020-10435-z.

(30) Park, S.; Schumann, W. Optimization of the Secretion Pathway for Heterologous Proteins in Bacillus Subtilis. *Biotechnol. Bioprocess Eng.* **2015**, *20* (4), 623–633. https://doi.org/10.1007/s12257-014-0843-5.

(31) Song, Y.; Nikoloff, J. M.; Zhang, D. Improving Protein Production on the Level of Regulation of Both Expression and Secretion Pathways in Bacillus Subtilis. **2015**, *25* (7), 963–977. https://doi.org/10.4014/jmb.1501.01028.

(32) Neef, J.; van Dijl, J. M.; Buist, G. Recombinant Protein Secretion by Bacillus Subtilis and Lactococcus Lactis: Pathways, Applications, and Innovation Potential. *Essays Biochem.* **2021**, *65* (2), 187–195. https://doi.org/10.1042/EBC20200171.

(33) Santos, K. O.; Costa-Filho, J.; Spagnol, K. L.; Marins, L. F. Comparing Methods of Genetic Manipulation in *Bacillus Subtilis* for Expression of Recombinant Enzyme: Replicative or Integrative (CRISPR-Cas9) Plasmid? *J. Microbiol. Methods* **2019**, *164*, 105667. https://doi.org/10.1016/j.mimet.2019.105667.

(34) Francis, D. M.; Page, R. Strategies to Optimize Protein Expression in E. Coli. *Curr. Protoc. Protein Sci.* **2010**, *Chapter 5* (1), 5.24.1-5.24.29. https://doi.org/10.1002/0471140864.ps0524s61.

(35) Ma, Y.; Shen, W.; Chen, X.; Liu, L.; Zhou, Z.; Xu, F.; Yang, H. Significantly Enhancing Recombinant Alkaline Amylase Production in Bacillus Subtilis by Integration of a Novel Mutagenesis-Screening Strategy with Systems-Level Fermentation Optimization. *J. Biol. Eng.* **2016**, *10* (1), 13. https://doi.org/10.1186/s13036-016-0035-2.

(36) Hong, K.-Q.; Liu, D.-Y.; Chen, T.; Wang, Z.-W. Recent Advances in CRISPR/Cas9 Mediated Genome Editing in Bacillus Subtilis. *World J. Microbiol. Biotechnol.* **2018**, *34* (10), 153. https://doi.org/10.1007/s11274-018-2537-1.

(37) Cui, W.; Han, L.; Suo, F.; Liu, Z.; Zhou, L.; Zhou, Z. Exploitation of Bacillus Subtilis as a Robust Workhorse for Production of Heterologous Proteins and Beyond. *World J. Microbiol. Biotechnol.* **2018**, *34* (10), 145. https://doi.org/10.1007/s11274-018-2531-7.

(38) Mattanovich, D.; Branduardi, P.; Dato, L.; Gasser, B.; Sauer, M.; Porro, D. Recombinant Protein Production in Yeasts. In *Recombinant Gene Expression*; Lorence, A., Ed.; Humana Press: Totowa, NJ, 2012; pp 329–358. https://doi.org/10.1007/978-1-61779-433-9_17.

(39) Zhang, N.; An, Z. Heterologous Protein Expression in Yeasts and Filamentous Fungi. In *Manual of Industrial Microbiology and Biotechnology*; John Wiley & Sons, Ltd, 2010; pp 145–156. https://doi.org/10.1128/9781555816827.ch11.

(40) Guo, Y.; Xiong, Z.; Zhai, H.; Wang, Y.; Qi, Q.; Hou, J. The Advances in Creating Crabtree-Negative Saccharomyces Cerevisiae and the Application for Chemicals Biosynthesis. *FEMS Yeast Res.* **2025**, *25*, foaf014. https://doi.org/10.1093/femsyr/foaf014.

(41) Eleutherio, E. C. A.; Boechat, F. C.; Magalhães, R. S. S.; Brasil, G. B. R. and A. A. Molecular Mechanisms Involved in Yeast Fitness for Ethanol Production. *Adv. Biotechnol. Microbiol.* **2019**, *12* (4), 1–10. https://doi.org/10.19080/AIBM.2019.12.555847.

(42) Baumann, K.; Dato, L.; Graf, A. B.; Frascotti, G.; Dragosits, M.; Porro, D.; Mattanovich, D.; Ferrer, P.; Branduardi, P. The Impact of Oxygen on the Transcriptome of Recombinant S. Cerevisiae and P. Pastoris - a Comparative Analysis. *BMC Genomics* **2011**, *12*, 218. https://doi.org/10.1186/1471-2164-12-218.

(43) Hamilton, S. R.; Gerngross, T. U. Glycosylation Engineering in Yeast: The Advent of Fully Humanized Yeast. *Curr. Opin. Biotechnol.* **2007**, *18* (5), 387–392. https://doi.org/10.1016/j.copbio.2007.09.001.

(44) Li, P.; Anumanthan, A.; Gao, X.-G.; Ilangovan, K.; Suzara, V. V.; Düzgüneş, N.; Renugopalakrishnan, V. Expression of Recombinant Proteins in Pichia Pastoris. *Appl. Biochem. Biotechnol.* **2007**, *142* (2), 105–124. https://doi.org/10.1007/s12010-007-0003-x.

(45) Heyland, J.; Fu, J.; Blank, L. M.; Schmid, A. Quantitative Physiology of Pichia Pastoris during Glucose-Limited High-Cell Density Fed-Batch Cultivation for Recombinant Protein Production. *Biotechnol. Bioeng.* **2010**, *107* (2), 357–368. https://doi.org/10.1002/bit.22836.

(46) Padmanabhan, A.; Nicaud, J.-M.; Fickers, P.; Kumar, S. Metabolic Engineering of *Yarrowia Lipolytica* to Produce Recombinant Proteins. In *Yarrowia Lipolytica Yeast*; Koubaa, M., Mitri, S., Louka, N., Eds.; Academic Press, 2025; pp 51–72. https://doi.org/10.1016/B978-0-443-22092-0.00004-9.

(47) Vandermies, M.; Fickers, P. Bioreactor-Scale Strategies for the Production of Recombinant Protein in the Yeast Yarrowia Lipolytica. *Microorganisms* **2019**, *7* (2), 40. https://doi.org/10.3390/microorganisms7020040.

(48) Vieira Gomes, A. M.; Souza Carmo, T.; Silva Carvalho, L.; Mendonça Bahia, F.; Parachin, N. S. Comparison of Yeasts as Hosts for Recombinant Protein Production. *Microorganisms* **2018**, *6* (2), 38. https://doi.org/10.3390/microorganisms6020038.

(49) Sassi, H.; Delvigne, F.; Kar, T.; Nicaud, J.-M.; Coq, A.-M. C.-L.; Steels, S.; Fickers, P. Deciphering How LIP2 and POX2 Promoters Can Optimally Regulate Recombinant Protein Production in the Yeast Yarrowia Lipolytica. *Microb. Cell Factories* **2016**, *15* (1), 159. https://doi.org/10.1186/s12934-016-0558-8.

(50) Theron, C. W.; Vandermies, M.; Telek, S.; Steels, S.; Fickers, P. Comprehensive Comparison of Yarrowia Lipolytica and Pichia Pastoris for Production of Candida Antarctica Lipase B. *Sci. Rep.* **2020**, *10* (1), 1741. https://doi.org/10.1038/s41598-020-58683-3.

(51) Celińska, E.; Borkowska, M.; Korpys-Woźniak, P.; Kubiak, M.; Nicaud, J.-M.; Kubiak, P.; Gorczyca, M.; Białas, W. Optimization of Yarrowia Lipolytica-Based Consolidated Biocatalyst through Synthetic Biology Approach: Transcription Units and Signal Peptides Shuffling. *Appl. Microbiol. Biotechnol.* **2020**, *104* (13), 5845–5859. https://doi.org/10.1007/s00253-020-10644-6.

(52) Hernández-Montañez, Z.; Araujo-Osorio, J.; Noriega-Reyes, Y.; Chávez-Camarillo, G.; Villa-Tanaca, L. The Intracellular Proteolytic System of Yarrowia Lipolytica and Characterization of an

Aminopeptidase. *FEMS Microbiol. Lett.* **2007**, *268* (2), 178–186. https://doi.org/10.1111/j.1574-6968.2006.00578.x.

(53) Ward, O. P. Production of Recombinant Proteins by Filamentous Fungi. *Biotechnol. Adv.* **2012**, *30* (5), 1119–1139. https://doi.org/10.1016/j.biotechadv.2011.09.012.

(54) El-Enshasy, H. A. Chapter 9 - Filamentous Fungal Cultures – Process Characteristics, Products, and Applications. In *Bioprocessing for Value-Added Products from Renewable Resources*; Yang, S.-T., Ed.; Elsevier: Amsterdam, 2007; pp 225–261. https://doi.org/10.1016/B978-044452114-9/50010-4.

(55) Ward, O. P.; Qin, W. M.; Dhanjoon, J.; Ye, J.; Singh, A. Physiology and Biotechnology of Aspergillus. *Adv. Appl. Microbiol.* **2006**, *58*, 1–75.

(56) Machida, M. Progress of *Aspergillus Oryzae* Genomics. In *Advances in Applied Microbiology*; Laskin, A. I., Bennett, J. W., Gadd, G. M., Eds.; Advances in Applied Microbiology; Academic Press, 2002; Vol. 51, pp 81–107e. https://doi.org/10.1016/S0065-2164(02)51002-9.

(57) Wang, W.; Blenner, M. A. Engineering Heterologous Enzyme Secretion in Yarrowia Lipolytica. *Microb. Cell Factories* **2022**, *21* (1), 134. https://doi.org/10.1186/s12934-022-01863-9.

(58) Celińska, E.; Borkowska, M.; Białas, W.; Korpys, P.; Nicaud, J.-M. Robust Signal Peptides for Protein Secretion in Yarrowia Lipolytica: Identification and Characterization of Novel Secretory Tags. *Appl. Microbiol. Biotechnol.* **2018**, *102* (12), 5221–5233. https://doi.org/10.1007/s00253-018-8966-9.

(59) Ehsan, A.; Mahmood, K.; Khan, Y. D.; Khan, S. A.; Chou, K.-C. A Novel Modeling in Mathematical Biology for Classification of Signal Peptides. *Sci. Rep.* **2018**, *8* (1), 1039. https://doi.org/10.1038/s41598-018-19491-y.

(60) Grasso, S.; Dabene, V.; Hendriks, M. M. W. B.; Zwartjens, P.; Pellaux, R.; Held, M.; Panke, S.; van Dijl, J. M.; Meyer, A.; van Rij, T. Signal Peptide Efficiency: From High-Throughput Data to Prediction and Explanation. *ACS Synth. Biol.* **2023**, *12* (2), 390–404. https://doi.org/10.1021/acssynbio.2c00328.

(61) Vidal, L.; Dong, Z.; Olofsson, K.; Nordberg Karlsson, E.; Nicaud, J.-M. Production of Rhizopus Oryzae Lipase Using Optimized Yarrowia Lipolytica Expression System. *FEMS Yeast Res.* **2023**, *23*, foad037. https://doi.org/10.1093/femsyr/foad037.

(62) Pignède, G.; Wang, H.; Fudalej, F.; Gaillardin, C.; Seman, M.; Nicaud, J.-M. Characterization of an Extracellular Lipase Encoded by LIP2 in Yarrowia Lipolytica. *J. Bacteriol.* **2000**, *182* (10), 2802–2810. https://doi.org/10.1128/jb.182.10.2802-2810.2000.

(63) Celińska, E.; Nicaud, J.-M. Filamentous Fungi-like Secretory Pathway Strayed in a Yeast System: Peculiarities of Yarrowia Lipolytica Secretory Pathway Underlying Its Extraordinary Performance. *Appl. Microbiol. Biotechnol.* **2019**, *103* (1), 39–52. https://doi.org/10.1007/s00253-018-9450-2.

(64) Gorczyca, M.; Kaźmierczak, J.; Fickers, P.; Celińska, E. Synthesis of Secretory Proteins in Yarrowia Lipolytica: Effect of Combined Stress Factors and Metabolic Load. *Int. J. Mol. Sci.* **2022**, *23* (7), 3602. https://doi.org/10.3390/ijms23073602.

(65) Bordes, F.; Fudalej, F.; Dossat, V.; Nicaud, J.-M.; Marty, A. A New Recombinant Protein Expression System for High-Throughput Screening in the Yeast Yarrowia Lipolytica. *J. Microbiol. Methods* **2007**, *70* (3), 493–502. https://doi.org/10.1016/j.mimet.2007.06.008.

(66) Nicaud, J.-M.; Madzak, C.; van den Broek, P.; Gysler, C.; Duboc, P.; Niederberger, P.; Gaillardin, C. Protein Expression and Secretion in the Yeast Yarrowia Lipolytica. *FEMS Yeast Res.* **2002**, *2* (3), 371–379. https://doi.org/10.1016/S1567-1356(02)00082-X.

(67) Madzak, C. Yarrowia Lipolytica Strains and Their Biotechnological Applications: How Natural Biodiversity and Metabolic Engineering Could Contribute to Cell Factories Improvement. *J. Fungi* **2021**, *7* (7), 548. https://doi.org/10.3390/jof7070548.

(68) Pignède, G.; Wang, H.-J.; Fudalej, F.; Seman, M.; Gaillardin, C.; Nicaud, J.-M. Autocloning and Amplification of LIP2 in Yarrowia Lipolytica. *Appl. Environ. Microbiol.* **2000**, *66* (8), 3283–3289. https://doi.org/10.1128/aem.66.8.3283-3289.2000.

(69) Yu, S.; Zhang, G.; Liu, Q.; Zhuang, Y.; Dai, Z.; Xia, J. Construction and Testing of Yarrowia Lipolytica Recombinant Protein Expression Chassis Cells Based on the High-Throughput Screening and Secretome. *Microb. Cell Factories* **2023**, *22* (1), 185. https://doi.org/10.1186/s12934-023-02196-x.

(70) Larroude, M.; Rossignol, T.; Nicaud, J.-M.; Ledesma-Amaro, R. Synthetic Biology Tools for Engineering Yarrowia Lipolytica. *Biotechnol. Adv.* **2018**, *36* (8), 2150–2164. https://doi.org/10.1016/j.biotechadv.2018.10.004.

(71) Gasmi, N.; Lassoued, R.; Ayed, A.; Tréton, B.; Chevret, D.; Nicaud, J. M.; Kallel, H. Production and Characterization of Human Granulocyte-Macrophage Colony-Stimulating Factor (hGM-CSF) Expressed in the Oleaginous Yeast Yarrowia Lipolytica. *Appl. Microbiol. Biotechnol.* **2012**, *96* (1), 89–101. https://doi.org/10.1007/s00253-012-4141-x.

(72) Gasmi, N.; Fudalej, F.; Kallel, H.; Nicaud, J.-M. A Molecular Approach to Optimize hIFN A2b Expression and Secretion in Yarrowia Lipolytica. *Appl. Microbiol. Biotechnol.* **2011**, *89* (1), 109–119. https://doi.org/10.1007/s00253-010-2803-0.

(73) Zhao, Y.; Liu, S.; Lu, Z.; Zhao, B.; Wang, S.; Zhang, C.; Xiao, D.; Foo, J. L.; Yu, A. Hybrid Promoter Engineering Strategies in Yarrowia Lipolytica: Isoamyl Alcohol Production as a Test Study. *Biotechnol. Biofuels* **2021**, *14*, 149. https://doi.org/10.1186/s13068-021-02002-z.

(74) Wang, C.; Lin, M.; Yang, Z.; Lu, X.; Liu, Y.; Lu, H.; Zhu, J.; Sun, X.; Gu, Y. Characterization of the Endogenous Promoters in *Yarrowia Lipolytica* for the Biomanufacturing Applications. *Process Biochem.* **2023**, *124*, 245–252. https://doi.org/10.1016/j.procbio.2022.11.023.

(75) Guo, Z.; Borsenberger, V.; Croux, C.; Duquesne, S.; Truan, G.; Marty, A.; Bordes, F. An Artificial Chromosome ylAC Enables Efficient Assembly of Multiple Genes in Yarrowia Lipolytica for Biomanufacturing. *Commun. Biol.* **2020**, *3*, 199. https://doi.org/10.1038/s42003-020-0936-y.

(76) Liu, J.; Zhu, Y.; Hou, J. Optimizing the CRISPR/Cas9 System for Gene Editing in *Yarrowia Lipolytica*. *Eng. Microbiol.* **2025**, *5* (2), 100193. https://doi.org/10.1016/j.engmic.2025.100193.

(77) Onésime, D.; Lebrun, E.; Petrovic, G. S.; Celińska, E.; Nicaud, J.-M. New Yarrowia Lipolytica Chassis Strains for Industrial Enzyme Production. *Microb. Cell Factories* **2025**, *24*, 164. https://doi.org/10.1186/s12934-025-02787-w.

(78) Ma, Y.; Shang, Y.; Stephanopoulos, G. Engineering Peroxisomal Biosynthetic Pathways for Maximization of Triterpene Production in Yarrowia Lipolytica. *Proc. Natl. Acad. Sci.* **2024**, *121* (5), e2314798121. https://doi.org/10.1073/pnas.2314798121.

(79) Aloulou, A.; Rodriguez, J. A.; Puccinelli, D.; Mouz, N.; Leclaire, J.; Leblond, Y.; Carrière, F. Purification and Biochemical Characterization of the LIP2 Lipase from *Yarrowia Lipolytica*. *Biochim. Biophys. Acta BBA - Mol. Cell Biol. Lipids* **2007**, *1771* (2), 228–237. https://doi.org/10.1016/j.bbalip.2006.12.006.

(80) Engler, C.; Kandzia, R.; Marillonnet, S. A One Pot, One Step, Precision Cloning Method with High Throughput Capability. *PLOS ONE* **2008**, *3* (11), e3647. https://doi.org/10.1371/journal.pone.0003647.

(81) Engler, C.; Gruetzner, R.; Kandzia, R.; Marillonnet, S. Golden Gate Shuffling: A One-Pot DNA Shuffling Method Based on Type IIs Restriction Enzymes. *PLOS ONE* **2009**, *4* (5), e5553. https://doi.org/10.1371/journal.pone.0005553.

(82) Weber, E.; Engler, C.; Gruetzner, R.; Werner, S.; Marillonnet, S. A Modular Cloning System for Standardized Assembly of Multigene Constructs. *PLOS ONE* **2011**, *6* (2), e16765. https://doi.org/10.1371/journal.pone.0016765.

(83) Patron, N. J.; Orzaez, D.; Marillonnet, S.; Warzecha, H.; Matthewman, C.; Youles, M.; Raitskin, O.; Leveau, A.; Farré, G.; Rogers, C.; Smith, A.; Hibberd, J.; Webb, A. A. R.; Locke, J.; Schornack, S.; Ajioka, J.; Baulcombe, D. C.; Zipfel, C.; Kamoun, S.; Jones, J. D. G.; Kuhn, H.; Robatzek, S.; Van Esse, H. P.; Sanders, D.; Oldroyd, G.; Martin, C.; Field, R.; O'Connor, S.; Fox, S.; Wulff, B.; Miller, B.; Breakspear, A.; Radhakrishnan, G.; Delaux, P.-M.; Loqué, D.; Granell, A.; Tissier, A.; Shih, P.; Brutnell, T. P.; Quick, W. P.; Rischer, H.; Fraser, P. D.; Aharoni, A.; Raines, C.; South, P. F.; Ané, J.-M.; Hamberger, B. R.; Langdale, J.; Stougaard, J.; Bouwmeester, H.; Udvardi, M.; Murray, J. A. H.; Ntoukakis, V.; Schäfer, P.; Denby, K.; Edwards, K. J.; Osbourn, A.; Haseloff, J. Standards for Plant Synthetic Biology: A Common Syntax for Exchange of DNA Parts. *New Phytol.* **2015**, *208* (1), 13–19. https://doi.org/10.1111/nph.13532.

(84) Gao, X.; Yan, P.; Shen, W.; Li, X.; Zhou, P.; Li, Y. Modular Construction of Plasmids by Parallel Assembly of Linear Vector Components. *Anal. Biochem.* **2013**, *437* (2), 172–177. https://doi.org/10.1016/j.ab.2013.02.028.

(85) Green, M. R.; Sambrook, J. *Molecular Cloning: A Laboratory Manual*, Fourth edition.; Cold Spring Harbor Laboratory Press: Cold Spring Harbor, N.Y., 2012.

(86) Sarrion-Perdigones, A.; Falconi, E. E.; Zandalinas, S. I.; Juárez, P.; Fernández-del-Carmen, A.; Granell, A.; Orzaez, D. GoldenBraid: An Iterative Cloning System for Standardized Assembly of Reusable Genetic Modules. *PLOS ONE* **2011**, *6* (7), e21622. https://doi.org/10.1371/journal.pone.0021622.

(87) Gibson, D. G.; Young, L.; Chuang, R.-Y.; Venter, J. C.; Hutchison, C. A.; Smith, H. O. Enzymatic Assembly of DNA Molecules up to Several Hundred Kilobases. *Nat. Methods* **2009**, *6* (5), 343–345. https://doi.org/10.1038/nmeth.1318.

(88) Bomfiglio, I. F.; Mendes, I. S. de M.; Bonatto, D. A Review of DNA Restriction-Free Overlapping Sequence Cloning Techniques for Synthetic Biology. *Biotechnol. J.* **2025**, *20* (7), e70084. https://doi.org/10.1002/biot.70084.

(89) Gibson, D. G. Chapter Fifteen - Enzymatic Assembly of Overlapping DNA Fragments. In *Methods in Enzymology*; Voigt, C., Ed.; Synthetic Biology, Part B; Academic Press, 2011; Vol. 498, pp 349–361. https://doi.org/10.1016/B978-0-12-385120-8.00015-2.

(90) Celińska, E.; Ledesma-Amaro, R.; Larroude, M.; Rossignol, T.; Pauthenier, C.; Nicaud, J.-M. Golden Gate Assembly System Dedicated to Complex Pathway Manipulation in Yarrowia Lipolytica. *Microb. Biotechnol.* **2017**, *10* (2), 450–455. https://doi.org/10.1111/1751-7915.12605.

(91) Larroude, M.; Nicaud, J.-M.; Rossignol, T. Golden Gate Multigene Assembly Method for Yarrowia Lipolytica. In *Yeast Metabolic Engineering: Methods and Protocols*; Mapelli, V., Bettiga, M., Eds.; Springer US: New York, NY, 2022; pp 205–220. https://doi.org/10.1007/978-1-0716-2399-2_12.

(92) Larroude, M.; Park, Y.; Soudier, P.; Kubiak, M.; Nicaud, J.; Rossignol, T. A Modular Golden Gate Toolkit for Yarrowia Lipolytica Synthetic Biology. *Microb. Biotechnol.* **2019**, *12* (6), 1249–1259. https://doi.org/10.1111/1751-7915.13427.

(93) Wong, L.; Engel, J.; Jin, E.; Holdridge, B.; Xu, P. YaliBricks, a Versatile Genetic Toolkit for Streamlined and Rapid Pathway Engineering in *Yarrowia Lipolytica*. *Metab. Eng. Commun.* **2017**, *5*, 68–77. https://doi.org/10.1016/j.meteno.2017.09.001.

(94) Li, Y.-W.; Yang, C.-L.; Shen, Q.; Peng, Q.-Q.; Guo, Q.; Nie, Z.-K.; Sun, X.-M.; Shi, T.-Q.; Ji, X.-J.; Huang, H. YALIcloneNHEJ: An Efficient Modular Cloning Toolkit for NHEJ Integration of Multigene Pathway and Terpenoid Production in Yarrowia Lipolytica. *Front. Bioeng. Biotechnol.* **2021**, *9*, 816980. https://doi.org/10.3389/fbioe.2021.816980.

(95) Liu, S.-C.; Xu, L.; Sun, Y.; Yuan, L.; Xu, H.; Song, X.; Sun, L. Progress in the Metabolic Engineering of Yarrowia Lipolytica for the Synthesis of Terpenes. *Biodesign Res.* **2024**, *6*, 0051. https://doi.org/10.34133/bdr.0051.

(96) Larroude, M.; Trabelsi, H.; Nicaud, J.-M.; Rossignol, T. A Set of Yarrowia Lipolytica CRISPR/Cas9 Vectors for Exploiting Wild-Type Strain Diversity. *Biotechnol. Lett.* **2020**, *42* (5), 773–785. https://doi.org/10.1007/s10529-020-02805-4.

(97) Xiong, Y.-R.; Fang, Y.-C.; He, M.; Li, K.-J.; Qi, L.; Sui, Y.; Zhang, K.; Wu, X.-C.; Meng, L.; Li, O.; Zheng, D.-Q. Patterns of Spontaneous and Induced Genomic Alterations in Yarrowia Lipolytica. *Appl. Environ. Microbiol.* **2024**, *91* (1), e01678-24. https://doi.org/10.1128/aem.01678-24.

(98) Connelly, C. F.; Wakefield, J.; Akey, J. M. Evolution and Genetic Architecture of Chromatin Accessibility and Function in Yeast. *PLoS Genet.* **2014**, *10* (7), e1004427. https://doi.org/10.1371/journal.pgen.1004427.

(99) Janusz, G.; Pawlik, A.; Świderska-Burek, U.; Polak, J.; Sulej, J.; Jarosz-Wilkołazka, A.; Paszczyński, A. Laccase Properties, Physiological Functions, and Evolution. *Int. J. Mol. Sci.* **2020**, *21* (3), 966. https://doi.org/10.3390/ijms21030966.

(100) Panchal, K.; Gera, R.; Garg, R.; Kumar, R. LACCASE ENZYME: A Sustainable Catalyst For Bioremediation Strategies. *Biosci. Biotechnol. Res. Asia* **2024**, *21* (4), 1277–1287. https://doi.org/10.13005/bbra/3303.

(101) Aza, P.; Camarero, S. Fungal Laccases: Fundamentals, Engineering and Classification Update. *Biomolecules* **2023**, *13* (12), 1716. https://doi.org/10.3390/biom13121716.

(102) Mateljak, I.; Alcalde, M. Engineering a Highly Thermostable High-Redox Potential Laccase. *ACS Sustain. Chem. Eng.* **2021**, *9* (29), 9632–9637. https://doi.org/10.1021/acssuschemeng.1c00622.

(103) Zofair, S. F. F.; Ahmad, S.; Hashmi, Md. A.; Khan, S. H.; Khan, M. A.; Younus, H. Catalytic Roles, Immobilization and Management of Recalcitrant Environmental Pollutants by Laccases: Significance in Sustainable Green Chemistry. *J. Environ. Manage.* **2022**, *309*, 114676. https://doi.org/10.1016/j.jenvman.2022.114676.

(104) Lee, K.-M.; Kalyani, D.; Tiwari, M. K.; Kim, T.-S.; Dhiman, S. S.; Lee, J.-K.; Kim, I.-W. Enhanced Enzymatic Hydrolysis of Rice Straw by Removal of Phenolic Compounds Using a Novel Laccase from Yeast *Yarrowia Lipolytica*. *Bioresour. Technol.* **2012**, *123*, 636–645. https://doi.org/10.1016/j.biortech.2012.07.066.

(105) Shraddha; Shekher, R.; Sehgal, S.; Kamthania, M.; Kumar, A. Laccase: Microbial Sources, Production, Purification, and Potential Biotechnological Applications. *Enzyme Res.* **2011**, *2011*, 217861. https://doi.org/10.4061/2011/217861.

(106) Dana, M.; Khaniki, G. B.; Mokhtarieh, A. A.; Davarpanah, S. J. Biotechnological and Industrial Applications of Laccase: A Review. *J. Appl. Biotechnol. Rep.* **2017**, *4* (4), 675–679.

(107) Khatami, S. H.; Vakili, O.; Movahedpour, A.; Ghesmati, Z.; Ghasemi, H.; Taheri-Anganeh, M. Laccase: Various Types and Applications. *Biotechnol. Appl. Biochem.* **2022**, *69* (6), 2658–2672. https://doi.org/10.1002/bab.2313.

(108) Yang, J.; Li, W.; Ng, T. B.; Deng, X.; Lin, J.; Ye, X. Laccases: Production, Expression Regulation, and Applications in Pharmaceutical Biodegradation. *Front. Microbiol.* **2017**, *8*. https://doi.org/10.3389/fmicb.2017.00832.

(109) Zhang, J.; Hong, Y.; Li, K.; Sun, Y.; Yao, C.; Ling, J.; Zhong, Y. Enhancing the Production of a Heterologous Trametes Laccase (LacA) by Replacement of the Major Cellulase CBH1 in Trichoderma Reesei. *J. Ind. Microbiol. Biotechnol.* **2023**, *50* (1), kuad002. https://doi.org/10.1093/jimb/kuad002.

(110) Piscitelli, A.; Pezzella, C.; Giardina, P.; Faraco, V.; Sannia, G. Heterologous Laccase Production and Its Role in Industrial Applications. *Bioeng. Bugs* **2010**, *1* (4), 252–262. https://doi.org/10.4161/bbug.1.4.11438.

(111) Liu, C.; Zhang, W.; Qu, M.; Pan, K.; Zhao, X. Heterologous Expression of Laccase From Lentinula Edodes in Pichia Pastoris and Its Application in Degrading Rape Straw. *Front. Microbiol.* **2020**, *11*, 1086. https://doi.org/10.3389/fmicb.2020.01086.

(112) Darvishi, F.; Moradi, M.; Jolivalt, C.; Madzak, C. Laccase Production from Sucrose by Recombinant *Yarrowia Lipolytica* and Its Application to Decolorization of Environmental Pollutant Dyes. *Ecotoxicol. Environ. Saf.* **2018**, *165*, 278–283. https://doi.org/10.1016/j.ecoenv.2018.09.026.

(113) Zhu, J.; Gu, Y.; Yan, Y.; Ma, J.; Sun, X.; Xu, P. Knocking out Central Metabolism Genes to Identify New Targets and Alternating Substrates to Improve Lipid Synthesis in Y. Lipolytica. *Front. Bioeng. Biotechnol.* **2023**, *11*. https://doi.org/10.3389/fbioe.2023.1098116.

(114) Lund, A. H.; Duch, M.; Skou Pedersen, F. Increased Cloning Efficiency by Temperature-Cycle Ligation. *Nucleic Acids Res.* **1996**, *24* (4), 800–801. https://doi.org/10.1093/nar/24.4.800.

(115) Darvishi, F.; Moradi, M.; Madzak, C.; Jolivalt, C. Production of Laccase by Recombinant Yarrowia Lipolytica from Molasses: Bioprocess Development Using Statistical Modeling and Increase

Productivity in Shake-Flask and Bioreactor Cultures. *Appl. Biochem. Biotechnol.* **2017**, *181* (3), 1228–1239. https://doi.org/10.1007/s12010-016-2280-8.

(116) Madzak, C.; Otterbein, L.; Chamkha, M.; Moukha, S.; Asther, M.; Gaillardin, C.; Beckerich, J.-M. Heterologous Production of a Laccase from the Basidiomycete *Pycnoporus Cinnabarinus* in the Dimorphic Yeast *Yarrowia Lipolytica*. *FEMS Yeast Res.* **2005**, *5* (6), 635–646. https://doi.org/10.1016/j.femsyr.2004.10.009.

(117) Jang, I.-S.; Yu, B. J.; Jang, J. Y.; Jegal, J.; Lee, J. Y. Improving the Efficiency of Homologous Recombination by Chemical and Biological Approaches in Yarrowia Lipolytica. *PLoS ONE* **2018**, *13* (3), e0194954. https://doi.org/10.1371/journal.pone.0194954.

(118) Blazeck, J.; Liu, L.; Redden, H.; Alper, H. Tuning Gene Expression in Yarrowia Lipolytica by a Hybrid Promoter Approach. *Appl. Environ. Microbiol.* **2011**, *77* (22), 7905–7914. https://doi.org/10.1128/AEM.05763-11.

(119) Pomraning, K. R.; Wei, S.; Karagiosis, S. A.; Kim, Y.-M.; Dohnalkova, A. C.; Arey, B. W.; Bredeweg, E. L.; Orr, G.; Metz, T. O.; Baker, S. E. Comprehensive Metabolomic, Lipidomic and Microscopic Profiling of Yarrowia Lipolytica during Lipid Accumulation Identifies Targets for Increased Lipogenesis. *PLOS ONE* **2015**, *10* (4), e0123188. https://doi.org/10.1371/journal.pone.0123188.

(120) Celińska, E.; Gorczyca, M. 'Small Volume—Big Problem': Culturing Yarrowia Lipolytica in High-Throughput Micro-Formats. *Microb. Cell Factories* **2024**, *23*, 184. https://doi.org/10.1186/s12934-024-02465-3.

(121) Snopek, P.; Nowak, D.; Zieniuk, B.; Fabiszewska, A. Aeration and Stirring in Yarrowia Lipolytica Lipase Biosynthesis during Batch Cultures with Waste Fish Oil as a Carbon Source. *Fermentation* **2021**, *7* (2), 88. https://doi.org/10.3390/fermentation7020088.

(122) Boeckx, J.; Hertog, M.; Geeraerd, A.; Nicolai, B. Kinetic Modelling: An Integrated Approach to Analyze Enzyme Activity Assays. *Plant Methods* **2017**, *13*, 69. https://doi.org/10.1186/s13007-017-0218-y.

(123) Kalyani, D.; Tiwari, M. K.; Li, J.; Kim, S. C.; Kalia, V. C.; Kang, Y. C.; Lee, J.-K. A Highly Efficient Recombinant Laccase from the Yeast Yarrowia Lipolytica and Its Application in the Hydrolysis of Biomass. *PLOS ONE* **2015**, *10* (3), e0120156. https://doi.org/10.1371/journal.pone.0120156.

(124) Theerachat, M.; Emond, S.; Cambon, E.; Bordes, F.; Marty, A.; Nicaud, J.-M.; Chulalaksananukul, W.; Guieysse, D.; Remaud-Siméon, M.; Morel, S. Engineering and Production of Laccase from *Trametes Versicolor* in the Yeast *Yarrowia Lipolytica*. *Bioresour. Technol.* **2012**, *125*, 267–274. https://doi.org/10.1016/j.biortech.2012.07.117.

8. APPENDICES

Appendix 1

	Primer		Length	Binding Sites		Tm
✓	**Lac01B**		49-mer	1 .. 49	→	65ºC
	/sequence	= gggGGTCTCtAATGAGATTTCCTTCAATTTTTACTGATGTTTTATTCGC				
		37% GC / 15,054,9 Da				
✓	**Lac06**		39-mer	69 .. 93	→	60ºC
	/sequence	= GGGGGTCTCTTGCCGCTCCAGTCAACACTACAACAGAAG				
		56% GC / 11,961,8 Da				
✓	**Lac05**		36-mer	279 .. 300	→	61ºC
	/sequence	= GGGGGTCTCTTGCCGAATTCAGCATTGGGCCAGTCG				
		61% GC / 11,124,2 Da				
✓	**Lac07**		81-mer	279 .. 300	→	61ºC
	/sequence	= GGTCTCTTGCCCTCCCTTCCCCCATCACTCCTTCTGAGGCCGCAGTTCTCCAGAAGCGAGAATTCAGCATTGGGCCAGTCG				
		59% GC / 24,694,9 Da				
	/note	= XP-Pro Lip2				
✓	**Lac03**		22-mer	632 .. 653	→	59ºC
	/sequence	= CTGTGACGGACTCAGGGGTCCG				
		68% GC / 6792,4 Da				
✓	**Lac04**		22-mer	632 .. 653	←	60ºC
	/sequence	= CGGACCCCTGAGTCCGTCACAG				
		68% GC / 6681,4 Da				
✓	**LacqPCR-R**		20-mer	1049 .. 1068	←	59ºC
	/sequence	= GAAGGGCACGGATCCAGTAG				
		60% GC / 6216,1 Da				
	/note	= qPCR-Rev				
✓	**Lac02**		31-mer	1759 .. 1789	←	70ºC
	/sequence	= CCCGGTCTCTTAGATCAGAGGTCGCTGGGGT				
		61% GC / 9559,2 Da				

Appendix 1: Map of the original Lac Vader sequence, for full cloning, before removal of the *Bsa*I site (GGTCTC) in the middle of the protein sequence. All the primers used for the design of the constructs are visible in purple. Software used: SnapGene (v8.1).

Appendix 2

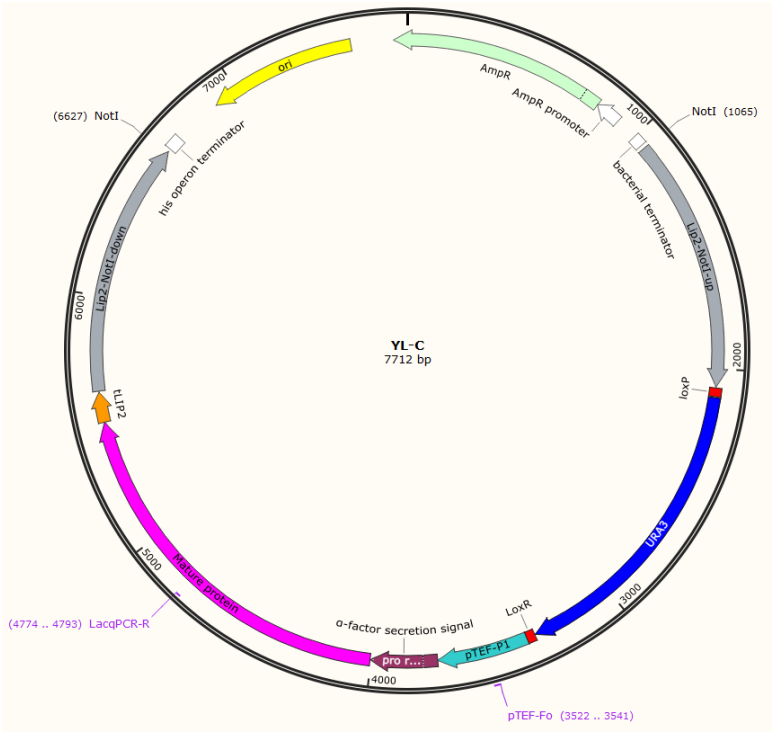

Appendix 2: Map of the YL-C Golden Gate Assembly, with the annealing primers p*TEF*-Fo and LacqPCR-R. NotI recognition sites (for plasmid linearization) are visible as well. Software used: SnapGene (v8.1).

Appendix 3

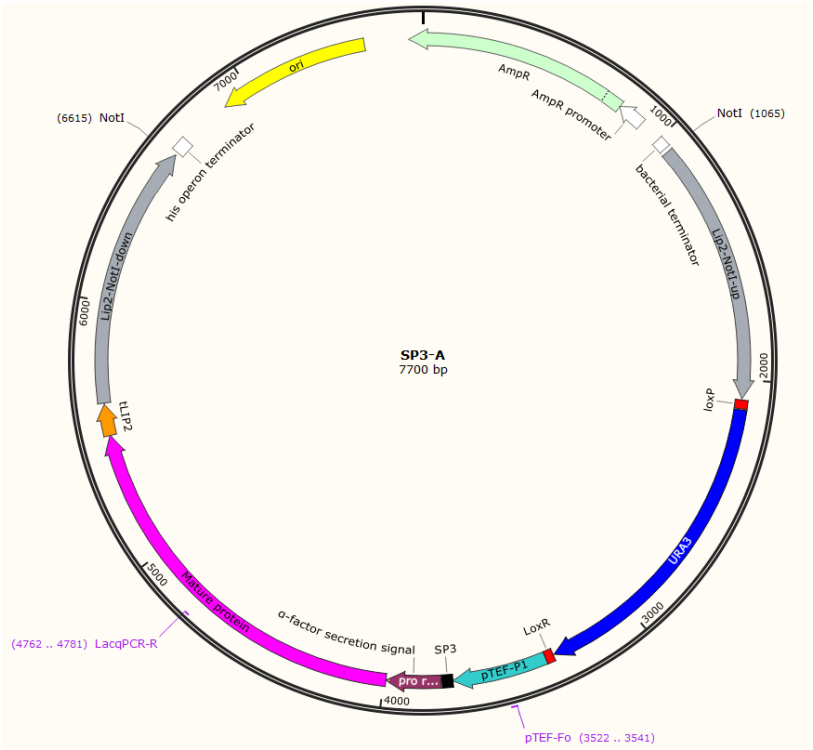

Appendix 3: Map of the SP3-A Golden Gate Assembly, with the annealing primers p*TEF*-Fo and LacqPCR-R. NotI recognition sites (for plasmid linearization) are visible as well. Software used: SnapGene (v8.1).

Appendix 4

Appendix 4: Map of the SP4-A Golden Gate Assembly, with the annealing primers p*TEF*-Fo and LacqPCR-R. NotI recognition sites (for plasmid linearization) are visible as well. Software used: SnapGene (v8.1).

Appendix 5

Appendix 5: Map of the SP6-A Golden Gate Assembly, with the annealing primers p*TEF*-Fo and LacqPCR-R. NotI recognition sites (for plasmid linearization) are visible as well. Software used: SnapGene (v8.1).

Appendix 6

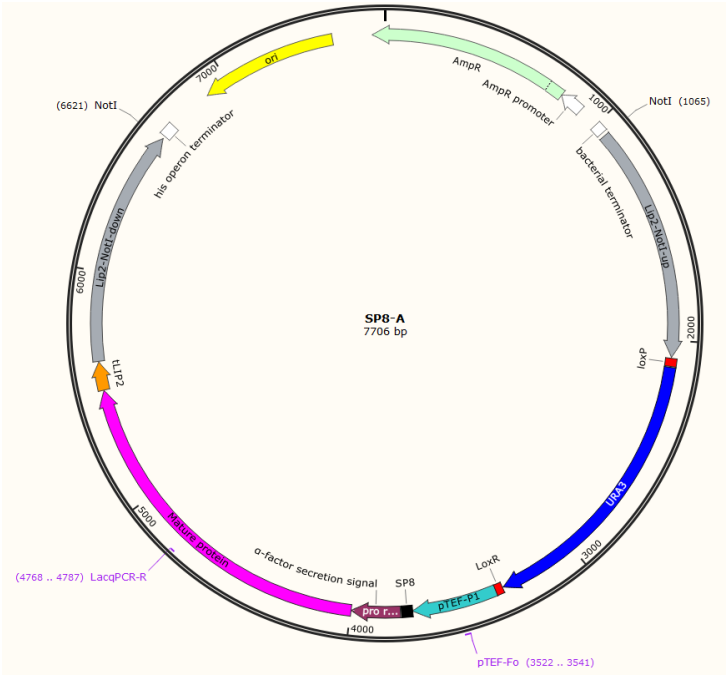

Appendix 6: Map of the SP8-A Golden Gate Assembly, with the annealing primers p*TEF*-Fo and LacqPCR-R. NotI recognition sites (for plasmid linearization) are visible as well. Software used: SnapGene (v8.1).

Appendix 7

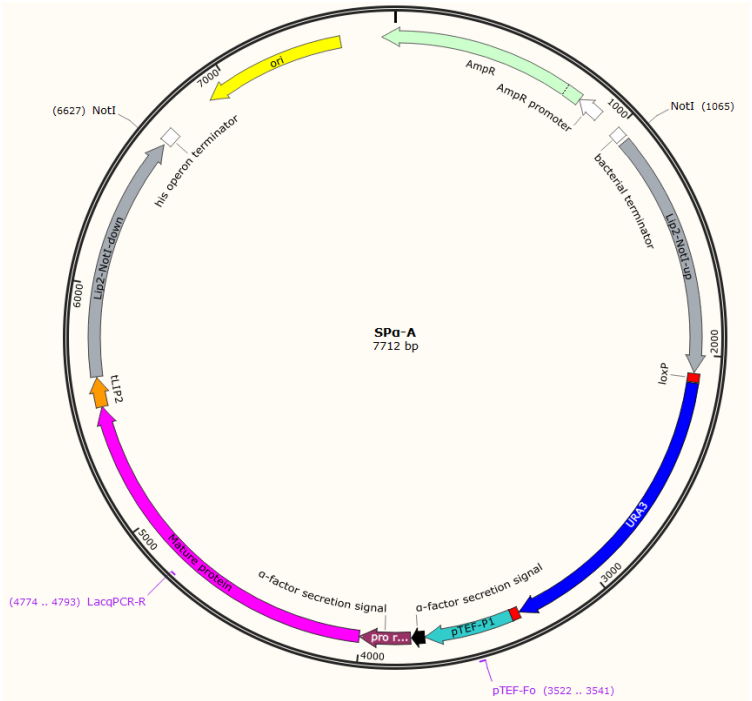

Appendix 7: Map of the SPα-A Golden Gate Assembly, with the annealing primers p*TEF*-Fo and LacqPCR-R. NotI recognition sites (for plasmid linearization) are visible as well. Software used: SnapGene (v8.1).

Appendix 8

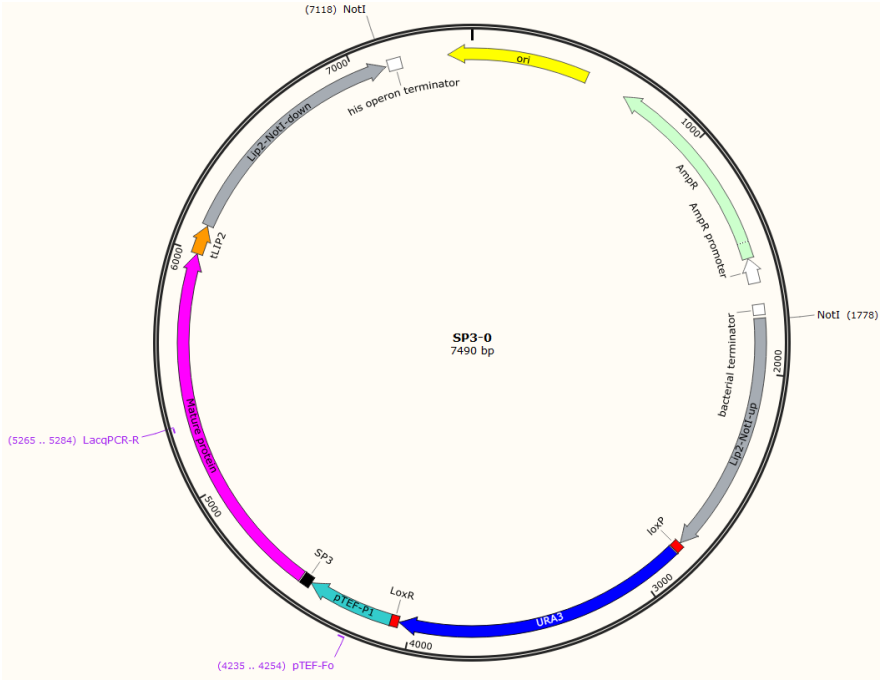

Appendix 8: Map of the SP3-0 Golden Gate Assembly, with the annealing primers p*TEF*-Fo and LacqPCR-R. NotI recognition sites (for plasmid linearization) are visible as well. Software used: SnapGene (v8.1).

Appendix 9

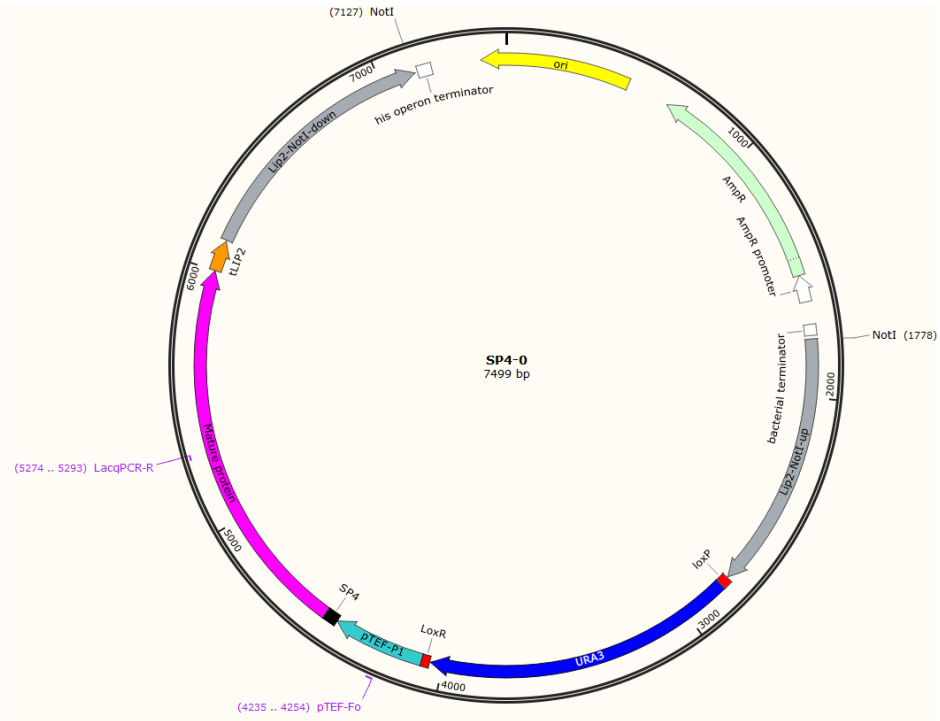

Appendix 9: Map of the SP4-0 Golden Gate Assembly, with the annealing primers p*TEF*-Fo and LacqPCR-R. NotI recognition sites (for plasmid linearization) are visible as well. Software used: SnapGene (v8.1).

Appendix 10

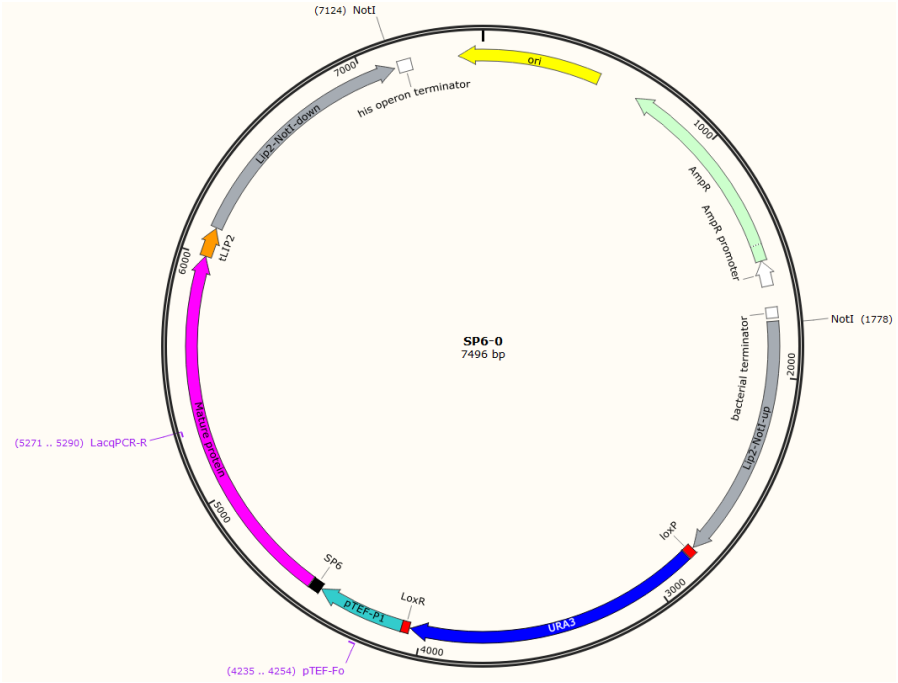

Appendix 10: Map of the SP6-0 Golden Gate Assembly, with the annealing primers p*TEF*-Fo and LacqPCR-R. NotI recognition sites (for plasmid linearization) are visible as well. Software used: SnapGene (v8.1).

Appendix 11

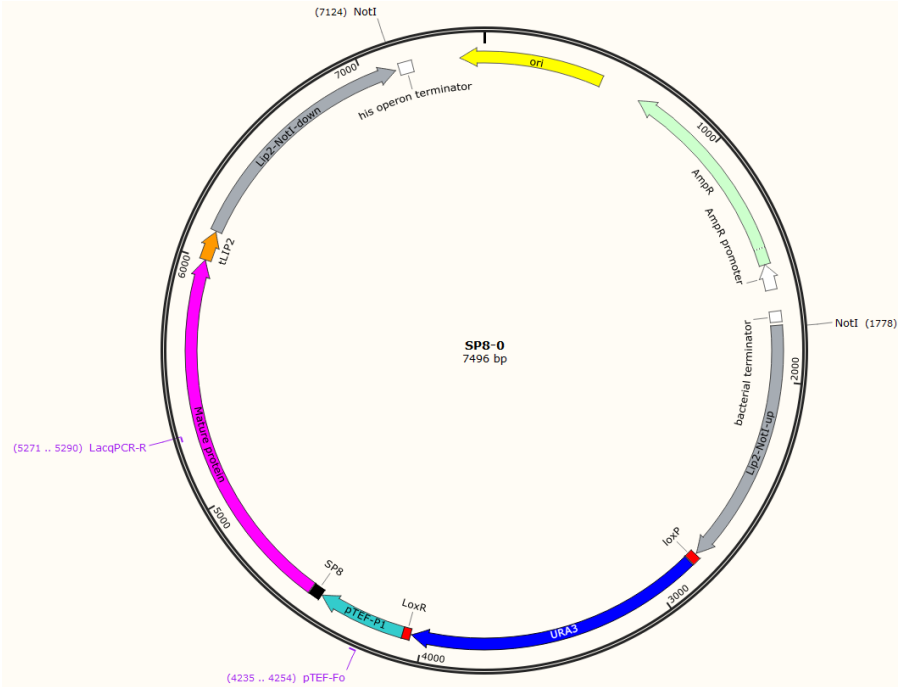

Appendix 11: Map of the SP8-0 Golden Gate Assembly, with the annealing primers p*TEF*-Fo and LacqPCR-R. NotI recognition sites (for plasmid linearization) are visible as well. Software used: SnapGene (v8.1).

Appendix 12

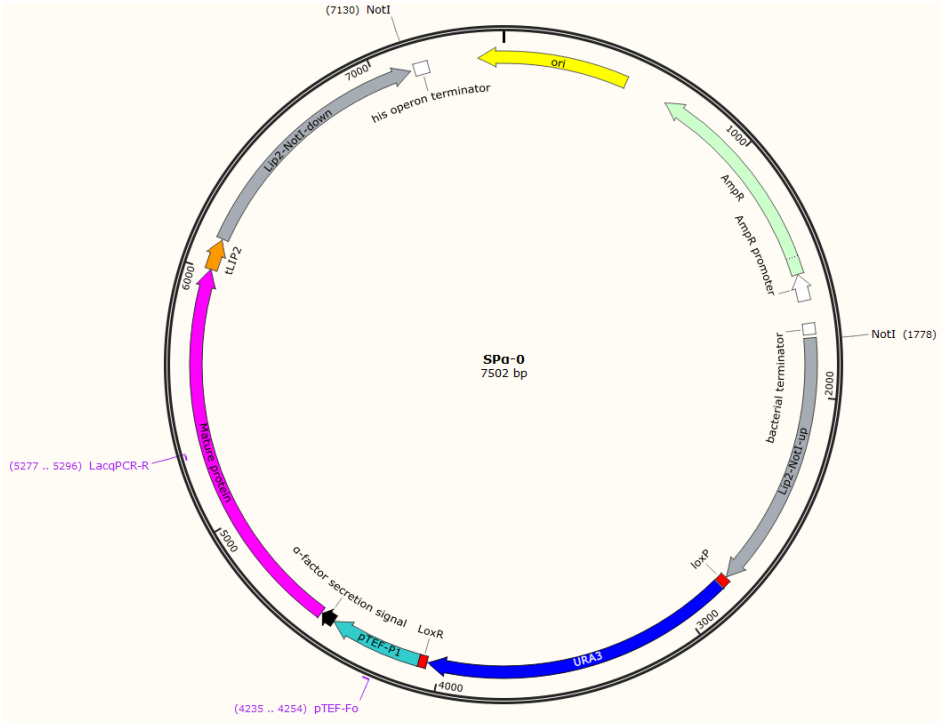

Appendix 12: Map of the SPα-0 Golden Gate Assembly, with the annealing primers p*TEF*-Fo and LacqPCR-R. NotI recognition sites (for plasmid linearization) are visible as well. Software used: SnapGene (v8.1).

Appendix 13

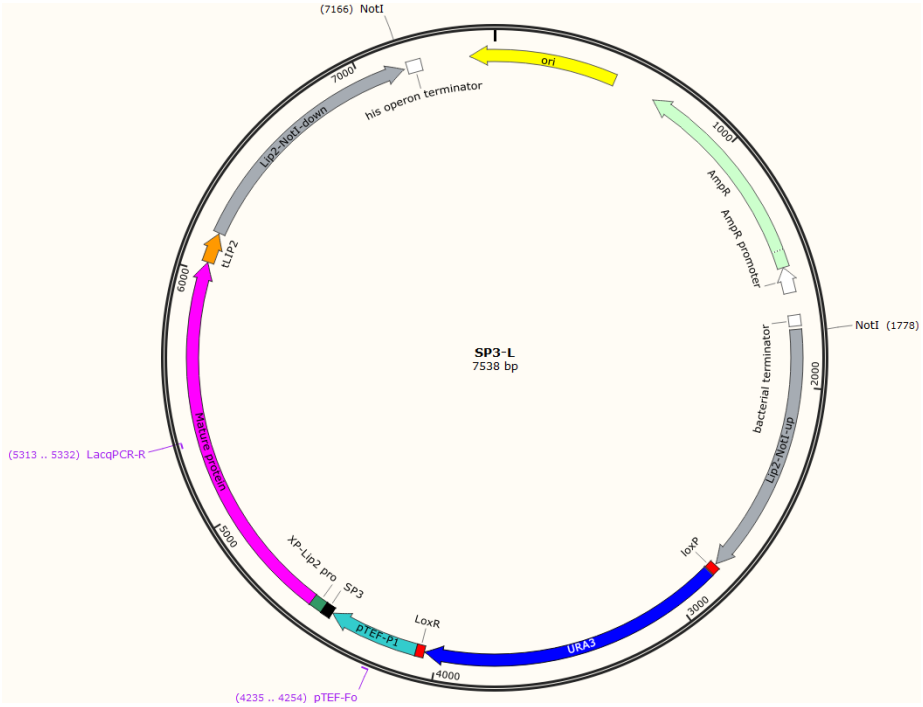

Appendix 13: Map of the SP3-L Golden Gate Assembly, with the annealing primers p*TEF*-Fo and LacqPCR-R. NotI recognition sites (for plasmid linearization) are visible as well. Software used: SnapGene (v8.1).

Appendix 14

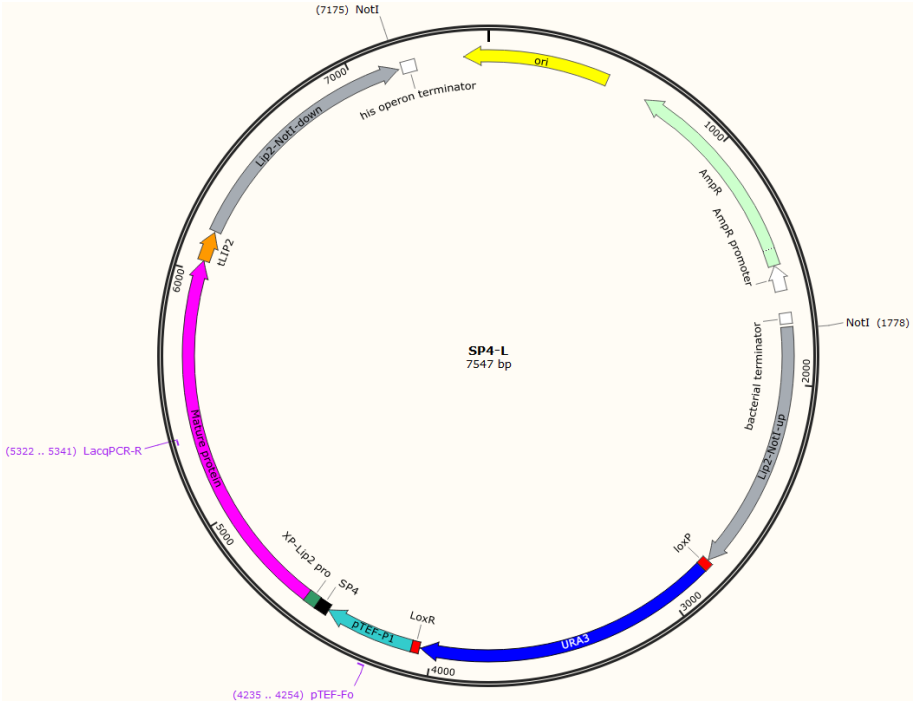

Appendix 14: Map of the SP4-L Golden Gate Assembly, with the annealing primers p*TEF*-Fo and LacqPCR-R. NotI recognition sites (for plasmid linearization) are visible as well. Software used: SnapGene (v8.1).

Appendix 15

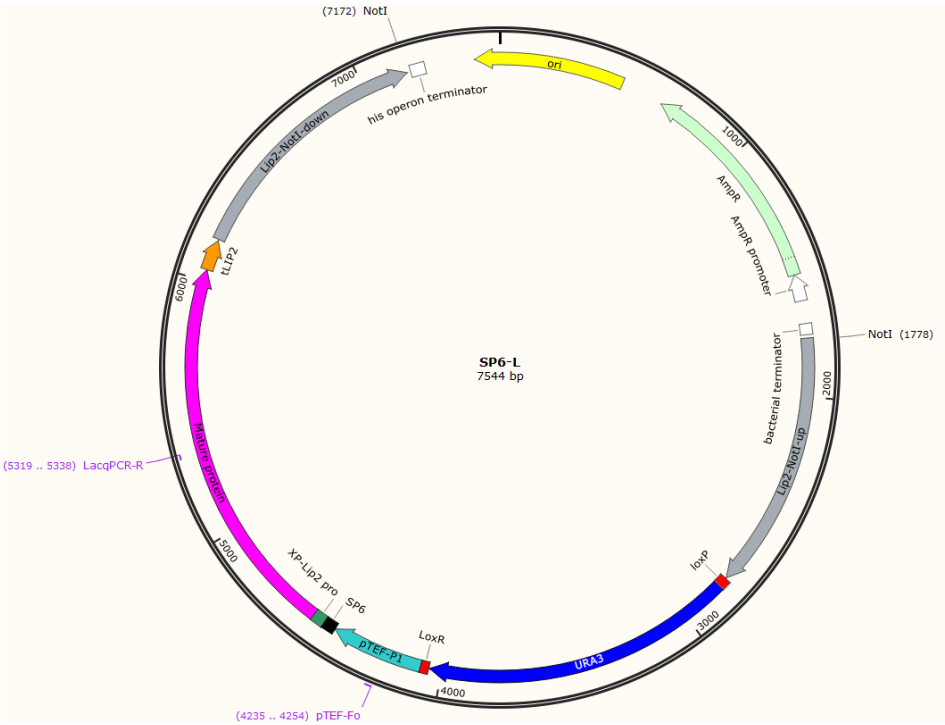

Appendix 15: Map of the SP6-L Golden Gate Assembly, with the annealing primers p*TEF*-Fo and LacqPCR-R. NotI recognition sites (for plasmid linearization) are visible as well. Software used: SnapGene (v8.1).

Appendix 16

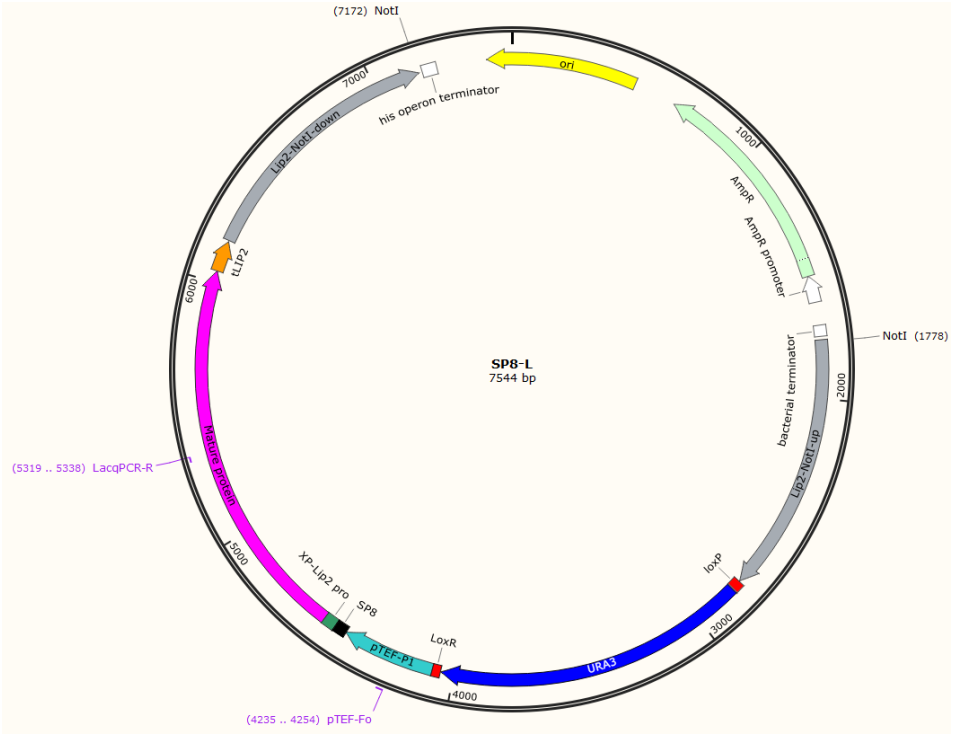

Appendix 16: Map of the SP8-L Golden Gate Assembly, with the annealing primers p*TEF*-Fo and LacqPCR-R. NotI recognition sites (for plasmid linearization) are visible as well. Software used: SnapGene (v8.1).

Appendix 17

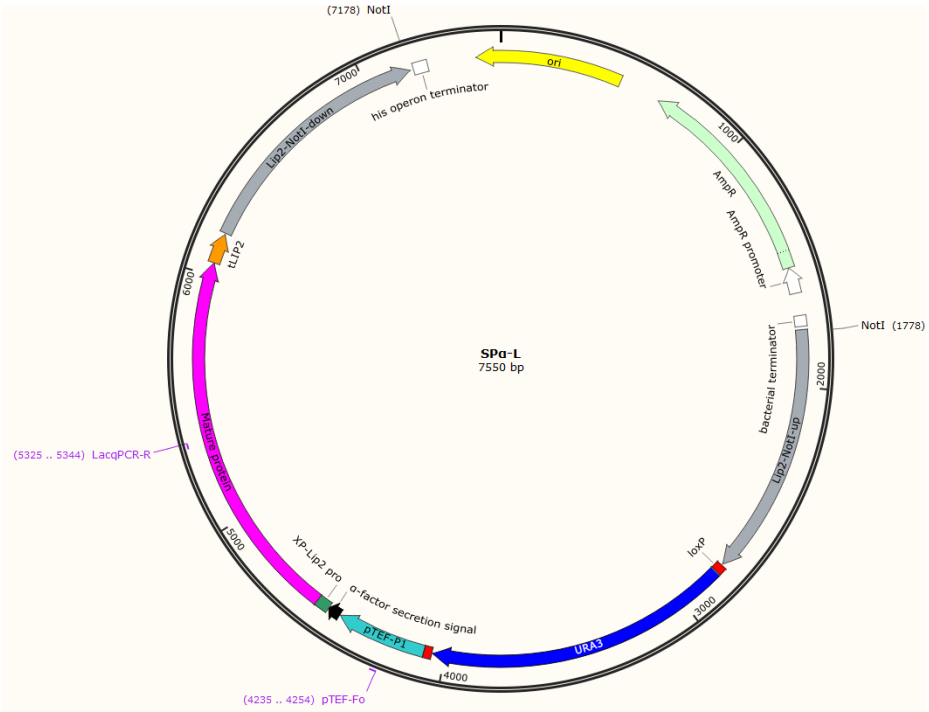

Appendix 17: Map of the SPα-L Golden Gate Assembly, with the annealing primers p*TEF*-Fo and LacqPCR-R. NotI recognition sites (for plasmid linearization) are visible as well. Software used: SnapGene (v8.1).

Appendix 18

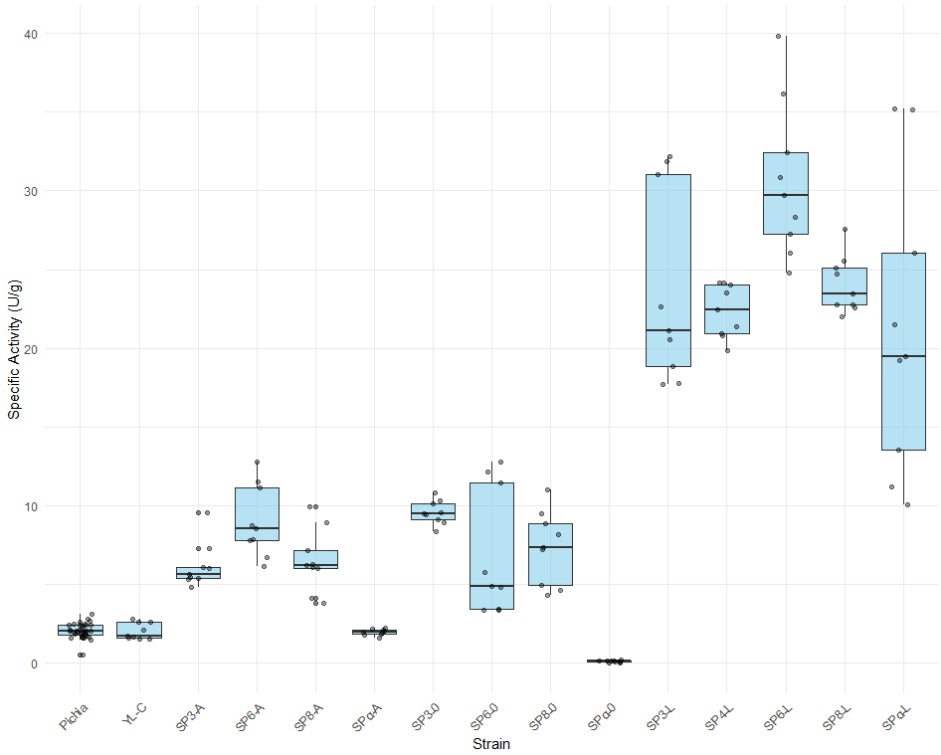

Appendix 1814: Box plot of the specific laccase activity (U/g) of the different *Y. lipolytica* strains and *P. pastoris* control after 48 hours of culture.

Appendix 19

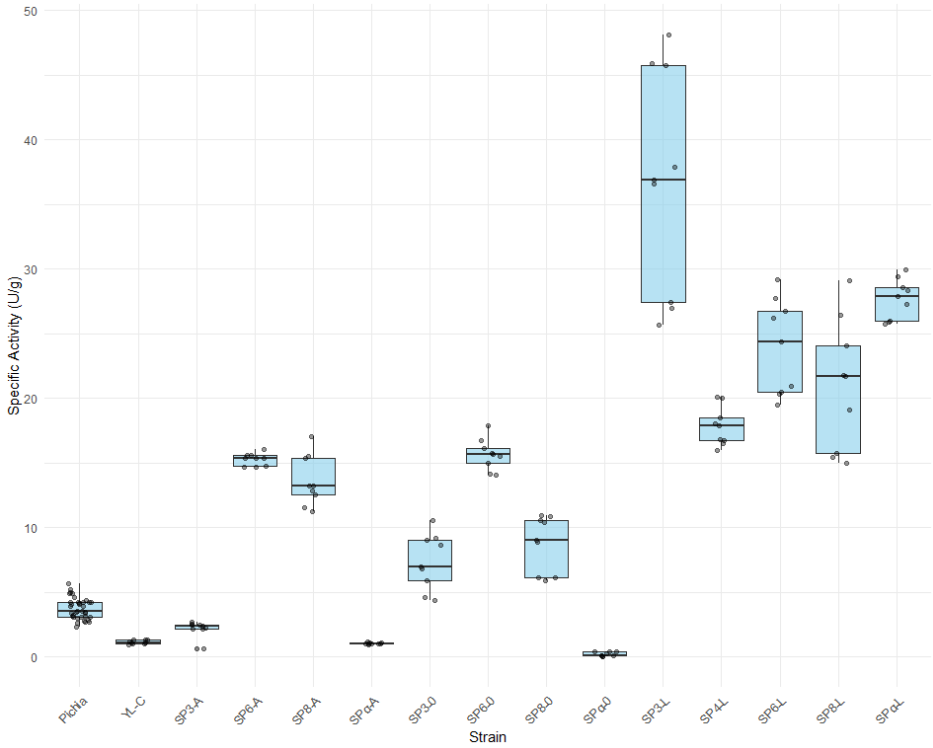

Appendix 19: Box plot of the specific laccase activity (U/g) of the different *Y. lipolytica* strains and *P. pastoris* control after 60 hours of culture.